Isolation and evaluation of extractable materials in commercial polyolefins.

By

Moses T. Kotsokoane

Thesis presented in partial fulfilment of the requirements of the degree of

Master of Science (Polymer Science) at the

University of Stellenbosch

Study leader

Dr. AJ van Reenen

Stellenbosch

March 2007

Declaration

I, the undersigned, hereby declare that the work contained in this thesis is my own original work and has not in its entirety or in part been submitted at any university as a degree.

13-March-2007

.....

Date

Abstract

Four homopolymer and five propylene-ethylene random copolymer samples produced from two different polypropylene production plants were used as test materials in this study. These materials were isolated into various fractions using the following techniques; xylene and decalin extractions, successive extractions and TREF. The types of fractions isolated with the abovementioned techniques were analysed using GPC, NMR and DSC. From the analytical results it was concluded that the extraction techniques isolate various types of fractions making up the polymer.

Opsomming

Vier homopolimeer en vyf lukrake kopolimeer monsters wat by twee verskillende polipropileen vervaardigingsaanlegte gemaak is, is gebruik as toetsmateriale in hierdie studie. Die materiale is in verskillende fraksies geisoleer deur gebruik te maak van xileen en dekalien ekstraksies, opeenvolgende ekstraksies, en stygende temperatuur uitloging fraksionering (Eng: "TREF"). Die fraksies wat sodoende geisoleer is, is deur GPC, KMR en DSC geanaliseer. Vanuit die analise-resultate is tot die gevolgtrekking gekom dat die ekstraksie-tegnieke almal verskillende fraksies van die oorpronklike materiale isoleer

Contents

List of schemes

Chapter 2. Historical and theoretical concepts.

List of Figures

Chapter 2. Historical and theoretical concepts.

Chapter 4. Results and discussions.

List of Tables

Chapter 2. Historical and theoretical concepts.

Chapter 4. Results and discussion.

List of abbreviations

DSC	Differential Scanning Calorimetry
Crystaf	Crystallization Analysis Fractionation
GPC	Gel Permeation Chromatography
MFI	Melt Flow Index
Mn	Number average molecular weight
Mw	Weight average molecular weight
MWD	Molecular Weight Distribution
NMR	Nuclear Magnetic Resonance
PP	Polypropylene
TREF	Temperature Rising Elution Fractionation

List of contents

Chapter 1. Introduction

Chapter 2. Historical and theoretical concepts

Chapter 3. Experimental

Chapter 4. Results and discussion

Acknowledgements

I would like to thank the following people for their valued contribution in making this study possible.

Dr. A.J van Reenen, for his willingness to supervise this study.

Dr. B. Sole, for his support and guidance.

Ms. M. Smith, for sharing of information throughout the study.

Ms. K. Ramphele, for all the GPC analysis.

Mr. J. Vermeulen, for TREF and GPC analysis.

Mr. R. Zwane, for the DSC analysis.

Dr. F. du Toit, for being my mentor and personal advisor.

Mr. J. Ferreira, for using your lab and knowledge sharing.

Ms. H. Assumption, for the NMR analysis.

Dr. R. Bekker, for helping with the NMR analysis.

I would like to extend my sincere gratitude to my family, colleagues and friends for their support throughout the study.

Chapter 1. Introduction and objectives

1.1 Introduction.

The isolation of polyolefins using various fractionation techniques is a key factor in many polymer institutions since it is a means of simplifying the complex nature of the polymer materials.

The homopolymer samples used in this study were sourced internally from Sasol, whereas the propylene-ethylene random copolymer samples were obtained from an external supplier. All these samples were produced using heterogeneous Ziegler-Natta catalysts but not necessarily of the same kind.

The basis for the present study was to isolate and evaluate the type of fractions generated from various extraction techniques. These extraction techniques differ in their extraction principles. For example, TREF fractionates the polymer according to variation in crystallizability with increasing temperature in a single solvent, while the successive extractions are dependent on a change in solubility in solvents with increasing the boiling points. Xylene and decalin extractions focused mainly on fractions obtained post extraction time at 20 °C [1,2,3,4]. Furthermore, these techniques were correlated with each other in order to determine their relationships.

1.2 Objectives.

The primary aim of this exercise was to differentiate between fractions obtained from xylene and decalin extractions. This is vital since xylene and decalin solubles measurements are used as product release criteria to the market. The extraction results were correlated to the "in-house" routine R21/calculated xylene solubles technique to establish the relationship existing between these measurements.

In addition, a comparison was made between the xylene solubles and successively extracted fractions to assist in elaborating on the molecular make-up of fractions extracted using xylene.

Since random copolymers were employed in the study it was imperative to determine the influence of the various amounts of comonomer incorporation on the chemical and physical properties of the polymers. This is important as comonomers act as chain defects, interrupting chain regularity and thus lowering chain crystallizability [5].

Preparative Temperature Rising Elution Fractionation, which is a more complete fractionation technique, was employed to separate the polymer into various fractions under strictly

controlled conditions. The fractions obtained were compared to the conventionally extracted fractions to establish any potential relationship existing amongst the generated fractions.

1.3 References.

1. Kakugo, M., Naito, Y., Mizunuma, K., and Miyatake, T. *Macromolecular Chemistry*, Volume 190 **(1989)**, pp. 849 - 864.
2. Xu, J., Feng, L., Yang, S. and Wu,Y. *Polymer,* Volume 38 **(1997)**, pp. 4381 - 4385.
3. Feng, Y and Hay, N. *Polymer,* Volume 39, Issue No. 25 **(1998)**, pp. 6589 - 6596.
4. Paukkeri, R. and Lehtinen, A. *Polymer,* Volume 35, Issue No. 8 **(1994)**, pp. 1673 - 1679.
5. Soares, J.B.P. and Anantawaraskul, S. *Journal of Polymer Science: Part B: Polymer Physics*, Volume 43 **(2005)**, pp. 1557 - 1570.

Chapter 2. Historical and theoretical concepts

2.1 Introduction.

In the early 1950's the processes for synthesizing most commodity polymers were established [1,2,3,4]. Semi-crystalline isotactic polypropylene was manufactured commercially following improvements in the catalyst systems. Before this period, polypropylene was just a branched low molecular weight substance no importance. The fundamental developments conducted on catalyst systems over the past five decades played a pivotal role in the making of crystalline polypropylene [1].

The catalyst systems used in the production of polypropylene are known as the heterogeneous Ziegler Natta catalysts [2,5-8]. These catalysts were named after two scientists, namely Giulio Natta from Italy and Karl Ziegler from Germany. They independently performed an extensive amount of work on the polymerization of olefins and in particular towards the achievement of isotactic polypropylene [2]. This work jointly earned them the Nobel Prize in chemistry [1].

Good physical properties inherent to polypropylene are achieved when using heterogeneous catalyst systems and this led to rapid growth in the demand for polypropylene in the market [1]. Heterogeneous catalysts are used in the majority of the polypropylene production plants around the world. The most commonly used type is the multi-sited $MgCl_2$-supported Ti catalyst [2,8-10]. Since the $MgCl_2$-Ti supported catalysts have multiple active sites, they require the addition of internal and external donors during polymerization [8,10].

External donors are added into the polymerization reaction to enhance the catalyst stereospecificity. Catalyst stereospecificity refers to the ability of the catalyst to reproduce the same methyl configuration along the polymer chain [2,3,8,10]. Alkoxy silanes are widely utilized external donors, employed to increase the polymer stereochemistry by poisoning the non-isospecific sites. These donors function on the steric hindrance principle, as the bulky nature of its molecular structure restricts monomer coordination at a specific site on the catalyst. Combination of the catalyst and a alkoxy silane result in the formation of highly isotactic polypropylene [3,5,9,11-13]. Proper selection of the alkoxy silane is critical since it has a significant influence on the product properties [11].

Tacticity is a very important feature in polypropylene since it influences the overall polymer properties. Process parameters such as polymerization temperature and hydrogen concentration do not influence the polymer tacticity as significantly as does changing the alkoxy silane concentration [5].

In practice, the silane/titanium ratio (Si/Ti) is the main parameter utilized to regulate the polymer stiffness-impact balance. Polymer stiffness and Si/Ti ratio have a directly proportional relationship, whereby, if the Si/Ti ratio increases, stiffness also increases. Increased polymer stiffness can be attributed to the increased crystalline regions in a polymer since the alkoxy silane promotes the formation of isospecific sites [1]. However this occurs at the expense of the polymer impact strength.

The chemistry around the polymerization process often leads to the formation of stereoerrors along the polymer chain. Stereoerrors refer to the unsystematic placement of methyl groups along the polymer chains. It is known that none of the polypropylene materials are 100% isotactic [4]. It is therefore important to use donors to control the polymer overall isotacticity.

Resconi et al. [14] gave a description of activities taking place during polymerization leading to the formation of stereoerrors. They further showed that for the transition metal catalysts, polyolefins are produced by multiple insertions of olefins into a metal-carbon bond, which occur through cis opening of the double bond. Although this reference by Resconi et al. [14] deals specifically with the homogenous catalysts, the polymerization mechanism illustrated in Scheme 2.1 also holds for the heterogeneous catalysts.

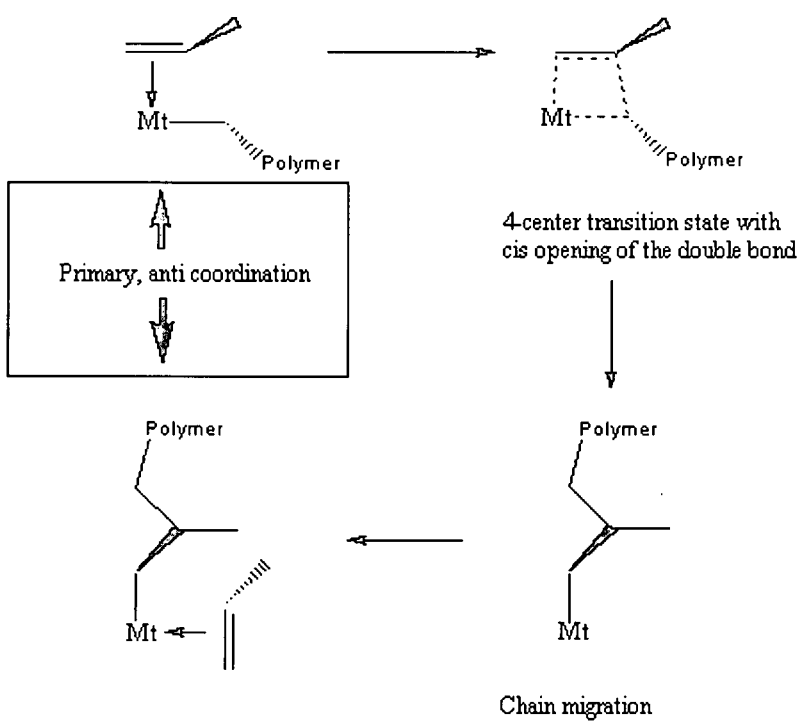

Scheme 2.1. *The basic polymerization mechanism* [14].

The consecutive insertion of the monomers into the polymer chain having the same enantioface produce polymer chains with chiral centers of the same configuration, known as

isotactic polypropylene. However, multiple insertion, whereby methyl groups are alternately placed relative to the polymer backbone, are known as syndiotactic polymer. Random enantioface insertions will produce a polymer chain with no conformational regularity, known as atactic polymer [15, 16].

Figure 2.1 illustrates the possible placement of the methyl groups along the polymer chain.

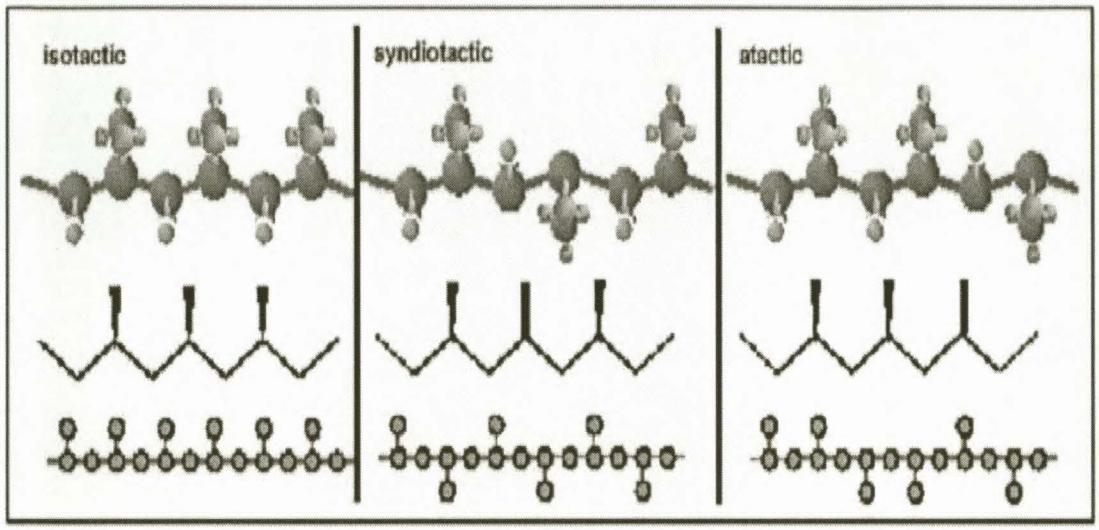

Figure 2.1 *Schematic illustration of the various stereochemical configurations of PP.*

Kukago et al. [8] indicated that, from an industrial perspective, the formation of atactic polymer is a major concern because of its influence on production costs and poor properties of the final products. Semi-crystalline isotactic polypropylene was for some time the only form of significant commercial importance [17]. The advancement in polypropylene production technologies has subsequently enabled the production of syndiotactic and atactic PP on commercial basis, however this is for highly specialized markets and applications.

2.2 Evaluation of polymer microstructure.

^{13}C Nuclear Magnetic Resonance (NMR) spectrometry is often employed to study the microstructure of polyolefins, thus distinguishing between the isotactic and non-isotactic polymer. NMR is currently the only technique that can provide a true reflection of the polymers' subtle microstructural features. Other techniques such as Differential Scanning Calorimetry (DSC) are often utilized to give an indication of the polymer average crystallinity. As a result the NMR is referred to as an absolute technique for the determination of polymer microstructure [6, 18]. The significance of NMR in the characterization of fractionated polymer samples arises from the fact that polymer separation is mainly dependent on stereoregularity. Therefore, its purpose is to differentiate the microstructure of the isolated fractions [19].

Production of polypropylene often results in the polymer comprised of methyl groups having different configurations known as isotactic, atactic and syndiotactic [1]. The formation of the syndiotactic and atactic sequences in the polymer causes a change in the chemical shifts of neighbouring carbon atoms. These chemical shifts are not only affected by stereoerrors but also by regioerrors, which are a deviation from the normal 1,2 or head-to-tail insertions. The resulting regioerrors are known as the tail-to-head and head-to-head misinsertions, or simply as 2,1 and 3,1 units, which are unlikely to occur in the case of heterogeneous catalysts due to the termination step [4].

Polypropylene microstructure has been studied extensively and a significant amount of information that can assist in the spectral interpretation is available in literature. Although polypropylene microstructure has been extensively studied, the information derived from literature should be used with caution since it is dependent on specific experimental conditions [4, 14].

2.3 The effect of controlled rheology processes on polymer properties.

The production of polymer grades of narrower molecular weight distribution (MWD) and higher melt flow index (MFI) values are a function of technology and catalyst systems. Controlled rheology (CR) or vis-breaking processes are often used in the production of grades required with high flow properties.

The CR process utilizes suitable organic peroxides in the extruder to modify the MWD and MFI of the extruded reactor powder [20,1]. MWD is significantly influenced by the catalyst and polymerization process parameters; however it can also be controlled outside the reactor by the addition of organic peroxides [5,21]. Additionally, there are a number of applications that require materials of narrower MWD in order to achieve optimum properties in the final product.

During the vis-breaking step, the polymer is subjected to high levels of shear and heat [20,22]. Figure 2.2 obtained from the testing of Polymers 1 and 3 by GPC illustrate the effect of controlled rheology on the polymer whereby the blue curve represents the MWD of a reactor grade polymer whereas the red curve represents the "vis-broken" polymer. Figure 2.2 is discussed in more detail in Chapter 4 under Section 4.4. The molecular weight (Mw) and MWD are determined by Gel Permeation Chromatography (GPC).

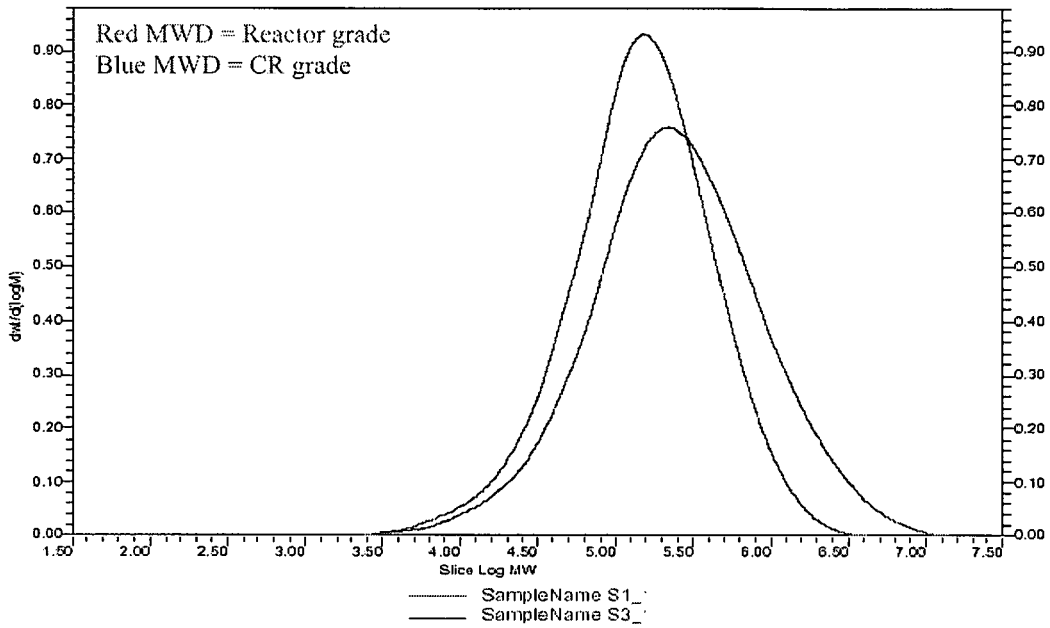

Figure 2.2 *A shift in Mw as result of controlled rheology.*

A shift towards a lower molecular weight occurs as a result of the formation of the highly reactive radicals. The formation of reactive radicals causes the abstraction of hydrogen atoms from the polymer backbone, resulting in the scission of the attacked polymer chain [22].

Canevarolo [20] quoted Beuche in his review article stating that "the probability of chain scission is higher for high molecular weight chains to yield smaller molecules of about half the original size". Controlled rheology grades have several secondary processing advantages over conventional reactor grades. The key advantage is the lower melt viscosity, which means less injection pressure is required to convey the melt for mould filling. Lower melt viscosity refers to a material with a higher melt flow index, capable of filling multi-cavity moulds with relative ease and also reducing secondary processing cycle times [23].

Tzoganakis et al. [24] have also studied controlled degradation of PP during extrusion using peroxide. They have shown that an increase in peroxide concentration induced a decrease in the average molecular weight and polydispersity. This in turn reduced the melt viscosity causing changes in the mechanical properties. The change in properties is dependent on the size of the vis-breaking step and the initial and final MFI. Table 2.1 shows the effect of the starting MFI and the peroxide concentration in the formulation [1].

Table 2.1 *The effect of the starting MFI and peroxide concentration on the final MFI of controlled rheology grades* [1].

	Starting MFI (g/10min)		
	0.8	3.5	12
Peroxide concentration (%)	**Final MFI (g/10min)**		
0.013	Not measured	Not measured	26
0.025	Not measured	17	44
0.05	8	33	58
0.075	14	51	74
0.1	33	64	Not measured
0.125	37	Not measured	Not measured

The base MFI, also referred to as the starting MFI, and peroxide concentration are critical in ensuring the achievement of the desired final MFI value.

Table 2.2 indicates some applications of polypropylene homopolymers based on average molecular weight.

Table 2.2 *Applications of PP homopolymers according to molecular weight* [1].

Mw (g/mol)	Application/Processing
<40 000	Wax, toner, pigment batch
100 000 – 125 000	Melt blown fibres
150 000 – 300 000	Injection moulding, fibres
250 000 – 500 000	Extrusion, blow moulding, tapes
>400 000	High melt strength, starting material for controlled rheology PP.

2.4 Copolymerization.

Copolymerization is defined as a process whereby two or more different monomers are incorporated into the same polymer [25]. It is a means of producing polymers with properties that are not achievable through homopolymerization. Polymer morphology, properties and consequently the final product applications are dependent on the copolymer composition [6].

Various types of copolymers are obtainable, for example, random and block copolymers. Their production depends on the amount of comonomer and the manner in which it is incorporated into the polypropylene backbone [1,6,26]. In this study, focus will be on the propylene-ethylene random copolymers. The primary reason for the production of random copolymers is to achieve improved optical properties [21, 26-28].

The comonomer insertion in polypropylene does not only affect the percentage crystallinity of the materials, but it also has an influence on the melting properties of the polymer. The comonomer inserted in polypropylene chains result in a melting temperature depression of the polymer [21,29]. Flory pointed out that the component, which causes depression in the melting point, might be part of the polymer chain such as the non-crystallizable comonomer unit [30]. Figure 2.3 clearly shows the influence of various amounts of comonomer incorporation on the polymer melting temperature. As comonomer content increases the melting temperature decreases.

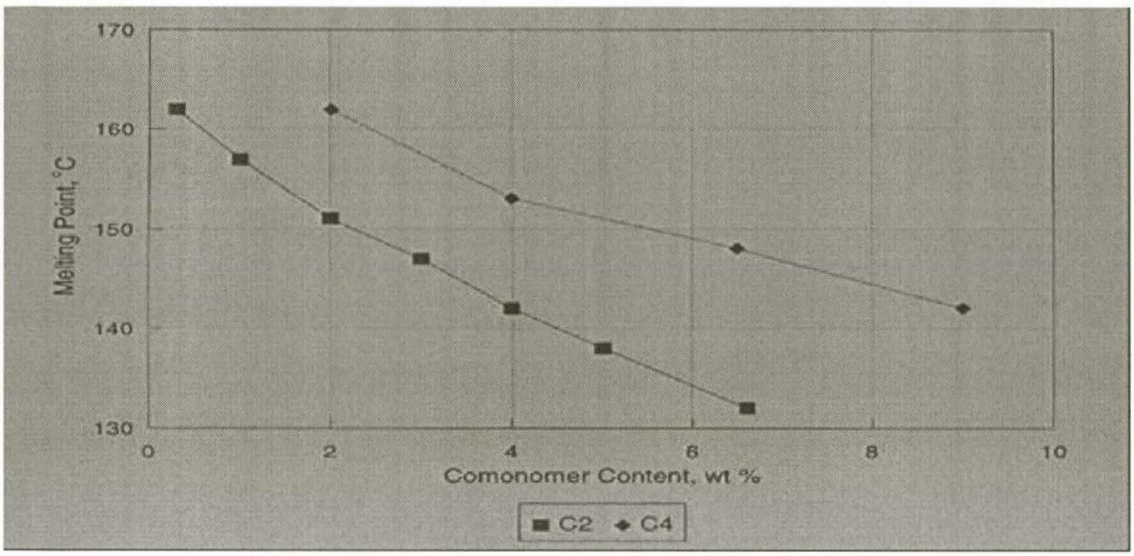

Figure 2.3 *The effect of comonomer content on the polymer melting temperature for propylene/olefin copolymers* [1].

The percentage crystallinity of polypropylene homopolymers and copolymers may be determined by DSC, by measuring the area under the peak melting curve. This is significantly affected by comonomer incorporation into the backbone of the polymer chain. The percentage crystallinity calculation (for propylene/ethylene copolymers) is based on a theoretical value for the heat of melting of 209 J/g for 100% crystalline polypropylene, and heat of melting obtained from the DSC [21]. The measured heat of melting is used in relationship to that of 100% crystalline PP (theoretically 209 J/g) to give the percentage crystallinity of the sample.

Additionally, the disruption in crystallinity by the comonomer leads to an increase in the formation of the non-crystalline regions within the polymer matrix. Materials having low or no crystallinity are soluble in specific solvents at specific temperatures. Figure 2.4 shows that the percentage of xylene soluble material of the polymer increases as the melting temperature decreases.

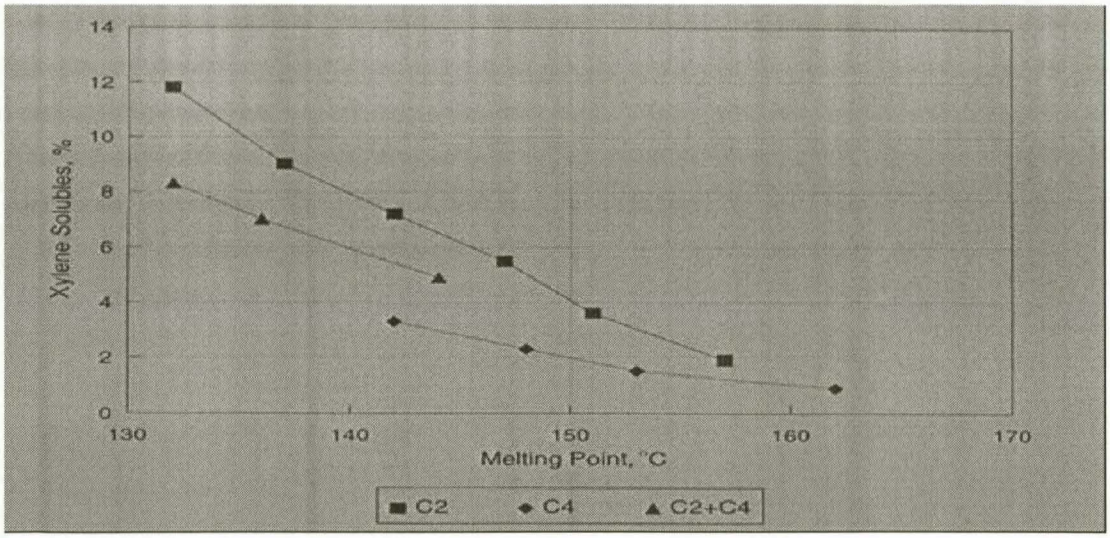

Figure 2.4 *The correlation of the melting temperature and xylene soluble percentage of the copolymer materials* [1].

The graph shown in Figure 2.4 indicates that polymers with lower melting temperature have a higher percentage of xylene soluble material. This shows that there are increased amounts of non-crystalline material resulting from the propylene sequences disrupted by the inserted comonomer. The types of comonomer used in copolymerization reactions affect the overall polymer properties differently. In this case, when the ethylene and butene copolymers are compared at about 4% xylene solubles, the ethylene copolymer has a higher melting temperature. This means that with copolymers, the percentage xylene solubles is not necessarily directly related to the melting temperature.

A linear decrease in the melting temperature is observed as the xylene solubles increases. This observation is consistent for all the comonomers constituting the graph.

2.5 Solvent extraction techniques.

Polymer materials are regarded as complex entities distributed in more than one direction of molecular heterogeneity [31]. To fully understand and explain the microstructure of the polypropylene and other polymers, it is important to isolate them into homogeneous fractions through solvent extractions and fractionation techniques [8,10,12,19,26,32-36].

Natta et al. [37] were among the first people to perform a separation of polypropylene according to stereoregularity. They used Soxhlet type apparatus, solvents of increasing boiling points, and conventional extraction techniques [2,19,32,38]. In this study, similar conventional extraction techniques were used in the xylene and decalin solvent extraction. The n-alkane solvents namely hexane and heptane were used in the successive extractions. The basis for successive extractions is the increasing boiling points of the solvents.

Luigi Cerruti stated in his review article that; "On the 11th March 1954, Paolo Chini fractionated the reaction product by boiling solvent extraction. He obtained three fractions, the last of which was a highly crystalline, high melting white powder. The very next day Paolo Corradini obtained a diffraction pattern from a sample stretched five times its length, and the pattern confirmed a high degree of crystallinity" [2]. These findings indicated the significance of extraction techniques and the type of information generated from such experiments regarding the polymer's chemical and physical composition.

Guilio Natta's group made important findings that led to the definition of polypropylene's different stereoregularities namely isotactic, syndiotactic and atactic polypropylene. Atactic polymer was defined as a polymer which is soluble in boiling ether, syndiotactic polymer as a polymer which is insoluble in boiling ether but soluble in boiling heptane, and finally isotactic polymer which is insoluble in both boiling ether and boiling heptane [19].

Fractional extraction methods were and are still widely used in polymer research. There are four basic requirements to be satisfied regarding the extraction and fractionation techniques:

1. The experiments must be fairly simple.
2. The apparatus must be user friendly and versatile enough to accommodate modifications.
3. The experimental period should be feasible for routine analysis.
4. Isolation of the molecules must occur according to stereoregularity and not on the basis of molecular weight.

Solvents of different physical and chemical properties were screened to determine their effectiveness in separating polymers into various fractions. The solvent selection criteria were based on differences in boiling points, solvating power and toxicity levels. For the conventional solvent extraction technique, decalin, tetralin and xylene were screened. From the solvent screening tests xylene emerged as the most preferred solvent. The choice of solvent was largely dictated by the economics, health implications and solvating power [19].

With the successive extractions, boiling points of n-alkane hydrocarbon solvents were the determining factor for the type of solvent to be used. The solvents that are mainly used in successive extractions are pentane, hexane, heptane and octane [10,36]. Although more advanced fractionation techniques such as Temperature Rising Elution Fractionation (TREF) and Crystallization Analysis Fractionation (Crystaf) are available today, the conventional extraction techniques are still an integral part of the analytical techniques used in industries and academic institutions. TREF and Crystaf are techniques that yield a lot of molecular information, but they are costly to perform [39].

Polymer solubility in a solvent chosen to conduct extractions is vital since the solubility determines the effectiveness of polymer separation. When the solvent fails to dissolve and

isolate the polymer into different fractions an alternative solvent of better solvating power should be tried. Polymer solubility depends on both the physical properties and chemical structure such as the molecular weight, branching and crystallinity. Additionally, inter- and intramolecular forces holding the polymer together highly influence the polymer solubility [10].

2.5.1 Xylene extractions.

The xylene extraction technique is temperature sensitive and the xylene soluble and insoluble test results are specific to particular techniques. Mingozzi et al. [36] provided a brief description of the xylene extraction procedure used in their study.

An undisclosed amount of the weighed polymer sample was dissolved in xylene solvent at 135 °C. The solution concentration was 1 g/dL and no antioxidants were added into the solvent to stabilize the polymer against heat. The extraction process continued for one hour. After extraction time elapsed, the solution was cooled down under controlled conditions to 25 °C and the insoluble fractions precipitated out of the solution. The insoluble fraction and solution were separated by means of filtration using filter paper. After the filtration, an aliquot of the solution was evaporated to dryness at 140 °C. A layer of the xylene soluble fraction remained on the inside of the evaporating dish. The soluble fraction was transferred into the vacuum oven at 70 °C to dry [40]. After drying it was then cooled down and weighed.

Kakugo et al.[8] did a similar experiment as part of their study, however the cooling to a set point differed slightly. Kakugo cooled the solution down to 20 °C and not 25 °C. The cooling process in the solvent extraction experiments is critical and should be kept constant to ensure homogeneity in the fractions obtained at that particular temperature. The variance between these two cooling points is significant; therefore the fractions generated are more likely to be different.

2.5.2 Successive extractions.

Polypropylenes produced from heterogeneous catalysts are a mixture of materials, varying in stereoregularity from highly isotactic to almost completely atactic. Successive extractions are an effective technique used to separate the polymer into simple homogeneous fractions using solvents of increasing boiling points [9]. A brief outline of the successive extraction technique and a schematic diagram are illustrated.

A polymer sample weighing 10 g was dissolved in 1 liter boiling xylene in an unspecified period. After extraction the solution was cooled down to 20 °C over a period of four hours. This approach causes less crystallizable polymer to deposit on the outer shell of the precipitate, leading to satisfactory extraction. The precipitate was extracted successively with higher boiling point hydrocarbon solvents in a Soxhlet extractor. The types of fractions

obtained from these experiments were the fraction insoluble in xylene at 20 °C, a fraction soluble in boiling hexane, and fractions soluble or insoluble in boiling heptane [10].

The schematic diagram of the successive extraction is shown in Scheme 2.2 to illustrate the experimental process followed.

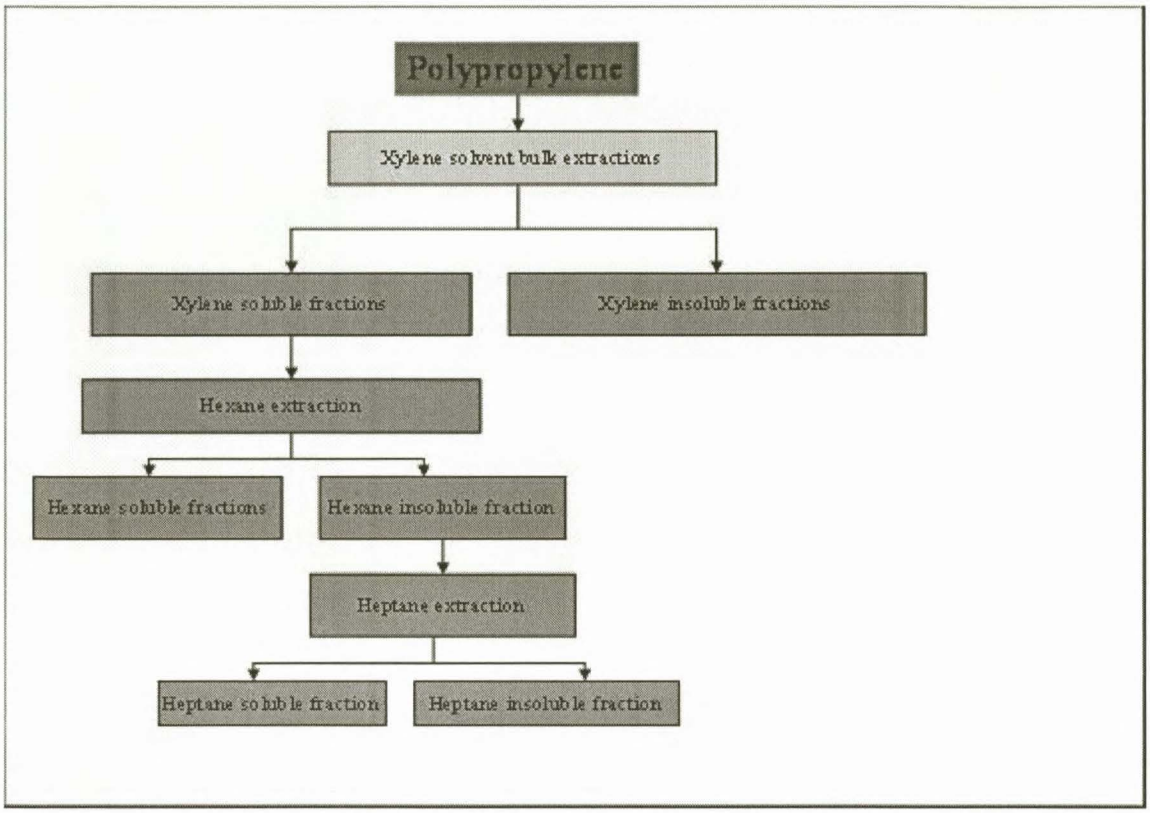

Scheme 2.2 *The successive extraction flow diagram.*

The bulk extraction step in the scheme is optional. However; it is beneficial since it is used to generate sufficient extraction test material for successive extractions. It is difficult to successively extract pellet samples when using the Soxhlet extractor because of poor polymer/solvent interaction and a reduced surface area. Normally, the successive extractions are performed on the reactor powder or ground pellets. In this study a slightly different approach was followed whereby the successive extractions were done on fractions extracted by xylene from the bulk polymer material.

The material obtained by xylene extraction from the bulk polymer were further extracted using hexane, and two fractions namely the hexane soluble and insoluble fractions were obtained. The hexane insoluble fraction was extracted further using heptane solvent. Also two different fractions were obtained, namely the heptane soluble and insoluble fractions. If further extraction on the insoluble fraction was necessary then a hydrocarbon solvent of higher boiling point such as octane could have been used.

The fractions obtained from the successive extractions are used to elucidate the polymer molecular composition. In this case, it is inappropriate to compare the successive extraction results of the xylene bulk extracted fractions with the reactor powder and ground pellets due to the significant differences in the nature of the samples.

2.5.3 Temperature rising elution fractionation (TREF).

Polymer characterization techniques are improved on a continuous basis to enhance the understanding of polymer properties and chemical composition. TREF is currently amongst the techniques in the forefront of modern polymer characterization [39].

A number of people contributed towards the development of TREF. Spiegels and Desreux were the first to describe the functioning of TREF in the 1950's. Wild and Ryle continued with the development work on this technique in the 1970's until they established the analytical TREF used in polyolefin industries [33]. Even though a significant amount of work was done on TREF by other scientists, Shirayama et al. [34] were the first to use the term TREF.

TREF is a separation technique for fractionating crystallizable polymers. The separation mechanism is based on the polymer crystallizability [40,41]. Initially, TREF was used to fractionate and elucidate the structure of low density polyethylene (LDPE) and linear low density polyethylene (LLDPE), however its application has now extended to PP [33].

TREF is a two-step process consisting of precipitation and elution steps [42]. In TREF, the sample is first dissolved in a suitable solvent at high temperature and the solution is then introduced into a column containing glass beads or other stationary phase. This is followed by a crystallization step at slow cooling rate, during which the polymer layers of increasing crystallinity are deposited on the glass beads [33]. This completes the first temperature cycle, which is referred to as the crystallization cycle. This phenomenon results in the formation of an onion-layer type structure [43].

In the second step, a solvent flows through the column while the temperature is steadily increased. The polymer precipitated in the first step will then be eluted. The concentration of the polymer eluted at each elution temperature is monitored with a mass sensitive detector [42].

TREF has been developed for both analytical and preparative fractionations over the last 40 years [31]. There are two distinct types of TREF systems, namely analytical and preparative TREF. Table 2.3 outlines the differences between the two systems.

Table 2.3 *Comparison between the analytical and preparative TREF* [43].

Preparative TREF	Analytical TREF
1. Fractions are collected at pre-determined temperature intervals. 2. Information about molecular structure is obtained off-line by additional analytical techniques. 3. Requires larger columns and larger sample sizes. 4. Time consuming but can generate detailed information about polymer microstructure.	1. Continuous operation. 2. Information about molecular structure is obtained on-line by means of a calibration curve. 3. Require smaller columns and smaller sample sizes. 4. Faster than preparative TREF but generates less information about polymer microstructure.

The crystallizability of PP is mainly dependent on stereoregularity and regioregularity and almost independent of the molecular weight. Thus, TREF curves are able to reflect the tacticity distribution of PP [41]. This technique relies on the ability of molecules with different composition to crystallize to a different extent and at different temperatures [44].

The schematic representation of TREF is shown in Figure 2.5, where (a) is the crystallization of the polymer solution in the stationary phase. The (b) part of the diagram illustrates the elution step.

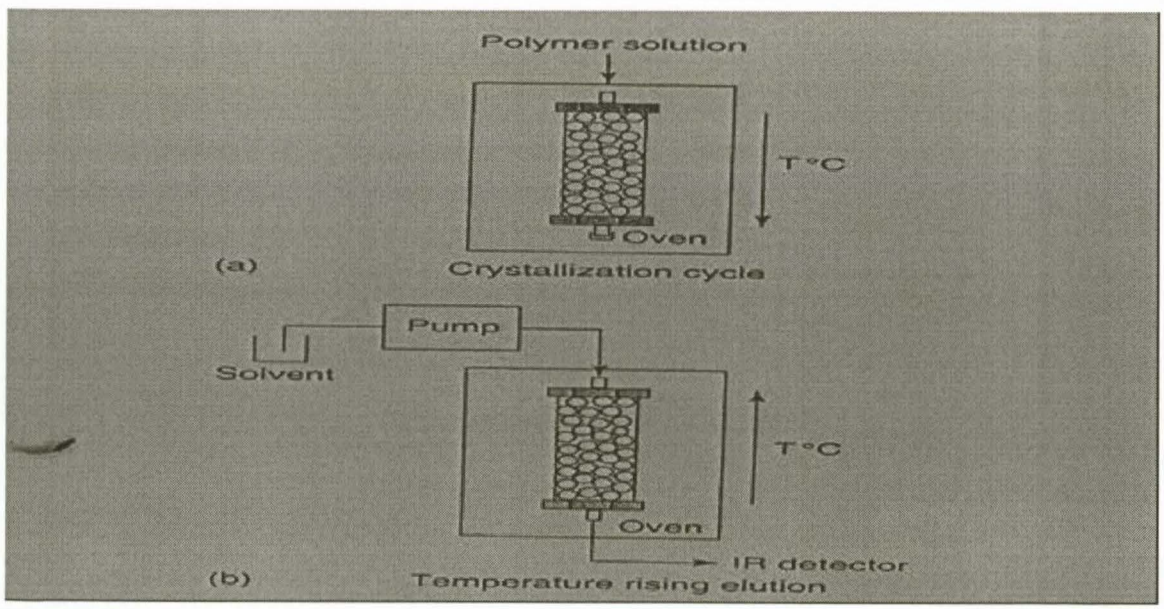

Figure 2.5 *A schematic diagram of TREF.*

In most papers published on this subject to date, the emphasis was mainly on the microstructures of the fractions eluted at higher temperature. However, these fractions are highly isotactic and lesser stereodefects are present along their polymer chains. Consequently, little information can be obtained from such fractions. On the other hand, it

should also be noted that for copolymers, the comonomer content units in the copolymer must be limited to low levels, since a large amount of comonomer units lead to an amorphous copolymer thus rendering TREF ineffective.

There are far fewer publications reporting on the TREF of propylene copolymers compared to LLDPE and propylene homopolymer. In propylene copolymers, composition distribution and sequence distribution must be taken into account besides tacticity distribution, because all of them affect the crystallinity of copolymers [41]. Therefore, alternative methods, including fractionation methods in differential scanning calorimetry (DSC), have been considered [39].

2.6 References.

1. Moore, Jr, E.P. *Polypropylene Handbook*. **(1996)** New York, Hanser/Garner.
2. Cerruti, L. *International Journal for Philosophy of Chemistry*, Volume 5, No.1 **(1999)**, pp. 3 – 41.
3. Viville, P., Daoust, D., Jonas A.M., Nysten, B., Legras, R., Dupire, M., Michel, J and Debras, G. *Polymer*, Volume 42 **(2001)**, pp.1953 – 1957.
4. Busico, V. and Cipullo, R. *Progress in Polymer Science*, Volume 26 **(2001)**, pp. 443 – 533.
5. Hungenberg, K.D. and Kersting, M. *New Advances in Polyolefins*, **(1993)**, pp. 31 - 45.
6. Faldi, A. and Soares, J.B.P. *Polymer,* Volume 42 **(2001)**, pp. 3057 - 3066.
7. Lovisi, H., Tavares, M.I.B., da Silva, N.M., de Menezes, S.M.C., de Santa Maria L.C. and Coutinho, F.M.B. *Polymer,* Volume 42 **(2001)**, pp. 9791 – 9799.
8. Kakugo, M., Miyatake, T., Naito, Y. and Mizunuma, K. *Macromolecules,* Volume 21 **(1988)**, pp. 314 – 319.
9. Xu, J., Yang, Y., Feng, L., Kong, X. and Yang S. *Journal of Applied Polymer Science,* Volume 62 **(1996)**, pp. 727 - 731.
10. Kakugo, M., Naito, Y., Mizunuma, K. and Miyatake, T. *Makromol. Chemistry,* Volume 190 **(1989)**, pp. 849 – 864.
11. Chadwick, J.C., Morini, G., Balbontin G., Camurati, I., Heere, J.J.R., Mingozzi, I. and Testoni, F. Macromol. *Chem. Phys.,* Volume *202* **(2001)**, pp. 1995 – 2002.
12. Xu, J., Feng, L., Yang, S. and Wu,Y. *Polymer,* Volume 38 **(1997)**, pp. 4381 – 4385.
13. Kakugo, M., Miyatake, T., Mizunuma, K. and Kawai, Y. *Macromolecules,* Volume 21 **(1998),** pp. 2309 – 2313.
14. Resconi, L., Cavallo, L., Fait, A. and Piemontesi, F. *Chemical Reviews,* Volume 100 **(2000)**, pp. 1253 – 1345.
15. Covezzi, M. and Mei, G. *Chemical Engineering Science,* Volume 56 **(2001)**, pp. 4059 – 4067.
16. Zhang, M., Lynch, D.T. and Wanke, E.S. *Journal of Applied Polymer Science,* Volume 75 **(2000)**, pp. 960 – 967.
17. Virkunen, V., Laari, P., Pitkanen, P. and Sundholm, F. *Polymer,* Volume 45, Issue 14 **(2004)**, pp. 4623 – 4631.
18. Kawamura, H., Hayashi, T., Inoue, Y. and Chujo, R. *Macromolecules,* Volume 22 **(1989)**, pp. 2181 – 2186.
19. Kamath, M. and Wild, L. *Polymer Engineering and Science*, Volume 3, Issue 6 **(1966)**, pp. 213 – 216.
20. Canevarolo, S.V. *Polymer Degradation and Stability,* Volume 70, Issue 1 **(2000)**, pp. 71 – 76.
21. Faldi, A. and Soares, J.B.P. *Polymer,* Volume 42 **(1998)**, pp. 6589 – 6596.
22. Busico, V., Cipullo, R. and Caporaso, L. *Macromolecules,* Volume 31 **(1990)**, pp. 2387 – 2390.

23. www.tangram.co.uk
24. He, S., Costeux, P., Wood-Adams and Dealy, J.M. *Polymer,* Volume 44, Issue 23 **(2003)**, pp. 7181 – 7188.
25. Mark, H.F., Bikales, M.N., Overberger, C.G. and Menges G. *Encyclopaedia of Polymer Science and Engineering,* Volume 4 **(1985)**, pp. 192.
26. Fan, Z., Zhang, Y., Xu, J., Wang, H and Feng, L. *Polymer,* Volume 42, Issue 13 **(2001)**, pp. 5559 – 5566.
27. Schwarz, O. *Polymer Materials Handbook, **(1995)***, The Natal Witness Printing and Publishing Company (Pty) Ltd.
28. Anantawaraskul, S., Soares, J.B.P., Wood-Adams, P and Monrabal, B. *Polymer*, Volume 44, Issue 8 **(2003)**, pp. 2393 – 2401.
29. Tanaka, N. *Polymer,* Volume 22 **(1981)**, pp. 647 – 648.
30. Kemp, A.R., Brown, D.S., Lattman, M. and Li, J. *Journal of Molecular Catalysis A: Chemical,* Volume 149, Issue 1-2 **(1999)**, pp. 125 – 133.
31. Pasch, H. *Advances in Polymer Science,* Volume 150 **(2001)**, pp. 1 – 60.
32. Mirabella Jr., F.M. *Journal of Liquid Chromatography*, Volume 17, Issue14 and 15 **(1994)**, pp. 3201 – 3219.
33. Monrabal B. *Journal of Applied Polymer Science,* Volume 52 **(1994)**, pp. 491 – 499.
34. Wild, L. *Advances in Polymer Science,* Volume 98 **(1990)**, pp. 1 – 47.
35. Wild, L., Ryle, T.R., Knobeloch, D.C. and Peat, I.R. *Journal of Polymer Science,* Volume 20 **(1982)**, pp. 441.
36. Mingozzi, I., Cecchin, G. and Morini, G. *International Journal Polymer. Analysis and Characterization,* Volume 3 **(1997)**, pp. 293 – 317.
37. Moore, W.R. and Boden, G.F. *Journal of Polymer Science*, Volume 9 **(1965)**, pp. 2019 – 2029.
38. Paukkeri, R. and Lehtinen, A. *Polymer,* Volume 35, Issue No. 8 **(1994)**, pp. 1673 – 1679.
39. Chen, F., Shanks, R.A. and Amarasinghe. *Polymer,* Volume 42 **(2001)**, pp. 4579 – 4587.
40. Virkkunen, V., Laari, P., Pitkanen, P. and Sundholm, F. *Polymer*, Volume 45, Issue 9 **(2004)**, pp. 3091 – 3098.
41. Xu, J. and Feng L. *European Polymer Journal,* Volume 36 **(2000)**, pp. 867 – 878.
42. Anantawaraskul, S., Soares, J.B.P. and Wood-Adams P. *Journal of Polymer Science: Part B: Polymer Physics,* Volume 4 **(2003)**, pp. 1762 – 1778.
43. Soares, J.B.P. and Hamielec, A.E. *Polymer,* Volume 36 **(1995)**, pp. 1639 – 1654.
44. Feng, Y and Hay, N. *Polymer,* Volume 39, Issue No. 26 **(1998)**, pp. 6723 – 6731.

Chapter 3. Experimental

3.1 Introduction.

A series of commercial polypropylene homopolymer and propylene-ethylene random copolymer samples were used in this study. These materials are produced from two different production technologies. The homopolymer samples were sourced in-house (Sasol) whereas the copolymers were obtained from another polypropylene polymer supplier.

3.2 Materials.

3.2.1 Solvents for extraction.

The extraction studies were conducted using o-xylene, boiling point (bp.) = 135 °C, decalin, bp. = 185 °C, n-hexane, bp. = 69 °C and n-heptane, bp. = 98 °C. All these solvents were supplied by Merck Chemicals (Pty) Ltd.

3.2.2 Polymers.

Five propylene-ethylene random copolymer samples of varying ethylene content, and four different homopolymer samples were used in the study.

3.3 Characterization.

3.3.1 Instruments.

There are certain in-house routine tests that were performed on the study materials. The routine analyses performed were melt flow index (MFI) measurements on a Thermo Haake melt flow indexer, and R21 values and calculated xylene solubles on the Bruker Minispec Nuclear Magnetic Resonance (NMR) spectrometer. The R21 value is an in-house measurement that determines the ratio between the atactic and isotactic regions in the polymer. Ethylene content was determined on Perkin Elmer 1600 Series Fourier Transform Infrared (FTIR) spectrometer.

The polymer samples and the extracted fractions were characterized using the following analytical instruments:

- TA Instruments 2920 Modulated Differential Scanning Calorimeter (DSC) was utilized to determine thermal properties of the samples.
- Varian ^{UNITY}INOVA® Nuclear Magnetic Resonance (NMR) spectrometer was used for polymer microstructural evaluations.

- Waters Alliance GPC V2000 Gel Permeation Chromatograph (GPC) was used to determine the weight average molecular weight (Mw), number average molecular weight (Mn) and molecular weight distribution (MWD).

3.4 Methods.

3.4.1 Determination of ethylene content.

The pellet samples analyzed for ethylene content were pressed into a film using a Graseby Specac press at a temperature of 180 °C and a pressure of 2 Bar. Film thickness was controlled using spacers. The pressed film was cooled down to room temperature before determining the ethylene content. A hot scan of 120 °C was performed on the FTIR equipped for ATR analysis to give the peak height. The ethylene content was calculated as follows:

Ethylene content = (peak height/sample thickness) / calibration slope
The calibration slope is established using copolymer samples of linearly increasing ethylene contents referencing the ethylene peak at approximately 732 cm^{-1}.

3.4.2 Determination of melt flow index.

The melt flow index was determined on the semi-automated Thermo Haake melt flow indexer. 5 grams of the polymer sample was placed into the heated barrel at 230 °C and pre-heated for a specified time to melt the pellets. Then, the dead weight piston of 2.16 kg was placed on top of the molten polymer to extrude it through the die orifice. Subsequently, the instrument measured the flow rate at specific time intervals as the extrudate comes out of the die.

3.4.3 Determination of R21 values and calculated xylene solubles.

The R21 values measured on the Minispec NMR were converted to calculated xylene solubles. The conversion is performed with the aid of a calibration curve established from the xylene extraction technique using polymers covering a range of xylene solubles. First, samples were conditioned in a vacuum oven for fifteen minutes at 120 °C to remove moisture and volatiles from the polymer. The samples were then transferred into a dry metal bath for thirty minutes at a temperature of 50 °C. Following the conditioning step, the sample was inserted into the magnetic probe to give the R21 reading.

3.4.4 Determination of the thermal properties.

A polymer sample of 5 mg was heated to 220 °C and held at that constant temperature for one minute to remove the sample's thermal history. The sample was then cooled down at a rate of 10 °C/min to 30 °C for the determination of the crystallization properties. It was then heated up again at a rate of 10 °C/min to 190 °C for the determination of the melting properties. The peak midpoints were quoted for the melting temperatures.

3.4.5 Determination of Mw, Mn and MWD.

A solution of 0.1% (w/v) was prepared by dissolving a polymer in a solution of trichlorobenzene/butylhydroxytoluene, (TCB/BHT (0.13% stabilizer)) at 150 °C for 3 hours. The sample was filtered into vials and placed in a carousel at 145 °C and analyzed under the following conditions:
Column temperature: 145 °C
Injector temperature: 145 °C
Solution temperature: 50 °C
Flow rate: 1 mL/min
The injection volume was set at 300 µl. Waters Styragel HT 3, HT 4, HT 5 and HT 6 columns were used. The GPC instrument was equipped with the refractive index (RI) detector. Easical polystyrene standards were utilized to calibrate the instrument.

3.4.6 Determination of polymer tacticity using ^{13}C NMR.

Quantitative ^{13}C NMR experiments were performed at 125 MHz on 5 mm pulsed field gradients (PFG) switchable/broadband probe on a Varian ^{UNITY}INOVA 500 MHz spectrometer at 130 °C.

Typically, 60 mg of polymer sample was dissolved in 0.6 mL deuterated tetrachloroethane (d-TCE) stabilized with di-tertiary butyl paraCresol (DBpC).
The polymer dissolution was performed in two steps:
First, only 0.3 mL of the solvent was added to the polymer in the NMR tube. The sample and the solvent were heated up using a heat gun to dissolve the polymer. This was to ensure that the polymer did not settle at the bottom of the NMR tube. Second, the remaining 0.3 mL of the solvent was added into the NMR tube and as a result the polymer was well dispersed in the solvent.

The NMR tube containing the solution was sealed with Teflon® tape and placed in a ventilated oven at 140 °C to homogenize for about two hours.

A 90° pulse width of 6 μs and delay time between pulses of 15 s were used with an acquisition time of 1.8 s. The number of scans was set at 2400 and the signal-to-noise parameter was at 750. Either the 2400 scans were acquired or the signal-to-noise ratio was reached. The analysis time ranged from 3 to 10 hours. Chemical shifts were referenced internally to the main backbone methylene carbon resonance (30 ppm).

3.5 Xylene extractions.

The xylene solvent extractions were performed under controlled conditions on various polypropylene grades to isolate and evaluate the extractable materials. A recently optimized xylene extraction technique was used in this study to enhance our understanding of polypropylene homopolymers and propylene-ethylene random copolymer properties and their microstructure [1].

3.5.1 Equipment.

- 1 L three-necked round bottom flask
- Overhead mechanical stirrer
- Cooler condenser
- Heating mantle
- Aluminium pots
- Evaporating dish
- Water bath
- Vacuum oven
- Analytical balances
- 100 mL and 500 mL measuring cylinders
- 15 cm diameter filter paper
- Glass funnel
- Stop watch

Care was taken with the handling of solvents and hot equipment. All experiments were carried out in well-ventilated areas.

3.5.2 Methods.

Precisely 500 mL of xylene was poured into a 1 liter three necked round bottom flask fitted with an overhead mechanical stirrer and condenser. This unit was placed on a heating mantle and water was allowed to circulate through the condenser before the heating was initiated.
The solvent was heated for fifteen minutes while stirring. 5 g of polymer sample was then added into the flask containing the hot agitated solvent. Caution was exercised during the sample addition into the flask to ensure that no polymer adhered to the walls of the flask. The

temperature was raised to the boiling point of xylene (135 °C). This temperature was maintained for two hours to ensure a complete dissolution of the polymer in the solvent.

After the dissolution process, the heating mantle was removed and replaced by an ice water bath. This was necessary to cool the solution to 5 °C within twenty minutes, whilst stirring. The bulk of the dissolved polymer started to precipitate during the cooling process. Once the 5 °C temperature was reached, the ice water bath was removed and replaced with warm water to raise the solution temperature to 20 °C within twenty minutes.

The solution was filtered to separate the soluble fractions and the insoluble fractions. 100 mL of the solution was filtered into a 100 mL measuring cylinder through the filter paper placed on a glass funnel. The filtered aliquot was then transferred into an evaporating dish of predetermined mass and then placed on the heated water bath to evaporate the solvent.

After the completion of the evaporation process, the evaporating dish and the polymer soluble fraction residual were transferred into the oven set at 105 °C. The soluble fractions were kept in an oven for one hour, to remove any residual solvent. Subsequent to the drying process, the dish was transferred from the oven into a desiccator to cool down the soluble fraction to room temperature.

The quantitative determination of xylene soluble fractions was calculated as follows:
Calculation:
$\%Xs = (g \times 500)/ (V \times G)*100$

Where: %Xs = xylene solubles in percentages
g = mass of the solvent soluble material (g)
G = sample mass (g)
V = volume of the aliquot (mL)
500 = volume of the solvent (mL)

3.5.3 Decalin extractions.

The method used to perform decalin extractions was similar to that used for the xylene extraction. The decalin extractions were done at 185 °C instead of 135 °C, which is the extraction temperature used in the xylene solvent extractions.

3.6 Bulk extractions.

The bulk extractions were performed using xylene to generate sufficient extractable materials to use in the successive extractions. Interest was mainly on the production of sufficient quantities of the xylene soluble fractions. There were two key parameters that were amended

from the conventional xylene solvent extraction method and these were solvent volume and sample mass.

The solvent volume changed from 500 mL to 750 mL whereas the sample mass was changed from 5 g to 15 g. The quantitative measurements of fractions were not essential in the bulk extractions exercise. Therefore, the intention of using more solvent and polymer material was only to generate as much xylene soluble material as possible. All other extraction conditions outlined in the xylene solvent extraction technique were adhered to.

Since the bulk extractions were conducted for qualitative purposes, the evaporation step was not performed in an evaporating dish of predetermined mass, but in a round bottom flask connected to the rotary evaporator. The rotary evaporator was used to accelerate solvent evaporation. After solvent evaporation, it was found that the polymer adhered onto the walls of the flask and thus acetone was used to remove it. The soluble fraction was kept in fume a hood with an extraction fan to dry over night.

3.7 Successive extractions.

3.7.1 Hexane extractions.

The successive or consecutive extractions conducted in this study used hydrocarbon solvents of increasing boiling points (hexane and heptane). These were used to successively extract the xylene soluble fractions obtained from the extraction of the bulk material with xylene and in so doing obtaining more homogeneous fractions. Successive extractions were performed on a Soxhlet type extractor.

The dried xylene soluble fraction was placed in a thimble plugged with glass wool to prevent the floating and spilling over of the test material during the extraction process. The thimble and the sample were inserted into the reflux condenser and then connected to a 250 mL round bottom flask containing 150 mL of hexane solvent. A cooler condenser was also mounted on the reflux condenser to prevent solvent evaporation; therefore water was continuously circulated during the extraction process.

The extraction process took place for eight hours at 90 °C under controlled temperature conditions. The Soxhlet system was heated up with the aid of silicon oil placed in a glass bath on a hot plate with built in magnetic stirrer. The temperature controller probe was permanently inserted in the heated oil during the extraction process to ensure that the 90 °C extraction temperature was maintained throughout the experiment.

After eight hours of extraction, the extraction unit was removed from the heated oil to cool down to room temperature before dismantling the Soxhlet unit. Once the unit was at room

temperature the solvent was recovered and evaporated on at rotary evaporator. The thimble with the hexane insoluble fraction was removed from the reflux condenser and placed in the fume hood for four hours to dry.

After the hexane solvent was evaporated, the hexane soluble fraction sticking on the walls of the round bottom flask was removed with the aid of acetone. This was followed by a drying step prior to characterization.

3.7.2 Heptane extractions.

The thimble, hexane insoluble fraction and new glass wool were placed in a clean Soxhlet extraction unit. A clean 250 mL round bottom flask containing 150 mL of heptane solvent was connected to the extraction unit. The extraction unit was then placed in the silicon oil bath, which was heated at 120 °C using the hot plate with a magnetic stirrer.

The extraction process continued for eight hours. After eight hours of extraction the unit was removed from the oil bath and allowed to cool down to room temperature. The solvent was then recovered and removed on the rotary evaporator. After all the solvent was evaporated the heptane soluble fraction was also found to stick on the walls of the round bottom flask and thus it was removed using acetone. The heptane soluble fraction was allowed to dry before it was analyzed.

3.8 Preparative Temperature Rising Elution Fractionation (TREF).

A polymer sample weighing 5 g was dissolved in 400 mL boiling xylene using the Holtrup Preparative TREF. The dissolved polymer was precipitated by cooling the solution linearly to 25 °C at rate of 6 °C/hr using programmable thermostat. The TREF used in the study does not use any inert stationary phase.

The precipitated polymer was introduced into the fractionation vessel and was heated up to 40 °C to elute the first fraction. The first fraction to be eluted was the least crystalline fraction. The polymer in solution is discharged through the lower drainage valve, whereas the more crystalline polymer remains in the fractionation vessel.

About 800 mL of acetone was poured into the solution eluted from the fractionation vessel to precipitate the polymer. The precipitated polymer was then filtered on a Buchner-funnel (glass frit No.3) and washed with acetone. The isolated polymer fraction was dried for 24 hours at 60 °C in vacuum a oven and then weighed after cooling down to room temperature.

Subsequent fractions were obtained in a similar fashion, at increasing elution temperatures.

3.9 References.

1. Kotsokoane, M. *The method development and optimization for solvent extraction of various polypropylene grades.* BSc. (Honours) Research Project, Department of Chemistry and Polymer Science, University of Stellenbosch **(2003)**.

Chapter 4. Results and discussion

4.1 Introduction.

The test samples consisting of four homopolymer samples and five propylene-ethylene random copolymers were analysed by GPC, NMR and DSC. In addition to these analyses, the techniques used on a daily basis for process and product quality control were also employed in this study. These techniques are namely, MFI, Mini Spec NMR and FTIR.

There is a perceived relationship between some of these techniques. For example, the MFI value, which is a rheological property, gives an indication of the average molecular weight of a polymer, which is in turn determined via GPC, a specialised technique [1]. An inverse relationship exists between MFI and $\overline{Mw}$. The higher the MFI value, the lower the $\overline{Mw}$ and vice versa.

The R21 values and calculated xylene solubles are "in-house" techniques used as an estimation of the polymer average isotacticity. The analytical results obtained from the above mentioned techniques are to a certain extent grouped according to their relationship to one another for ease of explanation.

For ease of understanding and for the logical interpretation of the findings, the results of the homopolymers are presented first, followed by the results of the propylene-ethylene random copolymers. The numbering of the samples however, does not follow suit, with the homopolymer samples numbered "Polymer 6" to "Polymer 9", and the propylene-ethylene random copolymers numbered "Polymer 1" to "Polymer 5". The reader should merely take cognizance of this when reading the thesis.

4.2 The evaluation of the un-fractionated homopolymer samples.

4.2.1 GPC analysis of the un-fractionated homopolymer samples.

The homopolymer samples were tested on the GPC and the results are shown in Table 4.1.

Table 4.1 *The MFI and GPC results of the un-fractionated homopolymer samples.*

Polymer number	MFI (g/10 min)	$\overline{Mw}$	$\overline{Mn}$	MWD
6	10	390 000	100 000	3.9
7	3	540 000	130 000	4.2
8	20	320 000	850 00	3.7
9	3	530 000	1250 00	4.2

The results in Table 4.1 show that the MFI and $\overline{M_w}$ have an inversely proportional relationship. Figure 4.1 shows a decrease in the $\overline{M_w}$ values as MFI values increases.

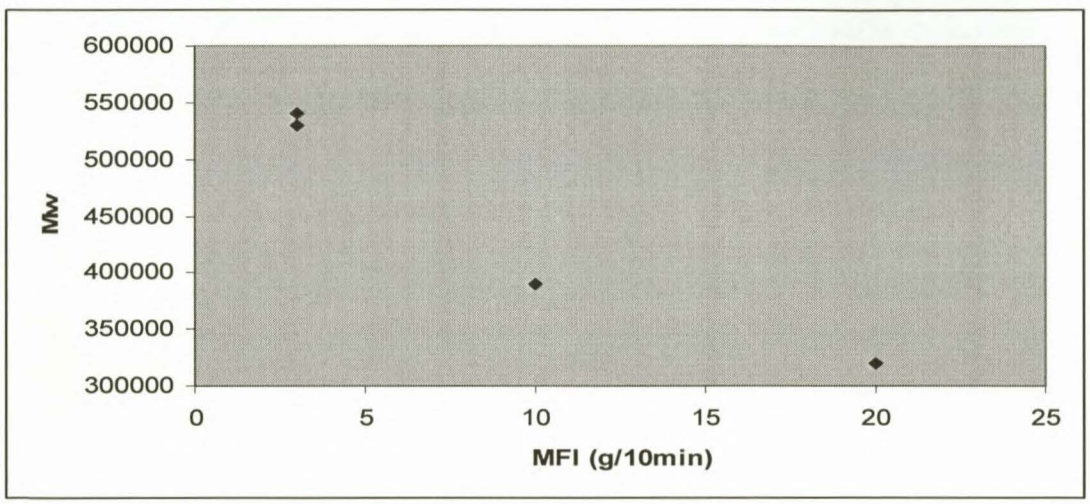

Figure 4.1: *MFI versus $\overline{M_w}$ for the homopolymer samples.*

Homopolymers 6 and 8 have almost similar molecular weights and $\overline{M_n}$ values; this is also reflected in their MWD results. Although Polymer 8 is a controlled rheology grade and Polymer 6 a reactor grade of slightly higher MFI value (i.e. 10 g/10 min), there are no significant differences between these samples according to the GPC. This also shows that the vis-break step was not significantly large. It is important to control the $\overline{M_w}$ and MWD of the polymer samples to optimize the mechanical properties and processability [2]. The results for Polymers 7 and 9 are almost equivalent in all respects.

4.2.2 The thermal properties of the homopolymer samples.

The thermal properties of the homopolymer samples are displayed in Table 4.2.

Table 4.2 *The thermal properties of the un-fractionated homopolymer samples.*

Polymer number	Crystallinity (%) (Based on PP ΔH)	Melting peak temperature (°C)
6	45	166
7	36	166
8	41	165
9	33	160

The crystallinity and peak melting temperature results shown in Table 4.2 are typical of homopolymer samples. The DSC thermograms of Polymers 6, 7 and 8 are shown in Figure 4.2 to illustrate the melting endotherms for individual samples.

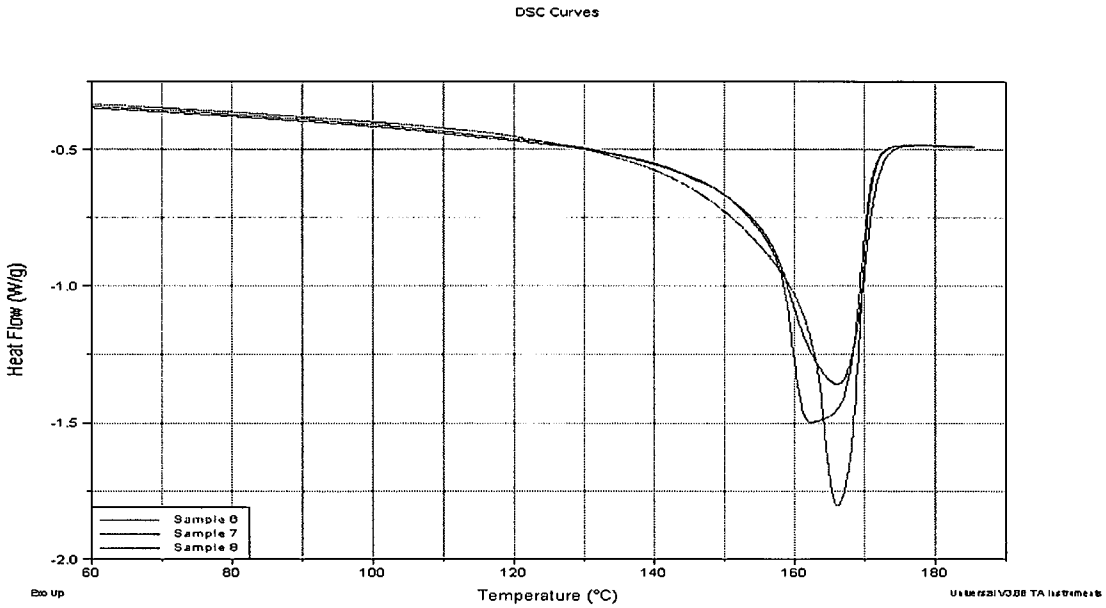

Figure 4.2 *The DSC thermogram of the homopolymer samples.*

The thermograms of the homopolymer samples used in this study are characterised by a well-defined, narrow and intense melting peak. In some cases the construction of the baseline tangent to pre- and post melting points on the curve is subjective. The error incurred in the estimation of the peak melting temperature area is usually small for sharp melting peaks such as that of the homopolymers. In this study a standard approach was adopted whereby the melting temperature range was measured between 100 °C and 180 °C to alleviate melting temperature range uncertainties.

Homopolymer 6, produced using higher amounts of stereomodifier, has a significantly higher percentage crystallinity than Polymer 7 which was produced at a lower Si/Ti ratio. The lower percentage crystallinity in Polymer 7 is due to increased non-crystalline regions caused by the addition of lesser amount of stereomodifier into the polymerization reaction. The variation in use of the stereomodifier is related to the final application of the polymer, hence Polymer 6 is typically targeted for applications where high stiffness is a prerequisite property.

4.2.3 ^{13}C NMR analysis of the homopolymers.

The microstructure of the homopolymer samples were analyzed by using ^{13}C NMR spectrometry [3]. The spectrum of Polymer 7, shown in Figure 4.3, was used as a representative spectrum for Polymers 6 and 8 since there were no major differences observed in their respective spectra **(See Appendix 1.1 (a,b))**

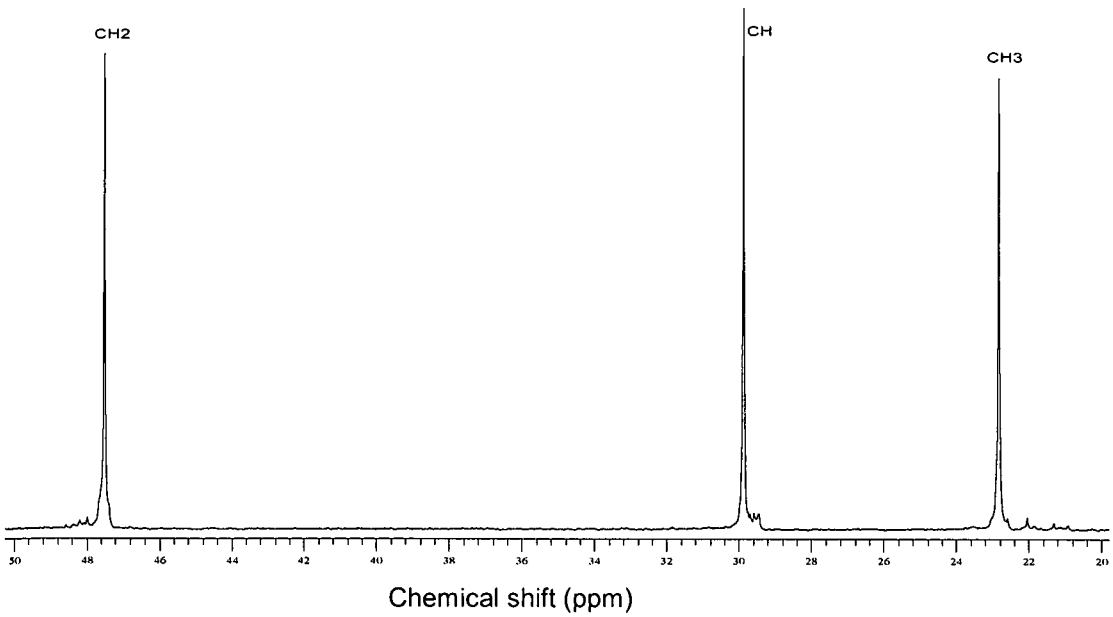

Figure 4.3: *The ^{13}C NMR spectra of Polymer 7 un-fractionated sample.*

The percentage isotacticity is determined by integrating the whole methyl region, and assigning to it an integral of 100 which is then equated to 100% isotacticity (the selection of the area to be integrated is dependent on the type of NMR software used and in this study Mestrec® Version 2.3 was used) [2]. Then the whole region can be individually integrated to get *mmmm*% (isotactic), *mmmr*% and so forth. The peaks with stereoerrors will have both the meso (*m*) and racemic (*r*) sequences.

The spectrum clearly shows that Polymer 7 is polypropylene of reasonably high isotacticity. Propylene peaks are clearly visible on the spectrum as cited in literature [4]. The isotacticity determination showed that Polymer 7 is 93% isotactic when compared to Polymer 6 and 8 with an average isotacticity of 96%. This corresponds to the DSC results, which indicate that Polymer 7 is less crystalline than Polymers 6 and 8.

4.3 Temperature rising elution fractionation results of the homopolymer samples.

Polymers 6 and 7 were fractionated by TREF and were used as representative samples for the homopolymers. The weight of individual recovered fractions is shown in Table 4.3.

Table 4.3 *The weights of the homopolymer TREF fractions.*

		Polymer 6	Polymer 7
Fraction number	**Elution temperature (°C)**	**Fraction weight (%)**	**Fraction weight (%)**
F1	**40**	1.42	3.65
F2	**80**	1.90	3.22
F3	**90**	1.48	1.77
F4	**100**	6.81	6.31
F5	**110**	70.46	70.57
F6	**125**	16.24	12.43
	Total weight fraction	**98.31**	**97.95**

Table 4.3 shows an increase in the quantities of the fractions as the elution temperature increases. The bulk of the material is eluted as F5 at 110 °C for both samples. Fractions F1 and F2 of Polymer 7 are slightly larger than the corresponding fractions of Polymer 6. This is expected since Polymer 7 is produced using lower amounts of the stereomodifier hence slightly higher fraction weights at lower elution temperatures. Simply put, Polymer 7 has higher amounts of amorphous material as a result of its production parameters.

4.3.1 The GPC results of the homopolymer TREF fractions.

The homopolymer sample 6 and 7 fractions generated from the TREF technique were tested on the GPC to determine their $\overline{Mw}$ and MWD. Their results are shown in Table 4.4. For Polymer 6, only fractions labelled as F4, F5 and F6 were analysed since the other fractions (i.e. F1, F2 and F3) were not recovered in sufficient quantities for GPC analysis. Polymer 7 yielded sufficient amount of fractions at all elution temperatures to allow for GPC analysis.

Table 4.4: *The GPC results of Polymer 6 and 7 TREF fractions.*

		Polymer 6			Polymer 7		
Fraction number	**Elution temperature (°C)**	$\overline{Mw}$	$\overline{Mn}$	**MWD**	$\overline{Mw}$	$\overline{Mn}$	**MWD**
F1	40				154210	26180	5.89
F2	80				129500	20400	6.35
F3	90				85160	22450	3.79
F4	100	97540	36720	2.66	111100	44900	2.47
F5	110	400300	146600	2.73	577440	166100	3.48
F6	125	581820	199500	2.92	638000	201010	3.17

Although TREF fractionates polymers according to their crystallizability, an increase in molecular weight is observed as the elution temperature increases [5, 6].

The fractions of Polymer 6 (i.e. F4 to F6) showed an increase in $\overline{Mw}$ as the elution temperature increases. Polymer 7 with fractions yielded at all the elution temperatures showed a decrease in $\overline{Mw}$ as the elution temperature increases from 40 °C to 90 °C (i.e. from F1 to F3). Polymer 7 F4 to F6 followed a similar trend as Polymer 6 fractions whereby the $\overline{Mw}$ of the fractions increased with an increase in the elution temperature.

The F1 and F2 fractions of Polymer 7 (eluted at 40 and 80 °C) have a much broader MWD relative to the fractions eluted at higher temperatures. These fractions are less crystalline since they are eluted first in the experiment. This, coupled with the fact that the molecular weight decreases as the elution temperature increases indicates that the fractionation of polypropylene with the TREF technique is not influenced by molecular weight [5]. In the case of Polymer 7, the isolation of fractions occurred according to polymer crystallizability as seen from the DSC results.

4.3.2 Thermal properties of the homopolymer TREF fractions.

Polymers 6 and 7 TREF fractions were analysed on the DSC and the results are shown in Table 4.5.

Table 4.5 *The DSC results of homopolymer TREF fractions.*

		Polymer 6		Polymer 7	
Fraction number	**Elution temperature (°C)**	**Melting temperature (°C)**	**Crystallinity (%) (Based on PP ΔH)**	**Melting temperature (°C)**	**Crystallinity (%) (Based on PP ΔH)**
F1	40				
F2	80	134	15.4	122	13
F3	90			139	21
F4	100	158	46	155	38
F5	110	166	46	164	38
F6	125	167	46	164	44

For Polymer 6, fractions F1 and F3 and for Polymer 7 fraction F1 were not analysed on the DSC because of an insufficient amount of sample yielded at those specified elution temperatures. From the available results it is clear that melting peak temperature and crystallinity increase as the elution temperature increases. Polymer 7 fractions have lower crystallinity than Polymer 6 because of the lower Si/Ti ratio which regulates polymer stereochemistry used in the production of this grade.

When focusing on the Polymer 6, and comparing fractions F2 and F4 (eluted at 80 and 100 °C, respectively), there is considerable variation in the melting temperature and crystallinity of

these two fractions. Very little difference is observed between the fractions F5 and F6 fractions, eluted at 110 and 125 °C, respectively. This shows that there are no major differences in the molecular composition of the fractions eluted at higher temperatures. Figure 4.4 shows the variations in the peak melting temperatures and peak areas of the Polymer 6 individual fractions.

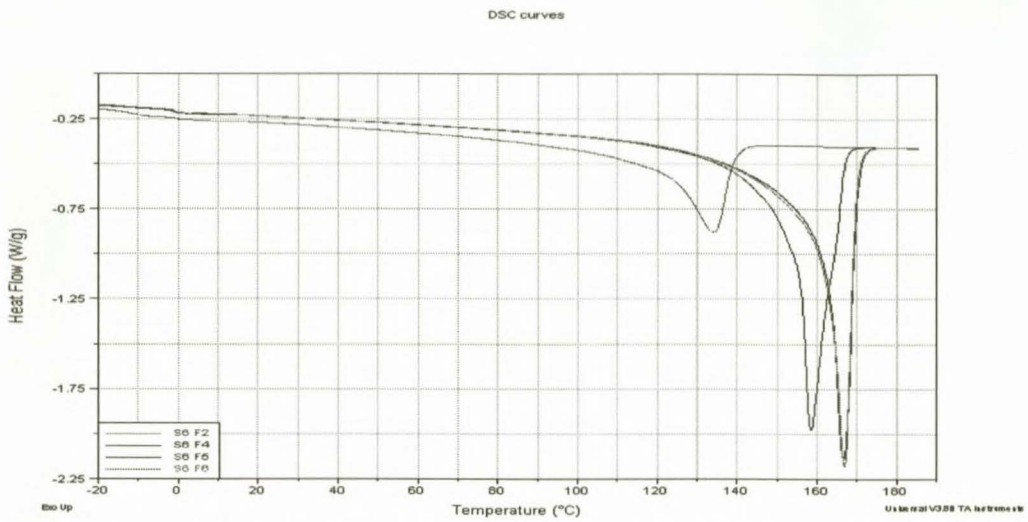

Figure 4.4 *Melting temperature overlays of Polymer 6 TREF fractions*

Figure 4.4 shows well defined and narrow melting curves. The F2 fraction has the smallest peak melting area, thus indicating a lower percentage crystallinity.

The peak melting temperature and crystallinity results of Polymers 6 and 7 were plotted as a function of elution temperatures. Figures 4.5 and 4.6 show the relationship of elution temperature to melting temperatures and crystallinity, respectively.

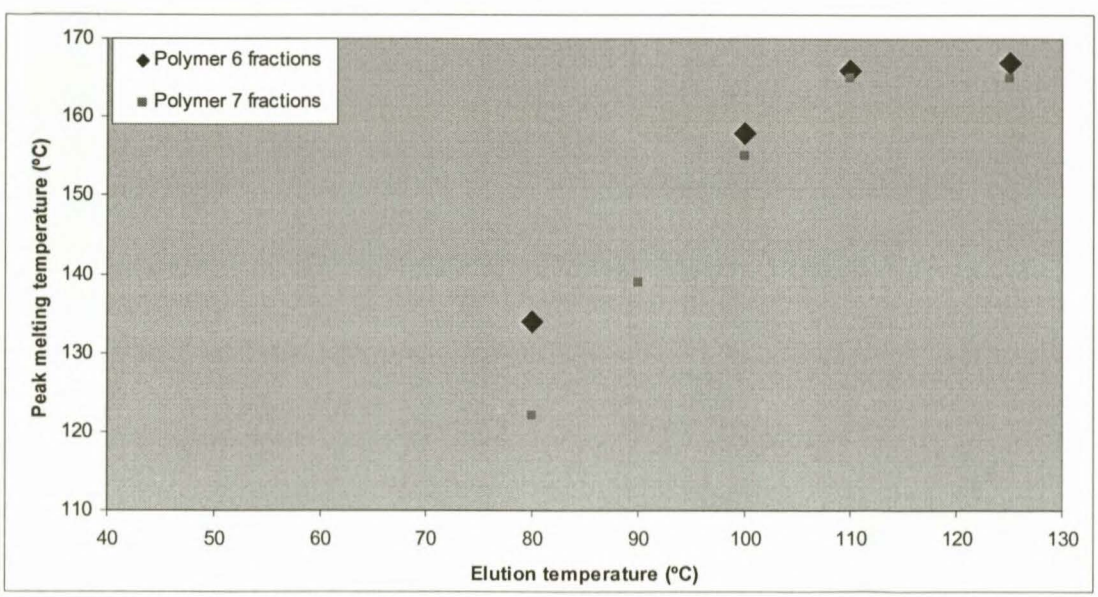

Figure 4.5 *The melting peaks of Polymers 6 and 7 TREF fractions.*

The fractions of Polymers 6 and 7 eluted at 100, 110 and 125 °C have essentially similar peak melting temperatures.

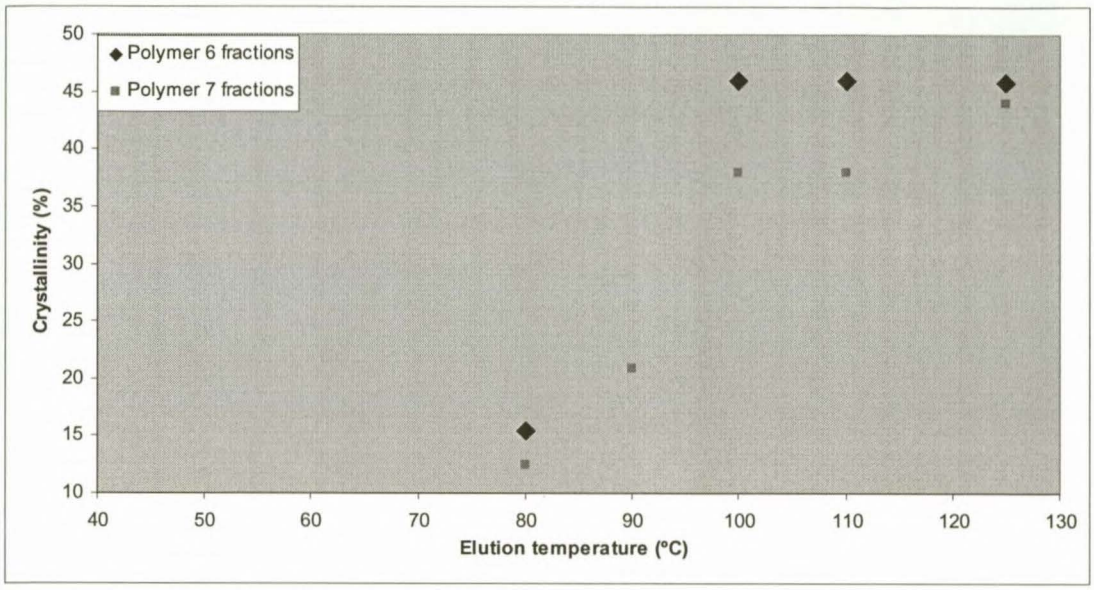

Figure 4.6: *Crystallinity plotted as a function of elution temperature.*

In contrast to the peak melting temperatures, a remarkable variation is observed in the crystallinity values for the fractions of Polymers 6 and 7, especially those eluted at 100 and 110 °C. The variations in crystallinity are minimised at an elution temperature of 125 °C. At 125 °C elution temperature the fractions are highly crystalline. It is apparent that the crystallinity of Polymer 6's fractions eluted in the region of 100 to 110 °C are higher than that of the comparable fractions of Polymer 7. All of this indicates a molecular composition difference between the polymers.

4.4 The evaluation of the un-fractionated propylene-ethylene random copolymer samples.

4.4.1 The GPC and MFI data interpretation.

Table 4.6 shows the MFI values and molecular weight data of the un-fractionated propylene-ethylene random copolymer samples.

Table 4.6 *The MFI values and the GPC results of the un-fractionated copolymer samples.*

Polymer number	MFI (g/ 10 min)	$\overline{Mw}$	$\overline{Mn}$	MWD
1	35.0	300 000	100 000	3.0
2	38.0	300 000	80 000	3.7
3	2.0	570 000	140 000	4.1
4	34.0	290 000	73 000	3.9
5	8.0	380 000	120 000	3.0

Polymers 1, 2 and 4 with MFI values of 35, 38 and 34 g/10 min, respectively, are controlled rheology grades, and they have molecular weight values in the region of 300 000. Polymer 5 with lower MFI value of 8 g/10 min has a slightly higher molecular weight of 380 000. Polymer 3 with the lowest MFI value of 2 g/10 min has the highest $\overline{Mw}$ of 570 000. Polymers 3 and 5 are different from Polymers 1, 2 and 4 since they are reactor grades. The results displayed in Table 4.6 confirm the existence of an inversely proportional relationship between molecular weight and MFI. Figure 4.7 further illustrates this relationship.

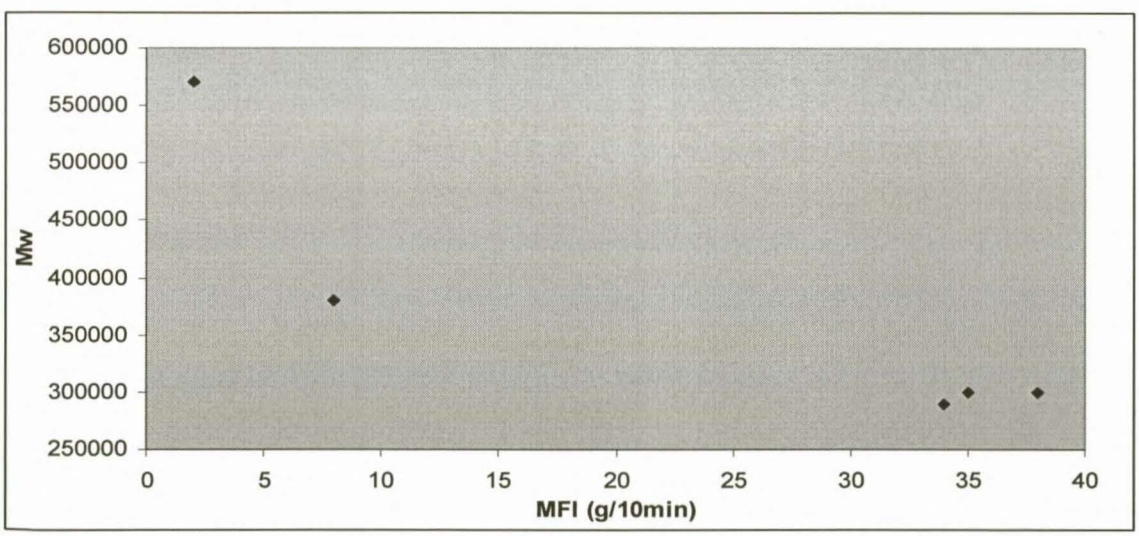

Figure 4.7 *The MFI-Mw inverse relationship for the ethylene random copolymers.*

Figure 4.7 shows that as the MFI increases $\overline{Mw}$ decreases. This observation is consistent with the findings made by other researchers [7]. Furthermore, the vis-break step largely determines the extent of chain scission, which in turn influences the polymer MWD. Slight differences in MWD are observed amongst Polymers 2, 3 and 4. Logically, this could mean that Polymers 2 and 4 were vis-broken from a polymer of very broad MWD. It is generally expected that the reactor grades should have a broader MWD than the controlled rheology grades.

Figure 4.8 illustrates the GPC overlay of Polymers 1 and 3, which are controlled rheology and reactor grades, respectively.

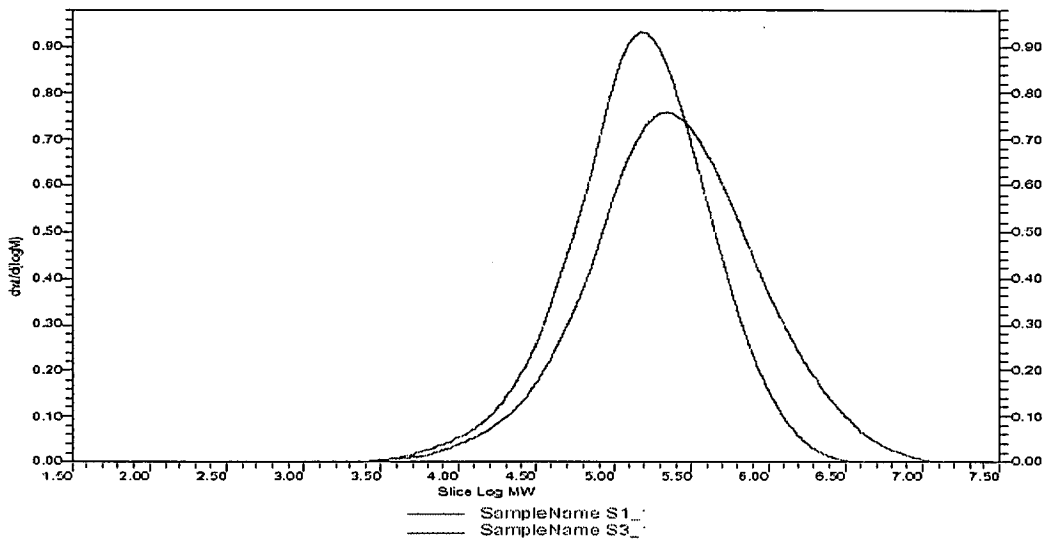

Figure 4.8 *The GPC overlay of Polymers 1 and 3.*

The chain scission induced by the addition of organic peroxide, which preferentially attacks longer polymer chains, results in the formation of shorter chains i.e. a shift to lower average Mw. This causes a drop in the molecular weight of individual chains constituting a polymer, as depicted by the blue curve on the chromatogram. Additionally, the blue curve also indicates the narrower MWD resulting from the controlled rheology.

4.4.2 Evaluation of the thermal properties of the un-fractionated samples.

Further studies were conducted on the un-fractionated propylene-ethylene random copolymer samples to determine their thermal properties. The ethylene content is not a thermal property, however it is included in the table of results since it influences the thermal properties. The results are illustrated in Table 4.7.

Table 4.7 *The thermal properties of the un-fractionated copolymer samples.*

Polymer number	Crystallinity (%) (Based on PP ΔH)	Melting peak temperature (°C)	Ethylene content (wt.%)
1	35	157	0.87
2	24	149 (137)	4.30
3	23	149	3.90
4	25	150 (137)	5.00
5	21	144	4.60

Polymers 1 to 5 have varying amounts of ethylene comonomer content, as shown in Table 4.7. The ethylene content of Polymers 4 and 5 were also determined by NMR to confirm the FTIR values. The results from the two instruments correlated well. The ethylene content results from the NMR were 5.38 and 4.44% for Polymers 4 and 5, respectively.

From the percentage crystallinity results shown in Table 4.7, the random copolymer samples of higher ethylene content have lower percentage crystallinity. Polymer 1, with the lowest ethylene comonomer content has a crystallinity of 35%, which is the highest amongst all the random copolymer samples. This shows that the extent of crystallinity disruption is also dependent on the amount of ethylene incorporated into the polymer backbone. Clearly, a low ethylene comonomer incorporation has little effect on the overall polymer crystallinity.

Figure 4.9 illustrates the type of relationship observed between polymer crystallinity and ethylene content.

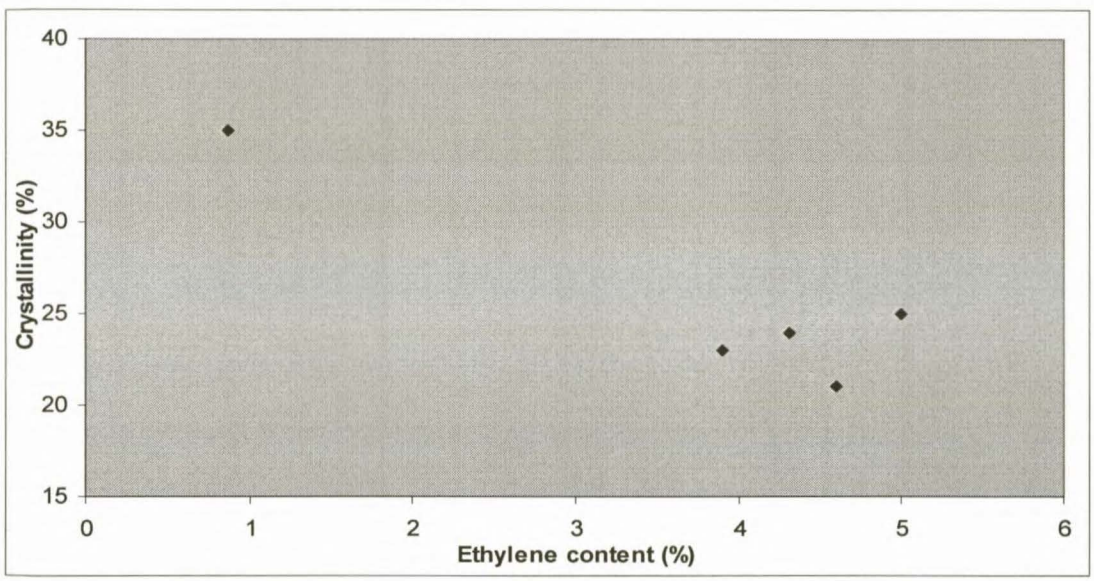

Figure 4.9 *The relationship between ethylene content and crystallinity for the propylene-ethylene random copolymer samples.*

Figure 4.9 show that Polymer 1 with the lowest ethylene content has a higher percentage crystallinity than the other random copolymer samples. Copolymer samples 2, 3, 4 and 5 with an ethylene content ranging between 3.90% and 5.00% show scattered data points when plotted against crystallinity, which indicates that ethylene content alone is not solely responsible for disruption in crystallinity.

Peak melting temperature is another characteristic feature strongly influenced by comonomer insertion in the polymer matrix. Ethylene comonomer incorporation tends to result in melting temperature depression. Although Polymers 2 and 4 have higher ethylene comonomer content, they lie in almost same region of peak melting temperature as Polymer 3. In

Polymers 2 and 4, the values in the brackets represent the second melting peak resulting possibly from a different crystalline species. The overlays of melting temperature of the un-fractionated random copolymer samples 1 to 5 are shown in Figure 4.10 to illustrate the effect of the comonomer insertion on the polymer thermal properties.

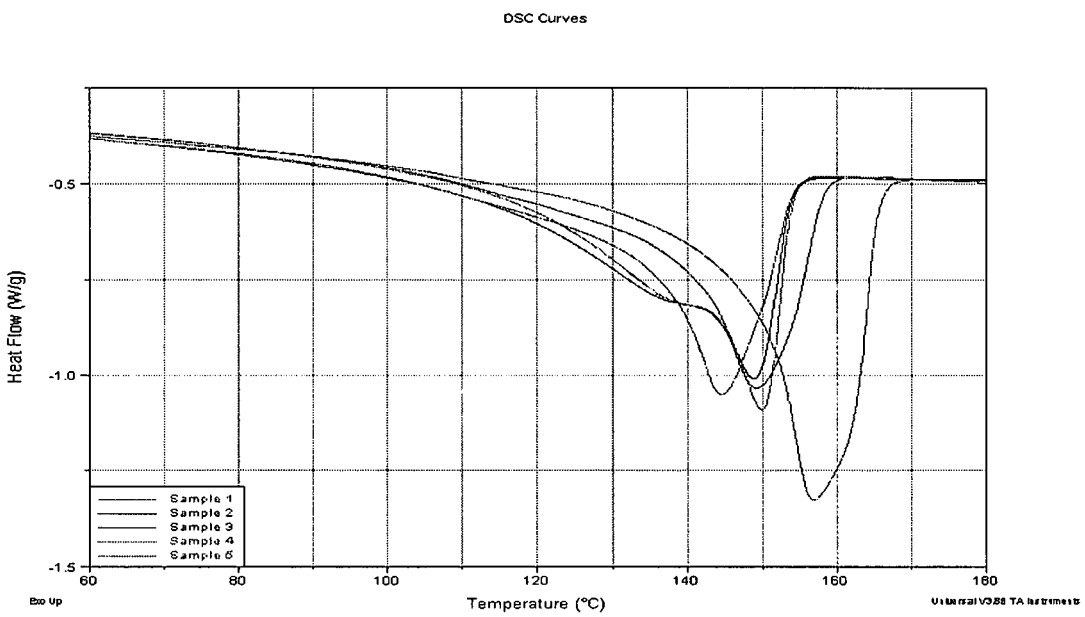

Figure 4.10 *DSC thermograms of the un-fractionated copolymer samples.*

The endothermic peaks observed in Figure 4.10 are representative of melting peaks for each individual polymer sample. Polymers 1, 3 and 5 exhibit one endothermic melting peak. However, the presence of ethylene comonomer in these samples is accounted for by lower peak melting temperatures and broader melting temperature ranges. Polymers 2 and 4 have shoulder peaks in their melting endotherms. These samples have broader melting temperature ranges as well.

The random copolymer samples have lower peak melting temperatures compared to the homopolymers, and melt over a wider temperature range and have irregularly shaped curves. The broadening of the melting temperature peaks, especially in Polymers 2 and 4 is indicative of the presence of more than one crystalline species in the respective polymers. These two polymer samples were nucleated and as a result this may have influenced the size of the crystals. These observations are supported by the higher re-crystallization temperatures (Tc) of 122 °C and 123 °C for Polymers 2 and 4, respectively.

The ethylene content versus peak melting temperature graph is shown in Figure 4.11 to establish the type of relationship existing between these two measurements.

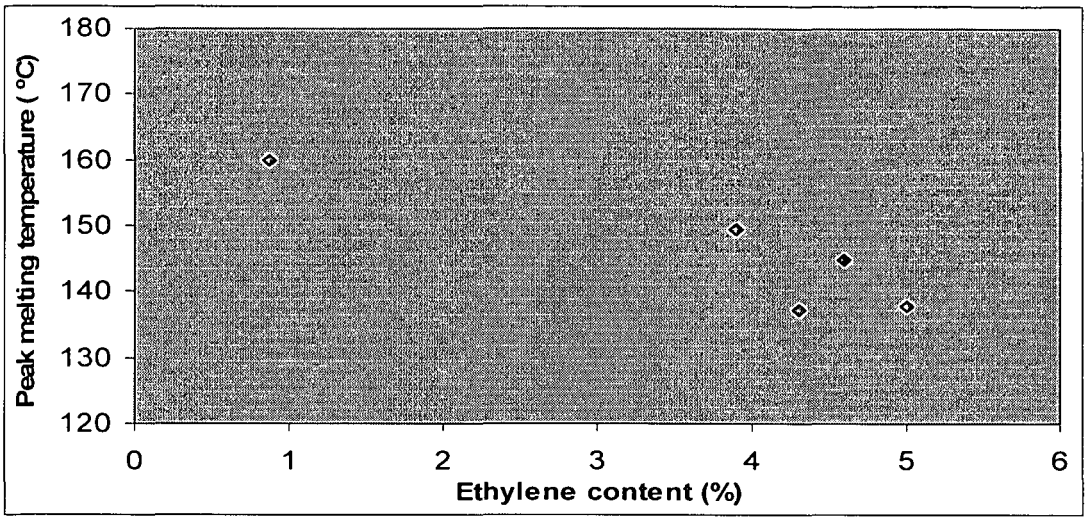

Figure 4.11 *The ethylene content versus peak melting temperatures.*

A simple relationship is observed whereby the melting peak temperature decreases as the ethylene content increases. The nucleation process in Polymers 2 and 4 may have had an influence on this relationship; hence there is some scatter towards the extreme end of the graph.

4.4.3 ^{13}C NMR analysis of the propylene-ethylene random copolymers

^{13}C NMR spectra were used to characterise the microstructure of Polymers 1 to 5. Propylene peaks, namely methyl (CH_3), methylene (CH_2) and methine (CH) appearing at approximately 22 ppm, 47 ppm and 30 ppm, respectively [4, 8], are clearly visible in Figure 4.12 for Polymer 1.

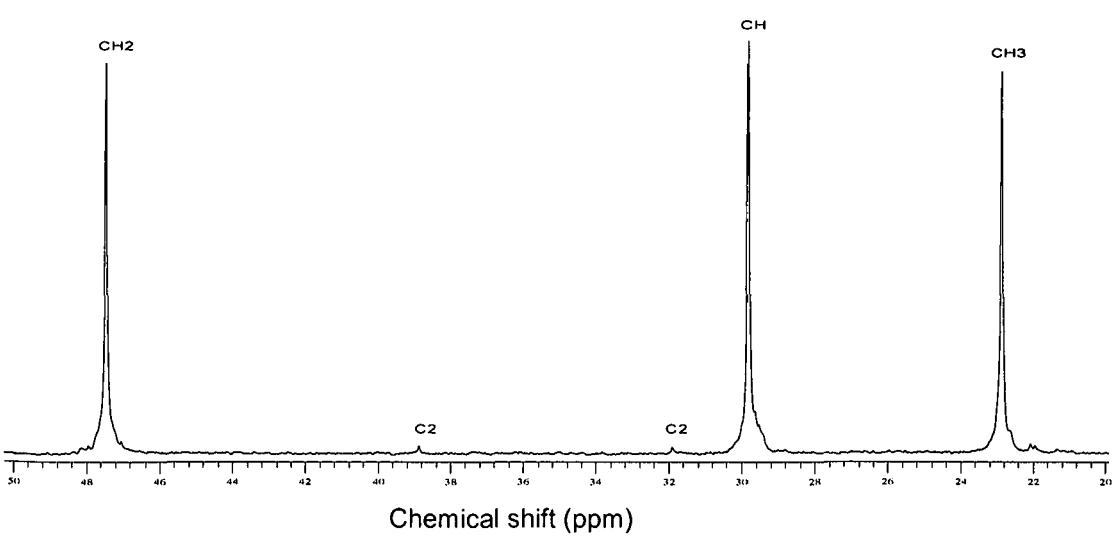

Figure 4.12 *The ^{13}C NMR spectrum of Polymer 1 un-fractionated sample.*

Figure 4.12 shows the presence of ethylene peaks that appear at approximately 32 ppm and 39 ppm in addition to the identified propylene peaks. These peaks are indicative of isolated ethylene insertions between polypropylene sequences.

The ^{13}C NMR spectrum of Polymer 1 differs slightly from that of Polymers 2 to 5. The variations in the spectra result mainly from the differences in the ethylene content of the polymers. This is illustrated by the fact that Polymers 2 to 5, with higher ethylene content, show more intense ethylene peaks. This is exemplified by the peak at 25 ppm in the spectra of Polymers 2 to 5, which is not visible in the spectrum of Polymer 1. Figure 4.13 represents the microstructure of Polymer 2, which is also used as a reference spectrum for Polymers 3-5 **(See Appendix 1.2 (a,b,c))**, since their spectra are similar.

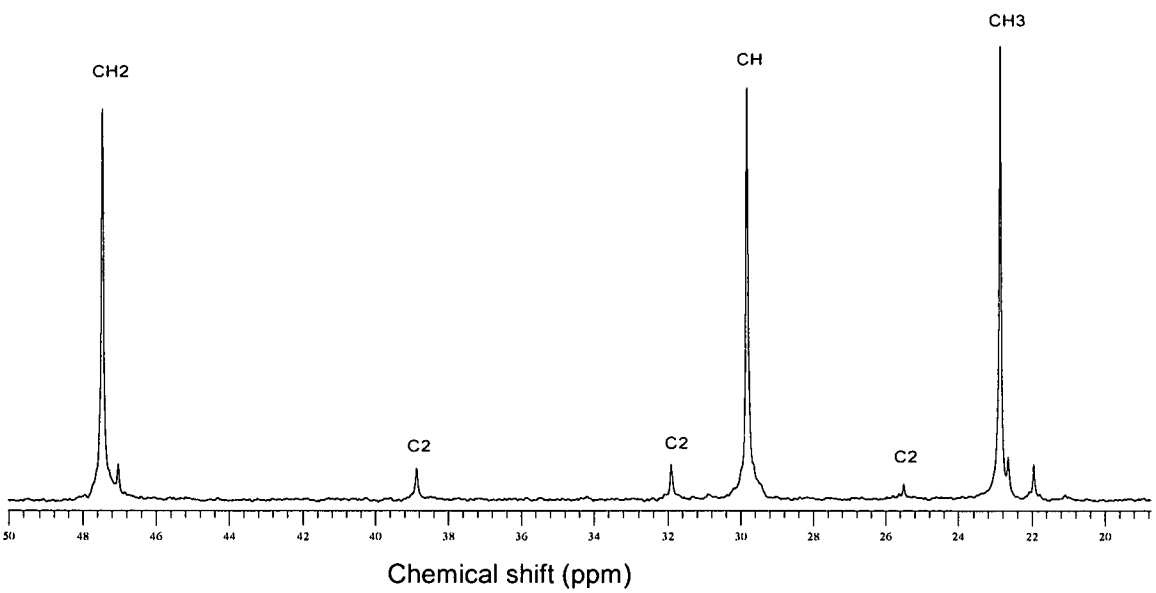

Figure 4.13 *The ^{13}C NMR spectrum of Polymer 2 un-fractionated sample.*

The ^{13}C NMR of Polymer 2 shows that the ethylene comonomer is inserted in a similar fashion as in Polymer 1, meaning that the ethylene appears to be mostly isolated insertions.

The methyl region of the ^{13}C NMR spectra of Polymers 1, 2 and 3 as shown in Figures 4.14, 4.15 and 4.16 is an indication that these samples have some degree of isotacticity. The methyl regions of these samples were integrated to quantify the isotacticity of each sample and to also evaluate the effect of comonomer content on their microstructure.

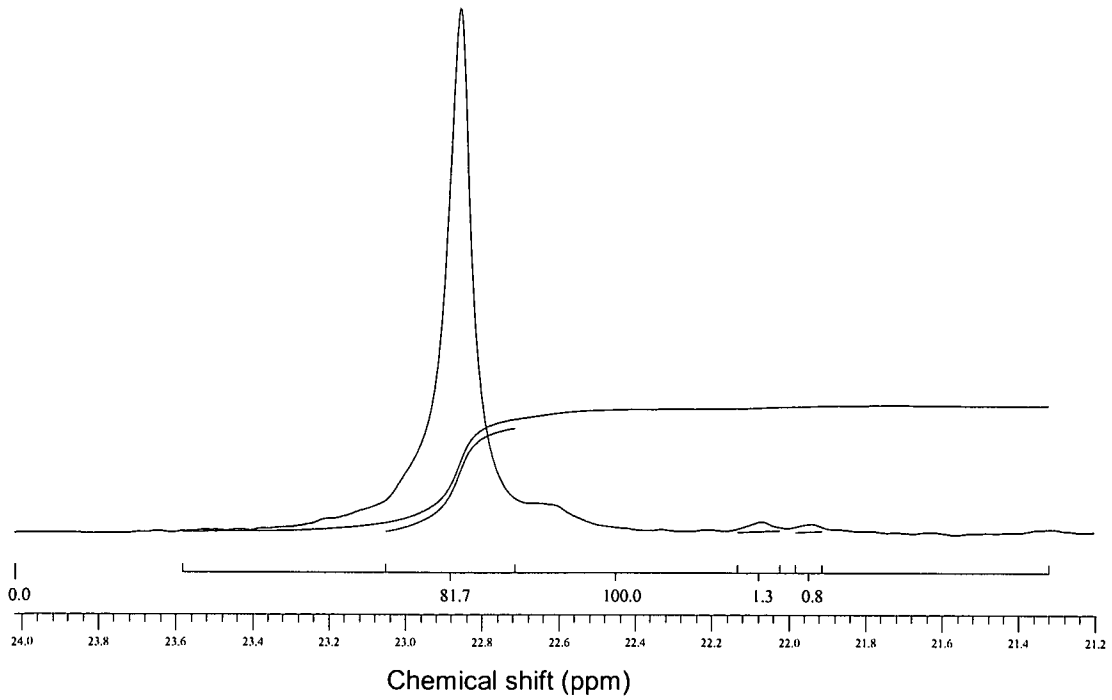

Figure 4.14 *The methyl region of Polymer 1 un-fractionated sample.*

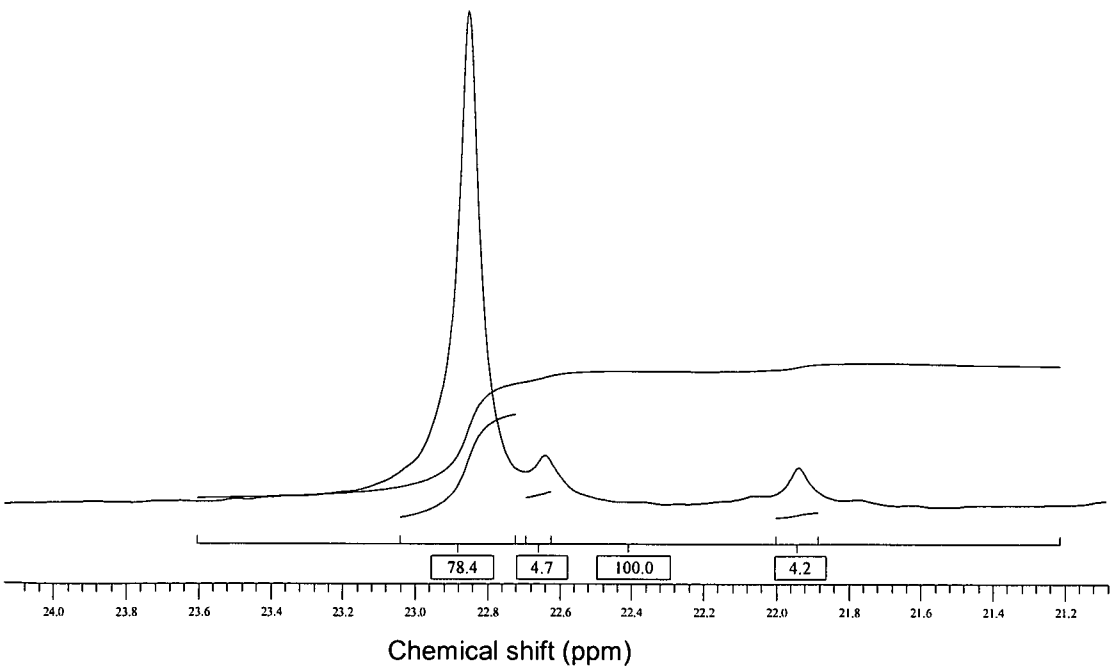

Figure 4.15 *The methyl region of Polymer 2 un-fractionated sample.*

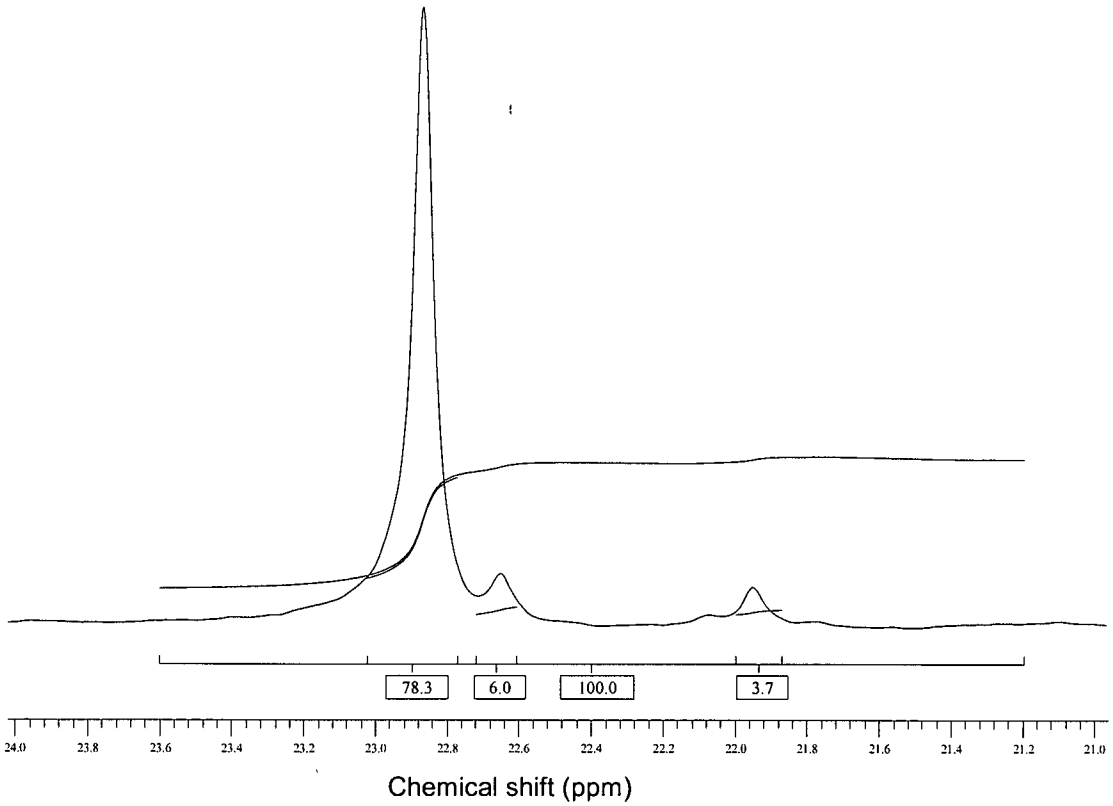

Figure 4.16 *The methyl region of Polymer 3 un-fractionated sample.*

The isotacticity values were found to be 81.7%, 78.4% and 78.3% for Polymers 1, 2 and 3, respectively. Polymer 1, with the least ethylene comonomer content, has the highest isotacticity. A general trend, which shows a decrease in tacticity as the comonomer content increases, can be deduced. These results correlate with the Minispec NMR results whereby the R21 values (xylene solubles) increases as the ethylene content increases, although the correlation appears less than perfect. The R21 results for Polymer 1, 2 and 3 were 9.4, 15.93 and 16.96, respectively. This will be discussed in more detail later in the chapter.

Furthermore, the above observations are aligned to the DSC results since the percentage crystallinity decreases as the comonomer content increases. This means that as the percentage crystallinity decreases the amount of the non-crystalline regions increases hence an increase in R21 (xylene solubles) and a drop in isotacticity. This is also influenced by the comonomer as well. The scatter in the results indicate that the relationship is not as straightforward as that found in the homopolymers.

4.5 Temperature rising elution fractionation of the propylene-ethylene random copolymer samples.

The temperature rising elution fractionation (TREF) technique was employed to separate the test samples according to their crystallizability. The fractions were eluted under strictly controlled conditions at 40, 80, 90, 100, 110 and 125 °C. Total polymer sample recovery was good and the weight of the recovered fractions is indicated in Table 4.8

Table 4.8 *The weight of the propylene-ethylene random copolymer TREF fractions.*

		Polymer 1	Polymer 2	Polymer 3
Fraction number	**Elution temperature (°C)**	**Fraction weight (%)**	**Fraction weight (%)**	**Fraction weight (%)**
F1	**40**	2.91	6.03	7.11
F2	**80**	3.71	15.84	16.84
F3	**90**	4.22	41.43	16.60
F4	**100**	21.93	29.16	48.02
F5	**110**	62.35	3.14	8.57
F6	**125**	3.75	0.43	0.49
	Total weight fraction	**98.87**	**96.03**	**97.63**

Table 4.8 shows the weights of individual fractions eluted at specific temperatures. It is apparent that there are differences in the molecular composition of Polymers 1, 2 and 3 because of the significant variations observed in the distribution of weights of the fractions at corresponding elution temperatures.

Polymer 1 with the lowest ethylene content (0.87 wt.%) shows that 62.35% of the total recovered sample was eluted at 110 °C followed by 21.93% at the elution temperature of 100 °C. Polymer 2 with an ethylene content of 4.3 wt.% has the highest fraction weight eluted at 90 °C whereas Polymer 3 with an intermediate ethylene content of 3.9 wt.% has the highest fraction weight eluted at 100 °C. A trend is established whereby the highest weight fractions are eluted at lower elution temperatures as the comonomer content increases.

4.5.1 The GPC analysis of the propylene-ethylene random copolymer TREF fractions

The fractions obtained from the TREF technique were analysed on the GPC to determine their molecular weight properties. These fractions were eluted at 40, 80, 90, 100, 110 and 125 °C. The results are shown in Table 4.9.

Table 4.9 *The GPC results of Polymer 1, 2 and 3 TREF fractions.*

		Polymer 1			Polymer 2			Polymer 3		
Fraction number	**Elution temp. (°C)**	$\overline{Mw}$	$\overline{Mn}$	**MWD**	$\overline{Mw}$	$\overline{Mn}$	**MWD**	$\overline{Mw}$	$\overline{Mn}$	**MWD**
F1	40	112480	18990	5.92	64920	19680	3.30	193500	36820	5.26
F2	80	82800	20900	3.96	125330	44390	2.82	260900	73900	3.53
F3	90	113900	37600	3.03	320470	137770	2.33	465100	162700	2.86
F4	100	216700	91600	2.37	402800	166190	2.24	736400	146400	2.99
F5	110	331800	148500	2.23	400880	140120	2.86	781000	289200	2.78
F6	125	340900	152000	2.24						

Table 4.9 shows a general increase in molecular weight of the fractions as the elution temperature increases. Conversely, a reduction in the MWD values is observed as the elution temperature increases. Clearly, the DSC results have shown that lower molecular weight fractions eluted at lower elution temperature are less crystalline than the fractions of higher molecular weights. Molecular weight may also influence the stability of the crystallite size, thus fractions of higher molecular weights have generally higher melting temperatures if molecular composition is similar.

Furthermore, the fractions of Polymers 2 and 3 with higher ethylene content were compared to distinguish between the types of fractions obtained at corresponding elution temperatures. These two samples are differentiated by the fact that Polymer 2 is a controlled rheology grade whereas Polymer 3 is a reactor grade. The fractions obtained from Polymer 2 have a lower molecular weight when compared to those from Polymer 3. However, the fractions of both samples have assumed a similar trend whereby the molecular weight increases as the elution temperature increases.

Generally, Polymer 3 fractions have broader MWD (as expected) compared to the Polymer 2 fractions. It can be concluded that controlled rheology does not only affect the properties of the bulk polymer materials but also the molecular weight properties of fractions eluted at different temperatures.

The TREF, xylene and successive extractions performed on the propylene-ethylene random copolymers provided different information on the physical and molecular composition on the fractions they yielded. The results of these techniques are not comparable due to differences in the extraction temperatures and also in the sample form, yet allows for a better understanding of the complex nature of these materials.

4.5.2 Thermal properties of the propylene-ethylene random copolymer TREF fractions.

The fractions obtained by TREF for Polymers 1, 2 and 3 were characterised on the DSC and the results are shown in Table 4.10. Fractions F6 of Polymers 2 and 3 did not yield sufficient material to allow DSC analysis.

Table 4.10 *The DSC results of Polymers 1, 2 and 3 TREF fractions.*

		Polymer 1		Polymer 2		Polymer 3	
Fraction Number	Elution temperature (°C)	Melting temperature (°C)	Crystallinity (%) (Based on PP ΔH)	Melting temperature (°C)	Crystallinity (%) (Based on PP ΔH)	Melting temperature (°C)	Crystallinity (%) (Based on PP ΔH)
F1	40	80	4.70	80	5.4	80	6.80
F2	80	128, 137	15.60	133	12.4	127	14.50
F3	90	147,156	28.40	145	25.3	143	23.70
F4	100	156	36.70	149	29.2	152	27.23
F5	110	159	35.60	149	20.8	151	29.20
F6	125	159	38.55				

The DSC results show an increase in the peak melting temperatures and crystallinity as the elution temperature increases. This shows that the less crystalline portions of the polymer were eluted first at lower temperatures. Polymer 1 with lower ethylene content has in general, a higher peak melting temperature and crystallinity than Polymers 2 and 3.

The F1 fractions of the individual samples have the lowest peak melting temperature and crystallinity. In all probability this means that these fractions contain more ethylene-rich copolymer compared to the rest of the fractions. The fractions F2 and F3 of Polymer 1 have two melting endotherms on their thermograms. These melting endotherms are attributed to the presence of more than one crystalline species in the fractions. Figure 4.17 illustrates the Polymer 1 TREF fractions DSC results for F1 to F6.

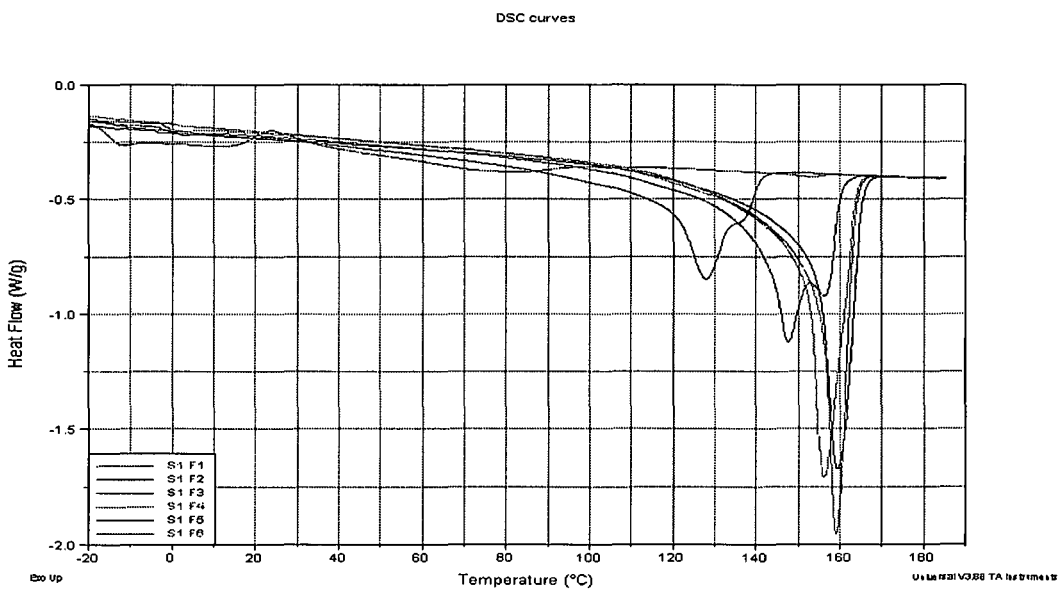

Figure 4.17 *Melting temperature overlays of Polymer 1 TREF fractions.*

The fractions F4, F5 and F6 of Polymer 1 have similar melting peak temperatures and crystallinity values. These are possibly purely polypropylene since the melting temperature

depression induced by the ethylene incorporation is minimal. Fractions F2 and F3 have two melting endotherms on their thermograms and they also melt over a wider temperature range.

Contrary to the thermogram of Polymer 1, none of Polymer 3 fractions have two melting endotherms on their thermogram as shown in Figure 4.18. This could be interpreted as representing a more homogeneous distribution of molecular and crystalline species over the fractions than in the case of Polymer 1.

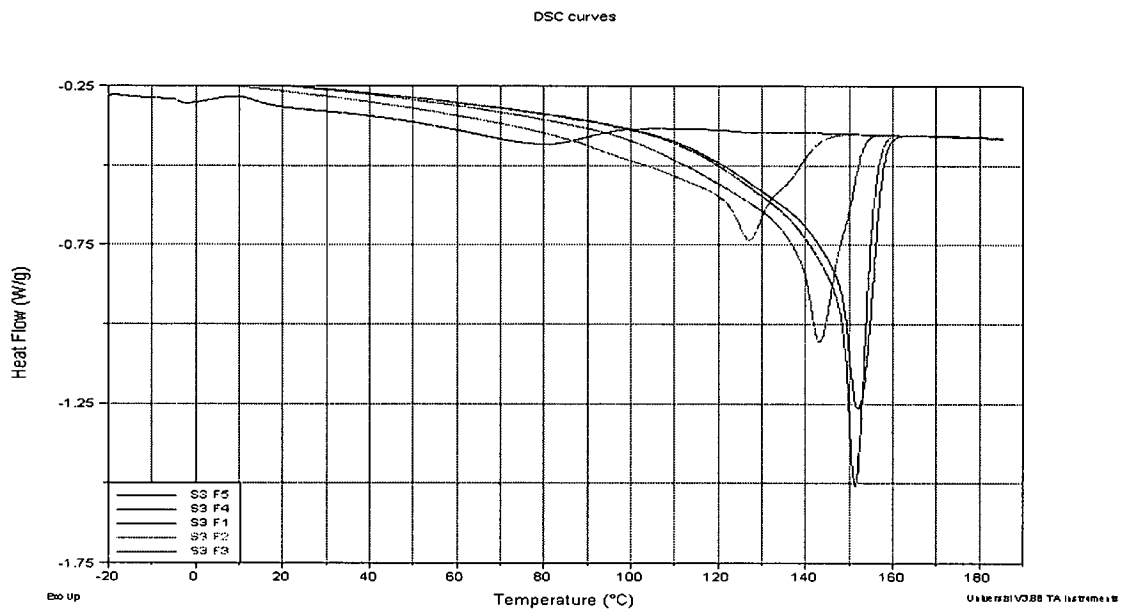

Figure 4.18 *Melting temperature overlays of Polymer 3 TREF fractions.*

Figure 4.18 clearly shows the lower peak melting temperatures for fractions F3, F4 and F5. The peak areas of these fractions are also smaller than the corresponding fractions of Polymer 1, indicating a lower precentage crystallinity in general. Again, this is thought to be due to the higher ethylene comonomer content in Polymer 3, which increases the non-crystalline regions and also lowers the peak melting temperature.

The relationship of the elution temperatures and the thermal properties namely, melting peak temperature and crystallinity was established. These two parameters were individually plotted as a function of elution temperature for Polymers 1, 2 and 3, fractions F1 to F6. Figures 4.19 and 4.20 illustrate the relationship between the elution temperature and the peak melting temperature and crystallinity, respectively, for the fractions, obtained by TREF, for the propylene/ethylene random copolymers.

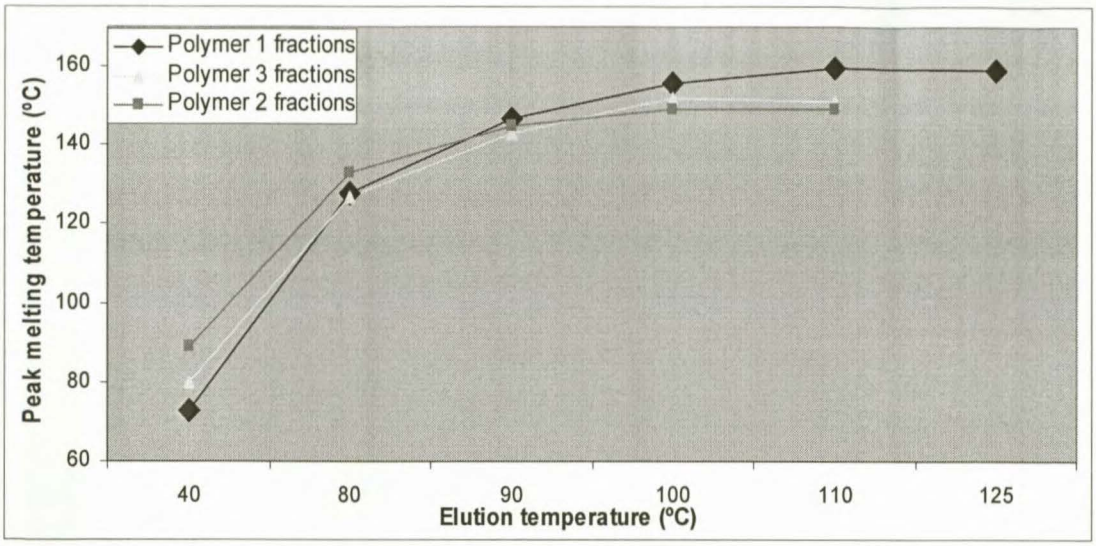

Figure 4.19 *The peak melting temperature versus elution temperature.*

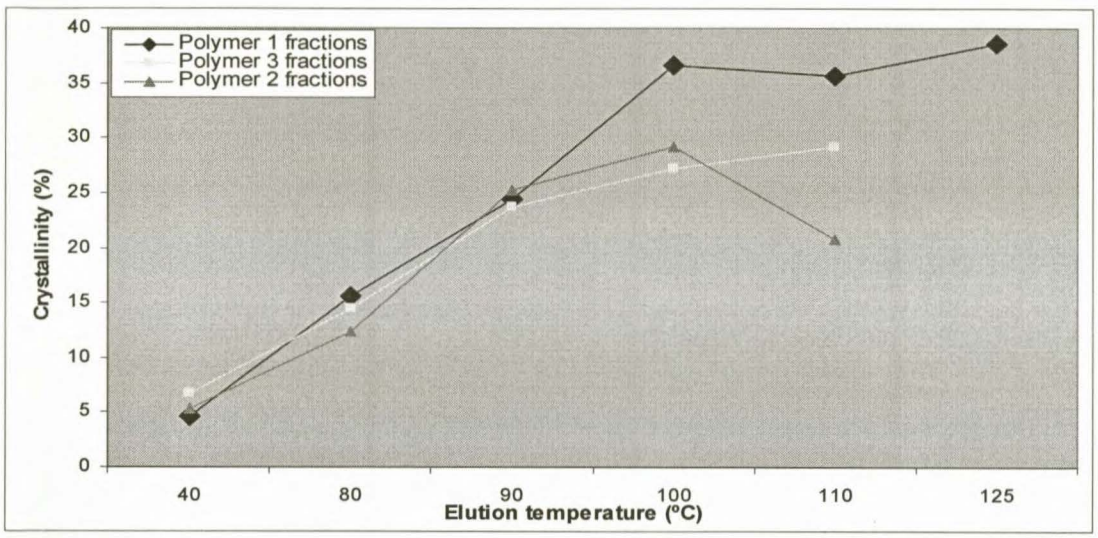

Figure 4.20 *The crystallinity of TREF fractions plotted as a function of elution temperature.*

From these two sets of results it is apparent that fractionation of the samples occurred in increasing order of the crystalline regions in the samples. The more crystalline materials were eluted at higher temperatures whereas less crystalline fractions were eluted at lower temperatures as stated in literature [8].

Polymer 2 fractions eluted at higher temperatures, for example between 100 °C and 110 °C have almost similar melting peak temperatures although their percentage crystallinity differs by an average of 9%. This observation confirms the fact that peak melting temperature is dependent only on the crystals lamellae size and not crystallinity itself. In Polymers 1, 2 and 3 differences in crystallinity at higher elution temperatures (100 and 110 °C) are mostly negligible for the respective fractions. It is clear from the TREF fractionation that the

distribution of ethylene in Polymers 2 and 3 are different; while the ethylene contents are very similar, the crystallization behaviour of the fractions are noticeably different, see for example the fraction eluted at 80 °C.

In general, the TREF principle for separation of various fractions is clearly evident in the results obtained from the DSC.

4.6 The interpretation of the homopolymer soluble fractions results.

The homopolymer samples labelled as Polymers 6 to 9 were analyzed on the Minispec NMR to determine their R21 values and, according to that, the calculated xylene solubles. The calibration curve used in the determination of the calculated xylene solubles was established using samples produced from the same plant that produced the homopolymer test samples.

This eliminates the uncertainty of the influence of "foreign" parameters such as catalyst and donor differences on the xylene solubles of a particular product. The catalyst and the external donors are known to have a substantial impact on the R21 and xylene solubles since they regulate the stereochemistry of the polymer [7]. This holds true for propylene homopolymers. In the case of the random copolymers, the amorphous (soluble) fractions can also be influenced by the comonomer incorporation.

Table 4.11 indicates the R21 values, calculated xylene solubles and the wet xylene solubles of the homopolymer samples.

Table 4.11: *The R21 values and the xylene solubles results of the homopolymer samples.*

Polymer number	R21	Calculated xylene solubles (%)	Wet xylene solubles (%)	Standard deviation
6	6.7	1.8	1.6	0.14
7	9.5	5.0	4.7	0.21
8	7.5	2.6	2.8	0.14
9	7.5	2.6	2.9	0.21

The R21 values were plotted as a function of wet xylene solubles in Figure 4.21 to establish the correlation between the calculated and wet xylene solubles. The standard deviations between the calculated and wet xylene solubles tests for Polymers 6, 7, 8 and 9 are insignificant. This indicates a good correlation between the wet and calculated xylene solubles measurements.

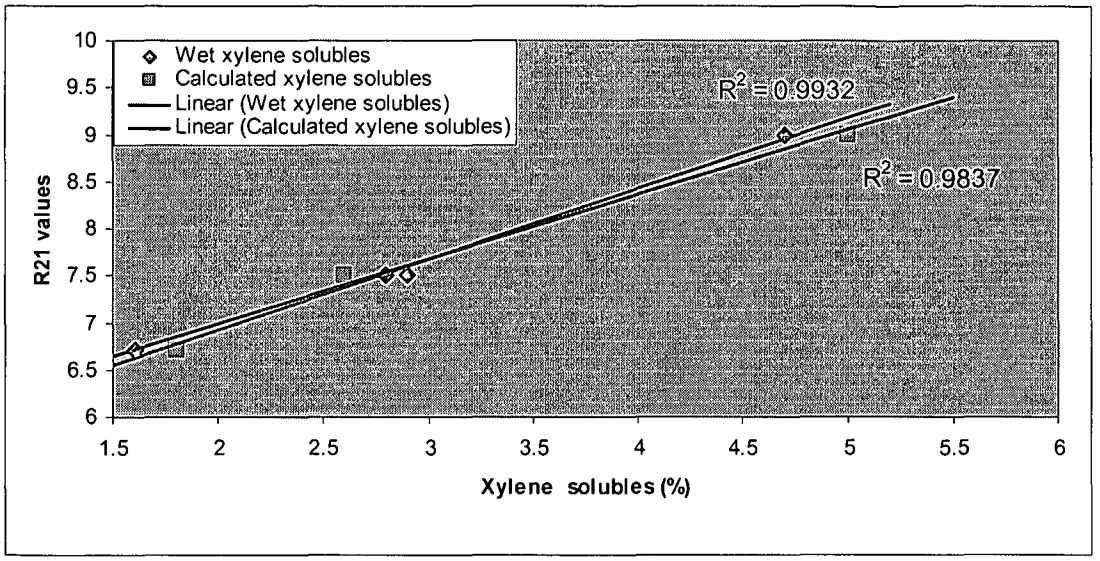

Figure 4.21 *The R21 values and xylene solubles correlation graph.*

Good correlation between the R21 and xylene solubles measurements is emphasized by the correlation coefficient values (R^2) of above 0.98, as shown in Figure 4.21.

It is also observed from the homopolymer results that the controlled rheology processing step does not have a great influence on the R21 and xylene solubles results. This statement is supported by the results of Polymers 8 and 9 which are a controlled rheology grade and reactor grade, respectively, and still exhibit the same xylene solubles results. This is an indication that the vis-breaking process mainly influences molecular weight and MWD, but does not affect the chemical make-up and stereochemistry of the materials significantly.

The homopolymer samples were also extracted using decalin as a solvent in order to perform a comparative study between extracts obtained with xylene and decalin. The results of the xylene and decalin solvent extractions are shown in Table 4.12

Table 4.12 *The results of the xylene and decalin homopolymer soluble fractions.*

Polymer number	Decalin solubles (%)	Calculated xylene solubles (%)	Wet xylene solubles (%)	R21 values
6	9.9	1.8	1.6	6.7
7	15.4	5.0	4.7	9.5
8	11.4	2.6	2.8	7.5
9	15.3	2.6	2.9	7.5

The results displayed in Table 4.12 show substantial differences in the amount of xylene and decalin solubles. Decalin extracts higher amounts of soluble fraction than xylene. This might be due to higher solvent strength of decalin. While it is known that the amount of xylene

solubles is used to give an estimate of the amorphous material in the polymer it is not clear as to what would the decalin solubles represent [9]. Elaboration on the decalin solubles is quite difficult because of the limited amount of publications or research work done on this subject.

Figure 4.23 illustrates the differences in the amount of decalin and xylene solubles. It also demonstrates the correlation existing between the R21 values and the xylene and decalin solubles.

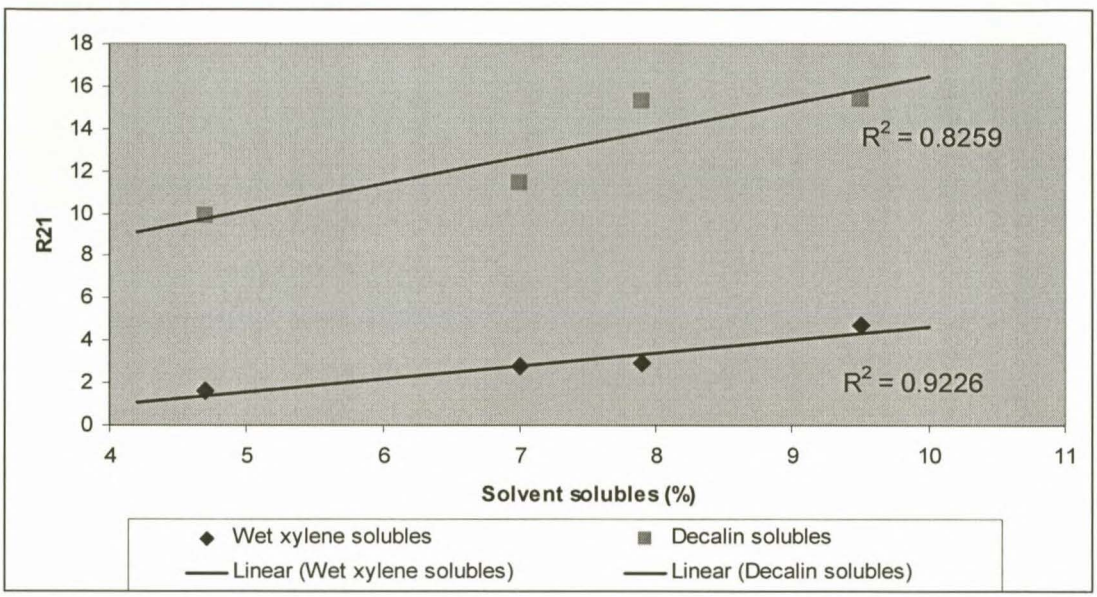

Figure 4.22 *The correlation between the homopolymer R21 values and the soluble fractions.*

Although there is an absolute difference between the xylene and decalin solubles results, a linear relationship is observed for both fractions when plotted against the R21 values. The xylene solubles and R21 values do however show a better correlation than that for the decalin solubles. The R^2 values are 0.9226 and 0.8259 for the xylene and decalin solubles, respectively.

The better correlation between the R21 and xylene solubles is expected since the current calibration line was established using xylene extractions of polymer samples of increasing xylene solubles produced from the same plant. Once again, the above leads to the conclusion that the R21 technique holds for homopolymers, but not for copolymers, the difference in xylene and decalin notwithstanding.

A correlation between the xylene and decalin solubles of the homopolymer samples was also determined. Figure 4.23 shows the relationship between the wet xylene solubles and decalin solubles.

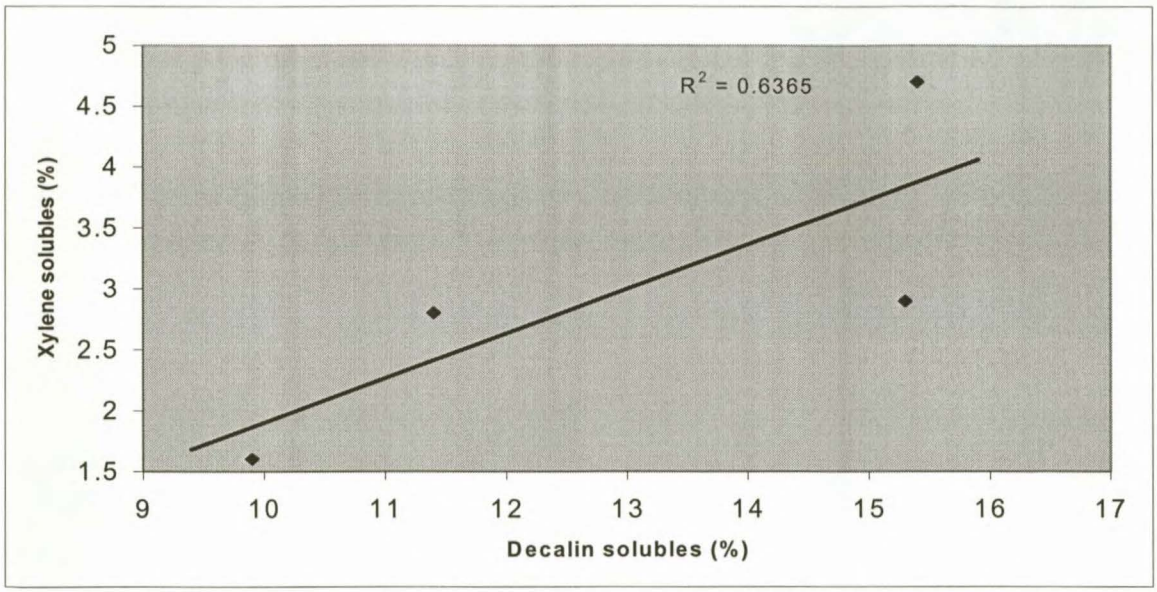

Figure 4.23 *Correlation between the xylene and decalin homopolymer soluble fractions.*

There is a poor correlation between the xylene and the decalin solubles since the data points are scattered on the graph.

4.6.1 The interpretation of the GPC results of the homopolymer soluble fractions.

The solvent soluble fractions were characterised on the GPC and the results are shown in Table 4.13.

Table 4.13 *The GPC results of the homopolymer solvent extracted fractions.*

	Xylene soluble fractions			Decalin soluble fractions		
Polymer number	$\overline{M_w}$	$\overline{M_n}$	MWD	$\overline{M_w}$	$\overline{M_n}$	MWD
6	50 000	2 000	25	50 000	20 000	2.5
7	130 000	8 000	17	115 000	35 000	3.5
8	60 000	3 000	20	30 000	20 000	1.5
9	135 000	9 000	15	55 000	25 000	2.2

In general, the xylene solubles have higher molecular weight than the decalin soluble fractions. Polymer 6 has equivalent molecular weight values for both the xylene and decalin fractions. On the contrary, the MWD value of Polymer 6 decalin soluble differs substantially from that of the xylene soluble fractions. The xylene soluble fractions have extremely broad MWD ranging from 15 to 25 whereas the decalin soluble fractions have MWD values of 1.5 to 2.5. This indicates that the molecular weight range extracted by xylene is far wider than that achieved by decalin.

4.6.2 The ^{13}C NMR analysis of the homopolymer soluble fractions

The ^{13}C NMR analyses were conducted on the xylene and decalin soluble fractions of the homopolymer samples as well. Polymer 7 was used as representative sample for the other homopolymers. The full-scale ^{13}C NMR spectra and their methyl region are shown in Figure 4.24 (a) and (b) and Figure 4.24 (b) and (c) for xylene and decalin solubles, respectively.

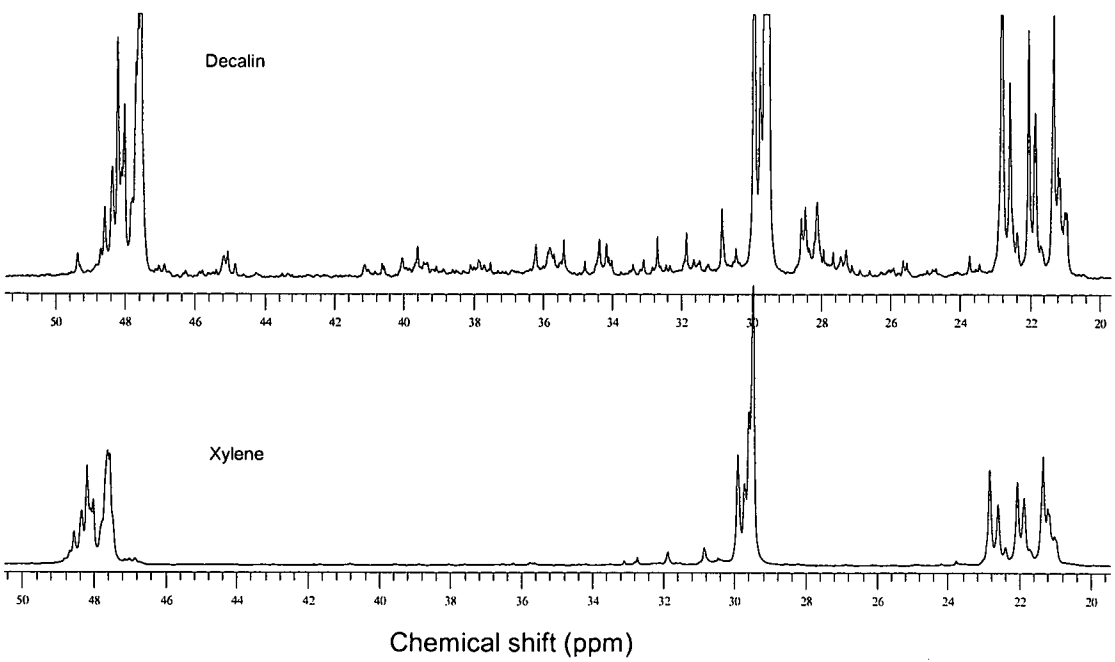

Figure 4.24 (a) *The ^{13}C NMR spectrum of the Polymer 7 xylene and decalin soluble fraction*

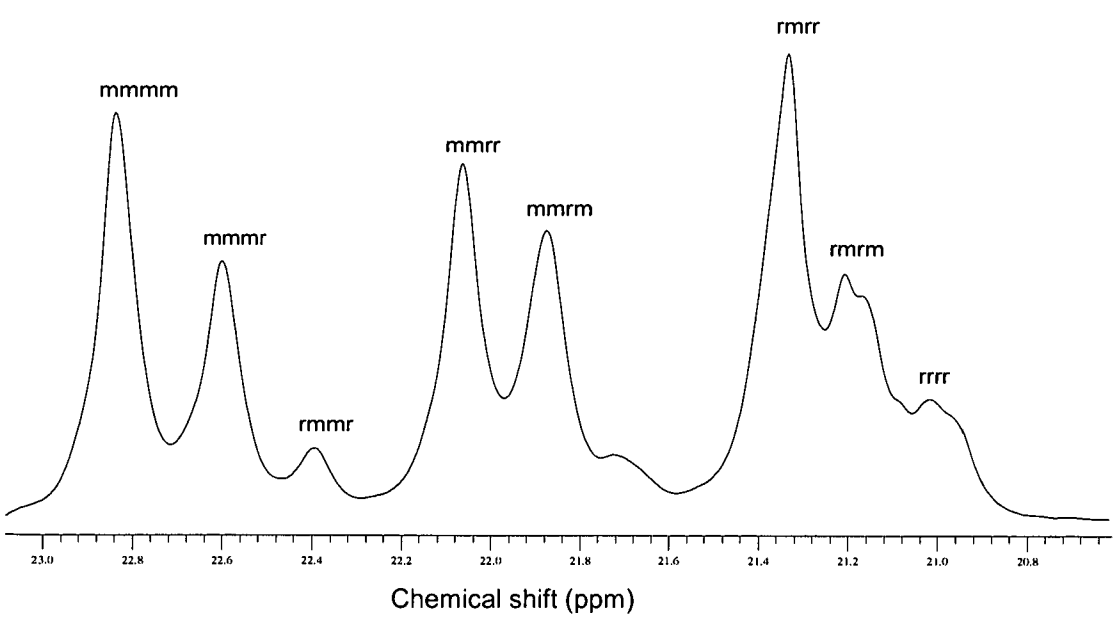

Figure 4.24 (b) *The methyl region of Polymer 7 xylene soluble fractions.*

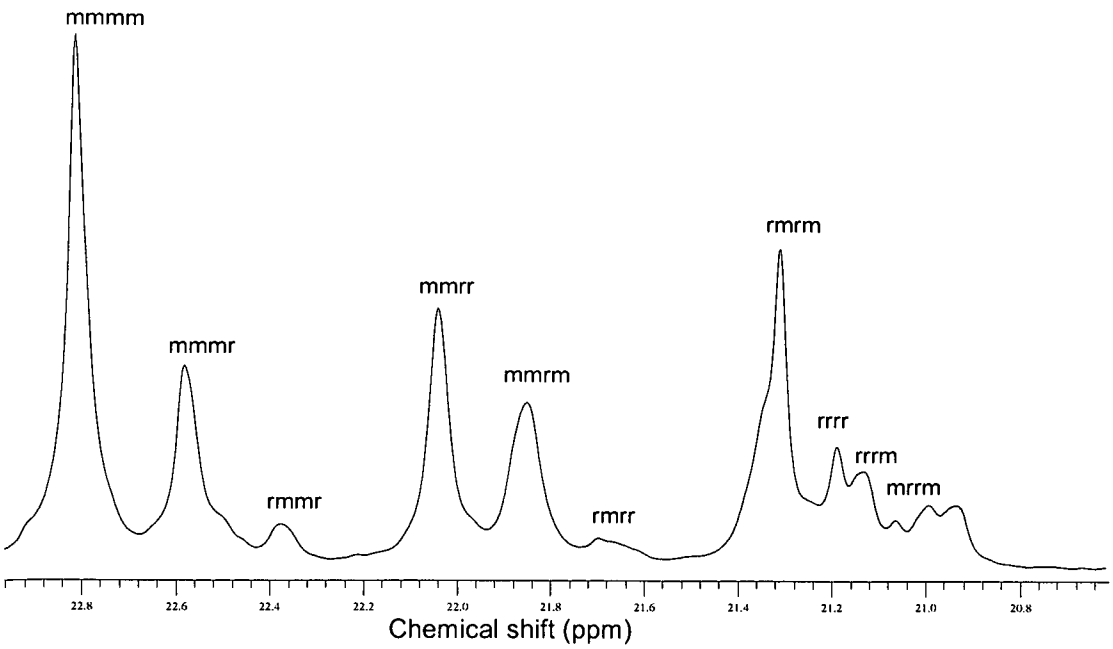

Figure 4.24(c) *The methyl region of Polymer 7 decalin soluble fractions.*

The spectrum for the decalin soluble fraction shown in Figure 4.24 (c) indicates that the sample is somewhat less atactic than it is the case with xylene soluble material (Figure 4.24 (b)). This observation, combined with the fact that more material is extracted by decalin than xylene (15.4% vs 4.7%) indicates that the decalin soluble fractions are much more complex than the xylene fractions.

The NMR spectra of the xylene and decalin solubles clearly show that xylene soluble fractions are more atactic than decalin solubles. This shows that decalin does extract some crystalline PP units in quantities not detectable on the DSC. Polymer 7 xylene soluble fractions have isotacticity of approximately 14% whereas the decalin soluble fractions are 20% isotactic.

The results indicate that decalin extracts what xylene does, as well as the low molecular weight isotactic polymer. Figure 4.24 (a) shows a higher number of regioerrors possibly resulting from the misinsertion of the propylene units. The latter might remain behind as a result of slow solution crystallization of PP out of decalin.

4.7 Evaluation of the R21 values and the solvent solubles of the propylene-ethylene random copolymers.

The benchtop Minispec NMR technique was employed to determine the R21 values and the calculated xylene solubles. The R21 measurement is an "in-house" technique utilized to provide an average value for polymer isotacticity. The results of the wet xylene solubles are included in Table 4.14 for comparison purposes. The ethylene content is included in the results since it affects the amount of extractable fractions significantly.

Table 4.14 *The R21 values and xylene solubles results of the copolymer fractions.*

Polymer number	R21	Calculated xylene solubles (%)	Wet xylene solubles (%)	Ethylene content (wt %)
1	9.0	4.4	3.2	0.87
2	16.0	12.0	5.9	4.3
3	17.0	13.0	7.7	3.9
4	16.0	12.0	6.9	5.0
5	17.0	13.0	6.8	4.6

The R21 values are obtained from the Mini Spec NMR spectrometer. These values are then converted to xylene solubles using an equation obtained from the xylene solubles calibration line. The wet xylene solubles results are obtained from the conventional solvent extraction method using the equation outlined in Chapter 3 under Section 3.5.2.

From Table 4.14 it can be seen that there are substantial differences between the R21 values of Polymer 1 and Polymers 2, 3, 4 and 5. The distinguishing feature between these samples is the variation in the ethylene content. The R21 (xylene solubles) results confirm that as the comonomer content increases the soluble materials also increases [2].

The variance between the calculated and wet xylene solubles was found to be higher than the maximum allowed experimental error of 10%. This variance result from the fact that the calibration curve used in the calculation propylene-ethylene random copolymer samples xylene solubles was established using materials produced from a different technology. Additionally, the results could also be influenced by different catalysts and donors utilised in the polymerisation processes by these two technologies.

What can be deducted from this observation is that a calibration curve needs to be established using the ethylene random copolymer samples of increasing xylene solubles produced from a similar technology. This will assist in eliminating the influence of factors such as catalyst and donor differences on the soluble materials.

In this instance, the wet xylene solubles are the preferred results over the calculated xylene solubles. The wet xylene solubles are obtained through the extraction technique, which does not necessarily discriminate the polymers based on their production technology. It appears as if the R21 calibration curve is inappropriate for ethylene random copolymers. Therefore, it can be concluded that there is no correlation between the R21 (calculated xylene solubles) and the wet xylene solubles of the propylene-ethylene random copolymer samples.

The xylene soluble results were further compared to the decalin soluble results. The major distinction between xylene and decalin extractions is the extraction temperature. The xylene

extractions were conducted at 135 °C and the decalin extractions at 185 °C. The same method was used in performing xylene and decalin extractions and complete solubility of polymer was observed in both cases.

The significance of this exercise originates from the fact that the technology from which the homopolymer samples were produced uses xylene solubles as a measure of the polymer isotacticity. Conversely, the technology used to produce the propylene-ethylene random copolymers utilizes decalin solubles for the same purpose. Consequently, it is imperative to understand the similarities and the differences in the fractions obtained from xylene and decalin. Table 4.15 indicates the results of xylene and decalin soluble material.

Table 4.15 *The results of the wet xylene and decalin soluble tests.*

Polymer number	Ethylene content (wt %)	Decalin solubles (%)	Xylene solubles (%)	R21 values
1	0.87	8.2	3.2	9.0
2	4.30	14.4	5.9	16.0
3	3.90	25.0	7.7	17.0
4	5.00	19.5	6.9	16.0
5	4.60	22.2	6.8	17.0

One of the vital points associated with solvent extracted fractions is the quantity of the soluble materials extracted by these solvents. The amount of extracted materials is used in industries to give an estimation of the polymer average isotacticity. From Table 4.15, Polymer 3 has higher amounts of soluble material, which translates to increased non-crystalline regions in the polymer matrix. On the contrary, Polymer 1 has the lowest percentage value of xylene and decalin solubles, primarily due to a much lower ethylene content.

The xylene and decalin solubles results of the ethylene random copolymers were plotted against the R21 values. This was to establish the relationship existing between the R21/xylene solubles and R21/decalin solubles as shown in Figure 4.25.

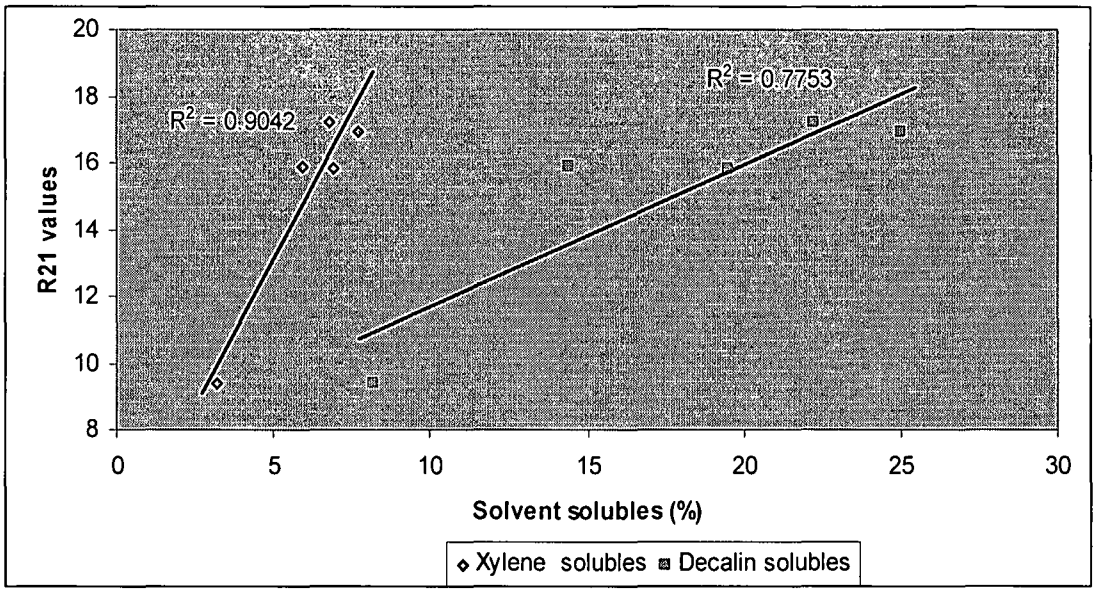

Figure 4.25 *The correlation of the solvent extracted soluble fractions and R21 values.*

Figure 4.25 shows a clear separation between the xylene and decalin extracted fractions. Figure 4.25 shows a better correlation between the R21 values and xylene solubles with a linearity value of 0.90 as compared to the R21 values and decalin solubles correlation having a correlation coefficient (R^2) value of 0.78.

The distribution of the solvent-soluble portion points on the graph indicates that the solvents may be extracting different soluble portions of the polymer material. This was investigated by using DSC, GPC and NMR. Overall, though, it appears as if the R21 technique for predicting xylene solubles (and decalin solubles) is inappropriate for the propylene-ethylene random copolymers.

The decalin soluble fractions were plotted against the xylene solubles to establish any relationship existing between these two measurements, as illustrated in Figure 4.26.

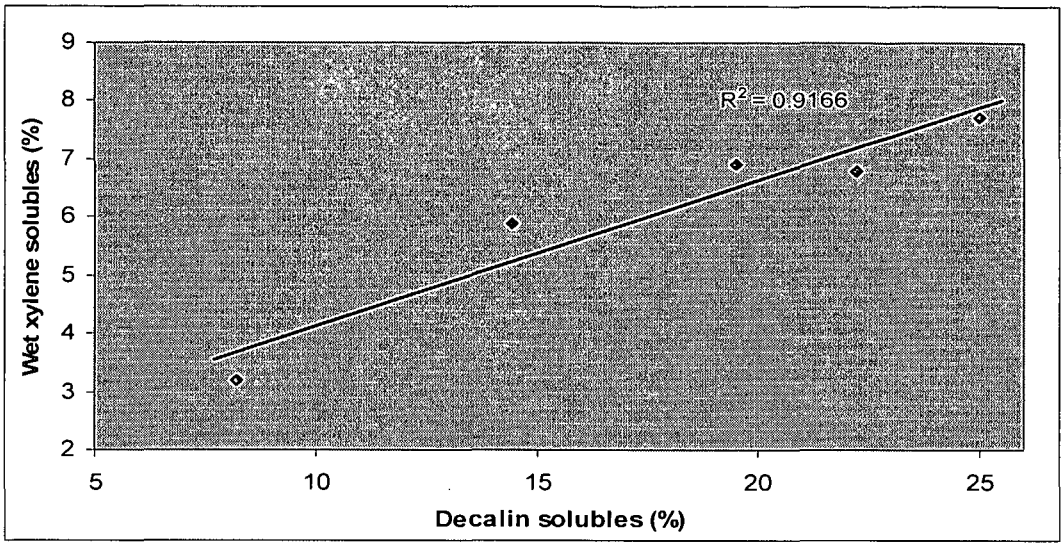

Figure 4.26 *The correlation between wet xylene solubles and decalin solubles.*

An almost linear relationship exists between the xylene and decalin solubles results. It is observed from the graph that as the xylene solubles increases the decalin solubles also increases. However, the absolute amounts of the soluble fractions are considerably different. The presence of un-evaporated decalin in the decalin soluble fractions might have also contributed towards the total mass of the fractions. At the time of this study the appropriate equipment capable of evaporating decalin solvent without subjecting the extractable materials to higher temperatures was not available. Consequently, the evaporation of decalin solvent was cautiously performed to prevent the degradation of the soluble fractions.

4.7.1 The GPC results of the solvent extracted propylene-ethylene random copolymers.

Gel Permeation Chromatography was used to determine the $\overline{Mw}$, $\overline{Mn}$ and MWD of the decalin and xylene soluble fractions and the results are shown in Table 4.16.

Table 4.16: *The GPC results of the copolymer xylene and decalin soluble fractions.*

	Xylene soluble fractions			Decalin soluble fractions		
Polymer number	$\overline{Mw}$	$\overline{Mn}$	**MWD**	$\overline{Mw}$	$\overline{Mn}$	**MWD**
1	90 000	5 000	17.0	120 000	30 000	4.0
2	45 000	5 000	9.0	35 000	15 000	2.3
3	135 000	15 000	9.0	35 000	15 000	2.3
4	45 000	50 00	9.0	30 000	10 000	3.0
5	95 000	10 000	9.5	65 000	25 000	2.6

Table 4.16 shows that xylene generally extracts fractions of higher molecular weight than decalin. However, the decalin soluble fractions have a narrower MWD when compared to the xylene soluble fractions. The differences in the MWD between these fractions are quite significant ranging from 9 to 17 and 2.3 to 4 for the xylene and decalin fractions, respectively.

4.7.2 Thermal properties of xylene and decalin soluble fractions.

The thermal properties of the propylene-ethylene random copolymers xylene and decalin solubles obtained from the DSC were not usable and therefore are not included. These fractions were essentially amorphous materials.

4.7.3 The ^{13}C NMR analysis of xylene and decalin soluble fractions.

The ^{13}C NMR spectrometer was utilized to evaluate the microstructure of the xylene and decalin soluble fractions. This was done in conjunction with the possible microstructures obtained from ACD Labs ^{13}C NMR prediction software as shown in Figures 4.27 and 4.28 [10]. These figures provide good guidelines regarding the type and positions of the ethylene insertions along the polymer chains, and can assist in the interpretation of the microstructure of the extracted fractions.

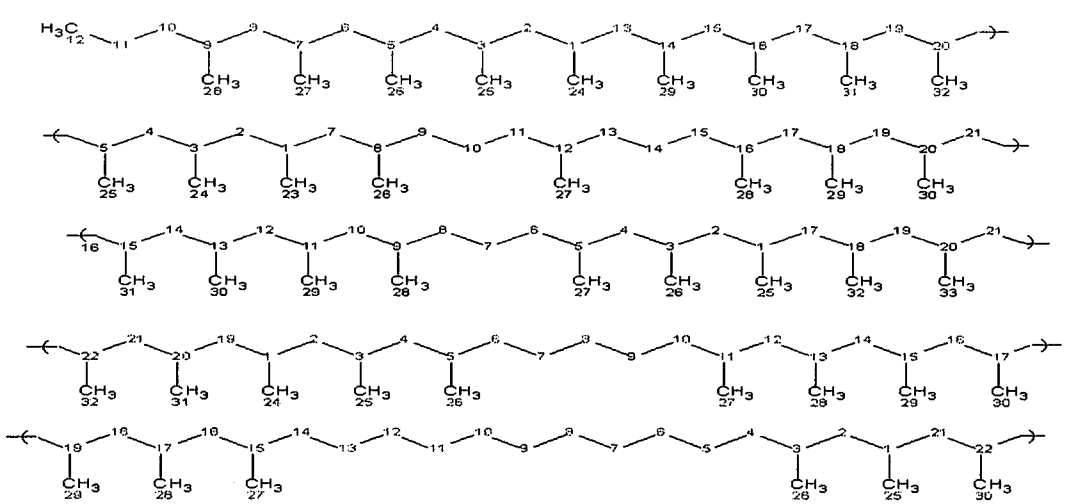

Figure 4.27 *The possible microstructures of the ethylene random copolymer fractions.*

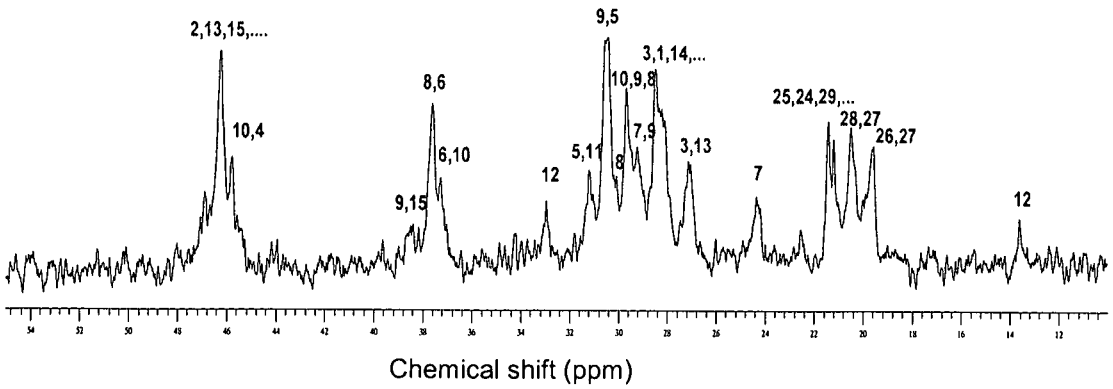

Figure 4.28 *^{13}C NMR spectrum of the ethylene random copolymer soluble fractions.*

The spectrum of the xylene soluble fraction of Polymer 1 is shown in Figure 4.29(a). Additionally, the expanded portion of its methyl region is also reflected in Figure 4.29(b) to allow comprehensive analysis of the polymer isotacticity.

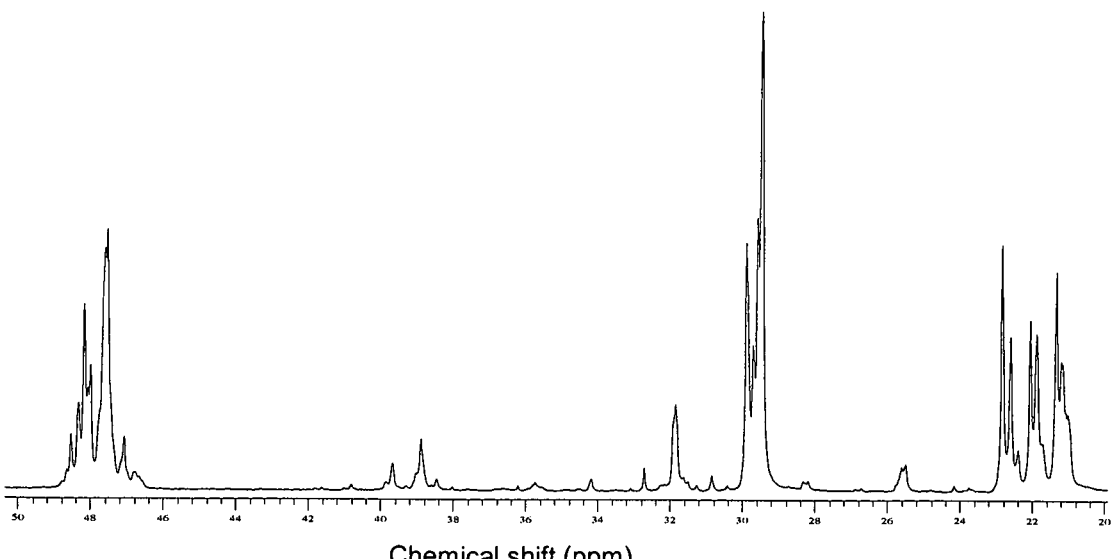

Figure 4.29(a) *The ^{13}C NMR spectrum of Polymer 1 xylene soluble fraction.*

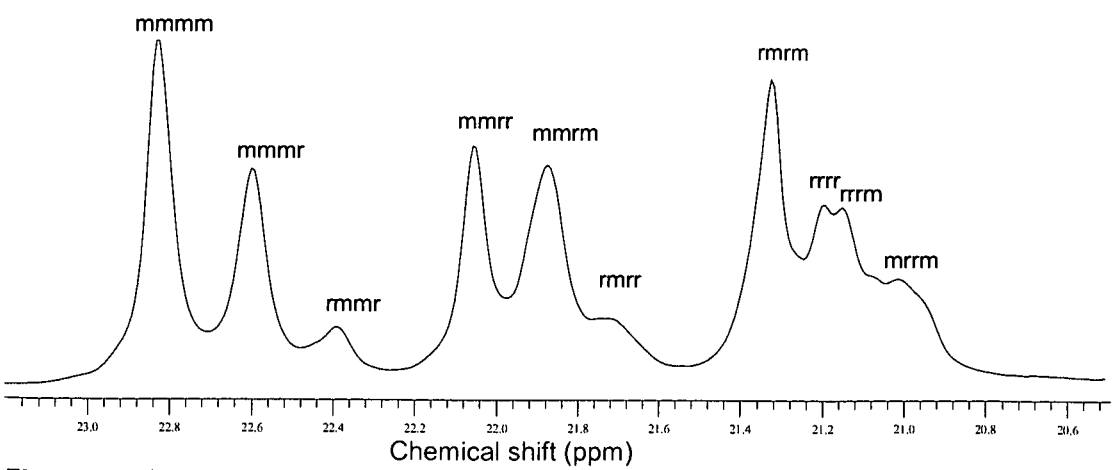

Figure 4.29(b) *The methyl region of Polymer 1 xylene soluble fraction.*

When looking at Figure 4.29(a) it is observed that the ethylene peaks are more pronounced in this spectrum than they were in the un-fractionated sample. Apparently material comprising the soluble fraction contain a significant amount of ethylene comonomer. The methyl region spectrum of the xylene soluble part of Polymer 1 shown in Figure 4.29(b) illustrates that the material is mainly atactic.

The ^{13}C NMR spectrum of the decalin soluble fraction of Polymer 1 are shown in Figures 4.30(a) and 4.30(b).

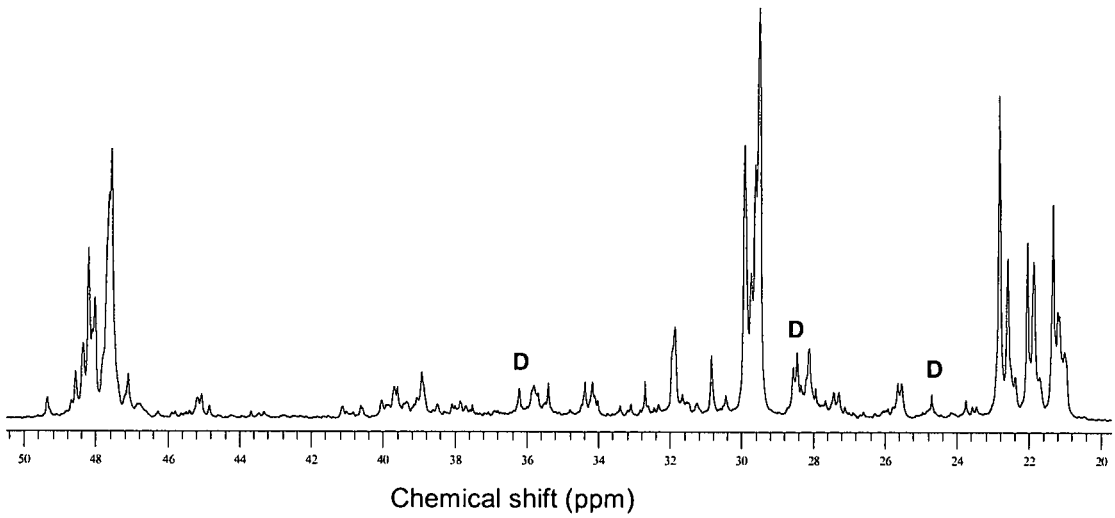

Figure 4.30(a) *The ^{13}C NMR spectrum of Polymer 1 decalin soluble fraction.*

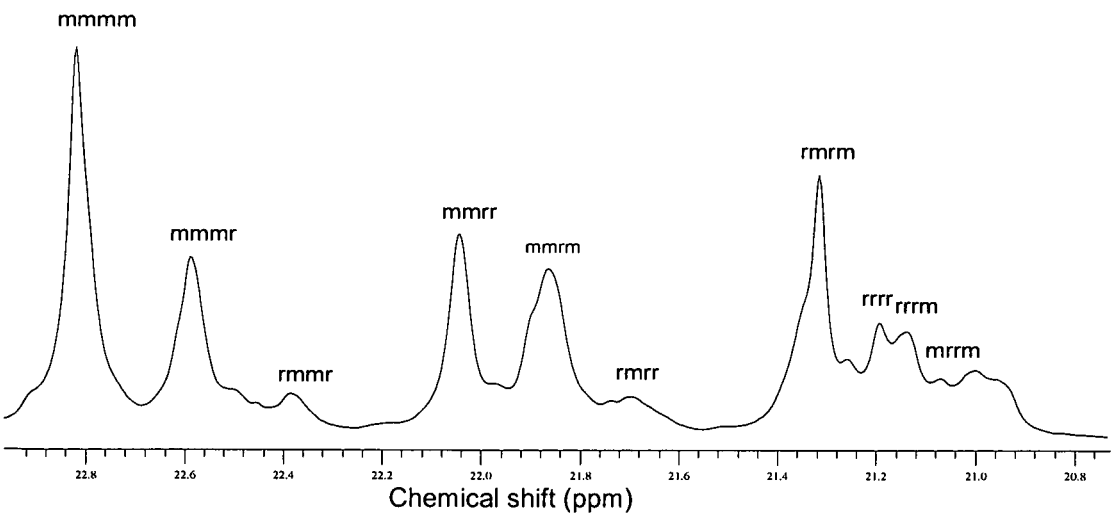

Figure 4.30(b) *The methyl region of Polymer 1 decalin soluble fraction.*

Comparatively, the ^{13}C NMR spectra of Polymer 1 xylene and decalin soluble fractions show that these fractions are chemically different. From the ^{13}C NMR spectra, it appears that the decalin soluble fraction contains less ethylene rich copolymer than the xylene soluble fraction. Isolated ethylene comonomer insertions are observed in both the xylene and decalin spectra. These peaks appear at ~ 26 ppm, 32 ppm, 39 ppm and 47 ppm.

In addition to the ethylene peaks observed on the decalin spectrum, peaks resulting from decalin itself **(marked with a D)** were also detected. These peaks appear at ~25 ppm, 29 ppm and 37 ppm. Again, this shows the difficulty to completely evaporate decalin from the soluble fractions without degrading the polymer due to the higher boiling point of the solvent.

Figure 4.29(b) and 4.30(b) representing the methyl region of the xylene and decalin solubles indicates that these fractions are essentially amorphous. Decalin soluble fractions appear to be slightly more isotactic. This was confirmed by the integration of the methyl regions of the respective fractions. The decalin soluble fraction has 17.6% isotacticity (*mmmm*%) against 13.7% isotacticity of the xylene soluble fraction. Furthermore, the GPC results showed that generally the decalin fractions have lower molecular weight than the xylene fractions. This can also be attributed to the slow solution crystallization of PP out of decalin.

Further comparison between the xylene and decalin solubles was conducted on the samples of higher ethylene content. Polymer 2 was selected as a representative sample for Polymers 3, 4 and 5. The ^{13}C NMR spectra of the xylene soluble fraction of Polymer 2, and its methyl region are shown in Figures 4.31(a) and 4.31(b) whereas, the decalin soluble fractions are shown in Figure 4.32(a) and 4.32(b).

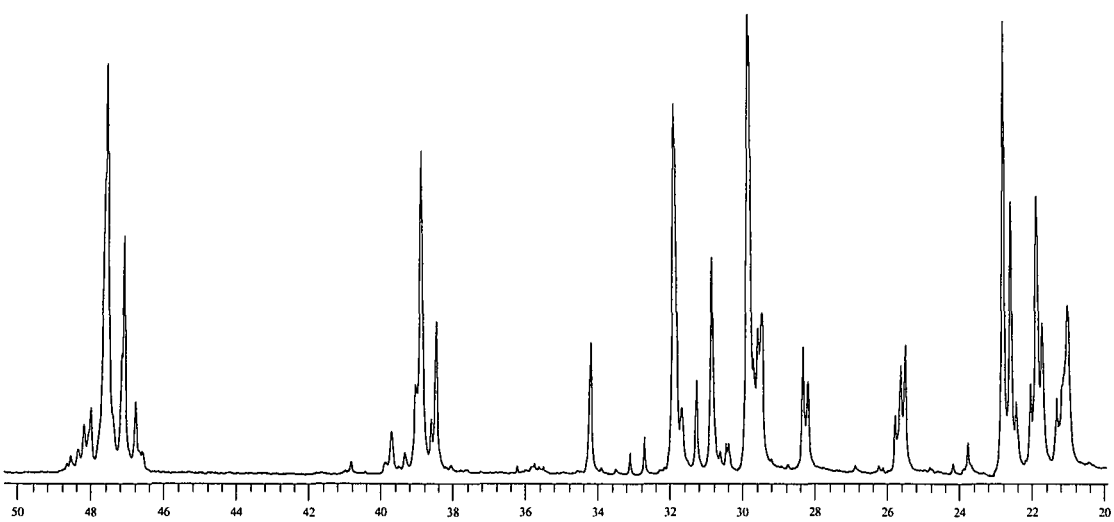

Figure 4.31(a) *The ^{13}C NMR spectrum of Polymer 2 xylene soluble fraction.*

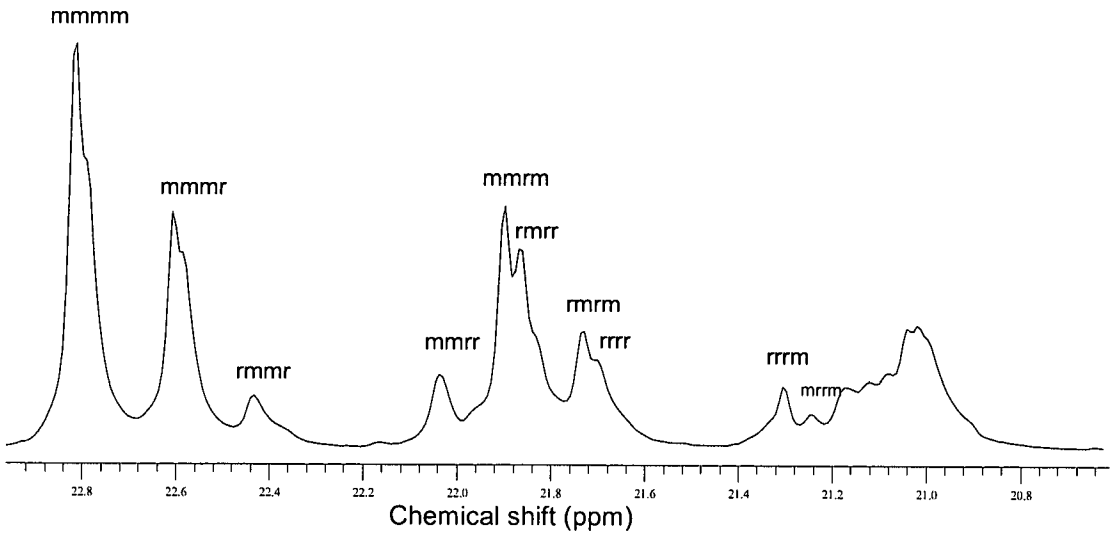

Figure 4.31(b) *The methyl region of Polymer 2 xylene soluble fractions.*

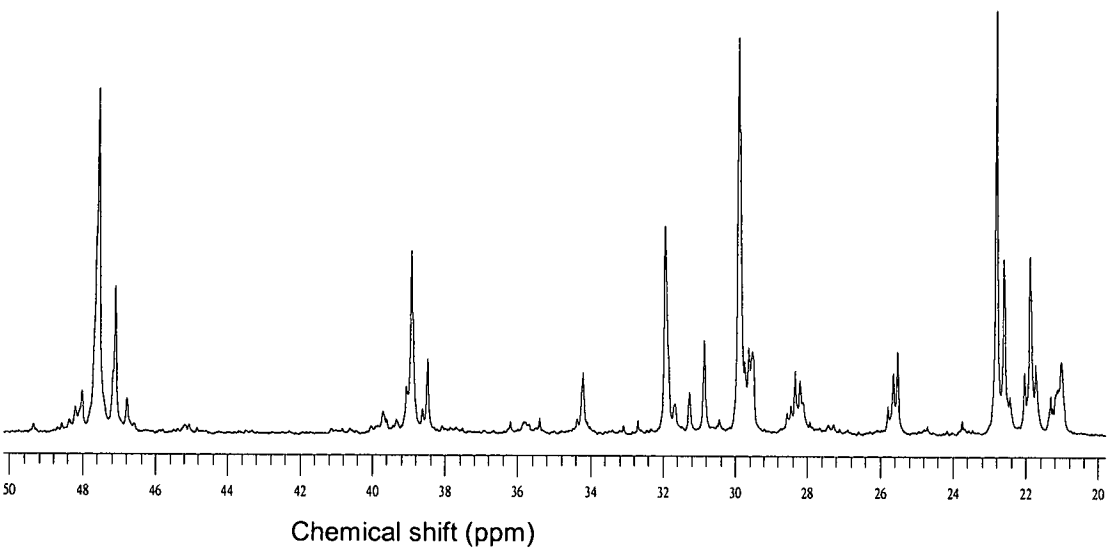

Figure 4.32(a) *The ^{13}C NMR spectrum of Polymer 2 decalin soluble fraction.*

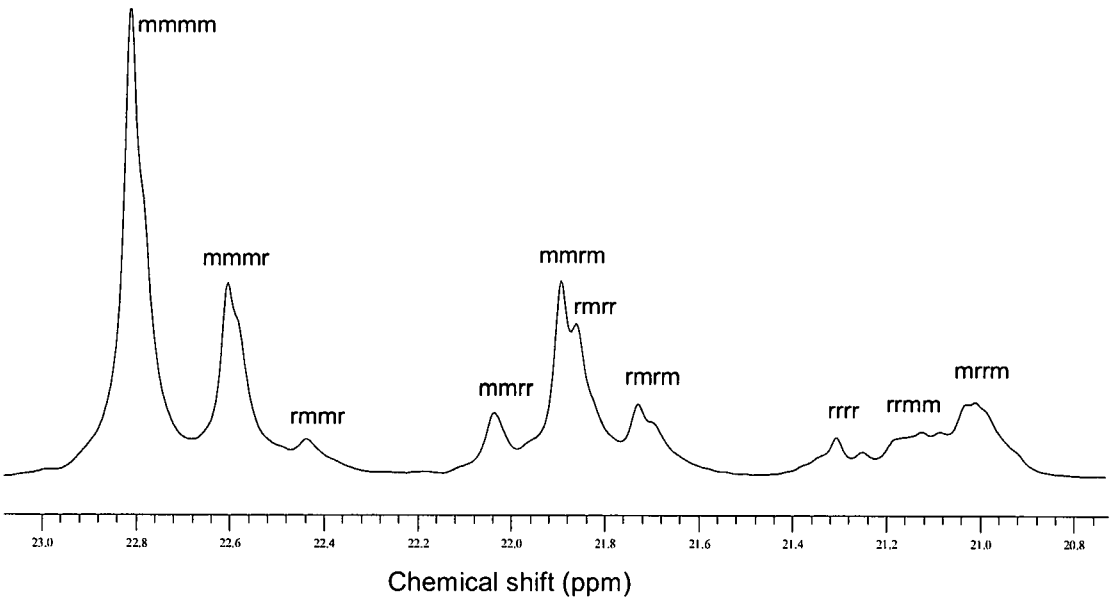

Figure 4.32(b) *The methyl region of Polymer 2 decalin soluble fractions.*

The ^{13}C NMR spectra of the xylene and decalin soluble fractions of Polymer 2 show similar results as those found for Polymer 1. This indicates that these fractions are mainly atactic. The trend observed in the results is that the decalin soluble materials have higher isotacticity percentage than the xylene soluble for both samples. The xylene and decalin soluble fractions of Polymer 2 have isotacticity values of 22% and 28%, respectively, which are higher than those of the Polymer 1 fractions.

The wet xylene and decalin solubles results and the R21 values show that Polymer 1 has lower amounts of soluble material than Polymer 2. However, the soluble fractions of Polymer 2 have more isotactic regions than Polymer 1 as shown by the ^{13}C NMR results.

Again, the ethylene peaks are more pronounced in the spectra of the xylene soluble materials, which indicate that the greatest percentage of the extracted material contains some ethylene. In the case of the decalin extracts, the conentration of ethylen is lower, but the amount of material extracted is more. This also indicates that decalin might be extracting everything that xylene extracts, as well as some crystalline material.

4.8 The evaluation of the homopolymer xylene and decalin insoluble fractions.

4.8.1 GPC analysis of the homopolymer insoluble fractions.

The xylene and decalin insoluble fractions of the homopolymer samples were characterized by GPC to determine molecular weight and MWD and the results are shown in Table 4.17.

Table 4.17 *The GPC analysis of the homopolymer decalin and xylene insoluble fractions.*

	Xylene insoluble fractions			Decalin insoluble fractions		
Polymer number	$\overline{M}_w$	$\overline{M}_n$	MWD	$\overline{M}_w$	$\overline{M}_n$	MWD
6	410 000	70 000	5.8	230 000	100 000	2.3
7	500 000	96 000	2.3	285 000	95 000	3.0
8	315 000	79 000	4.0	195 000	75 000	2.6
9	330 000	93 000	4.2	290 000	115 000	2.5

From Table 4.17, it is observed that the xylene insoluble fractions have higher molecular weight than decalin fractions. This observation means that the xylene and decalin solvents extract various components of the polymer from a molecular weight perspective. GPC overlays of the xylene and decalin insoluble fractions are also attached as Figures 4.33 and 4.34 to illustrate the molecular weight shifts of various fractions on the chromatograms.

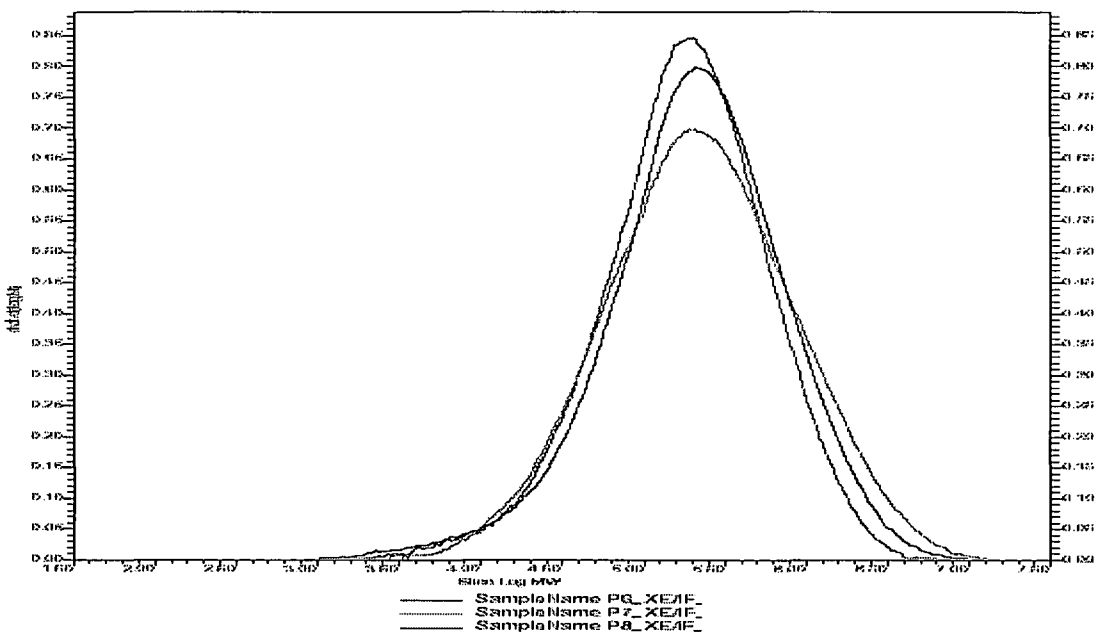

Figure 4.33 *GPC overlays of the homopolymer xylene insoluble fractions.*

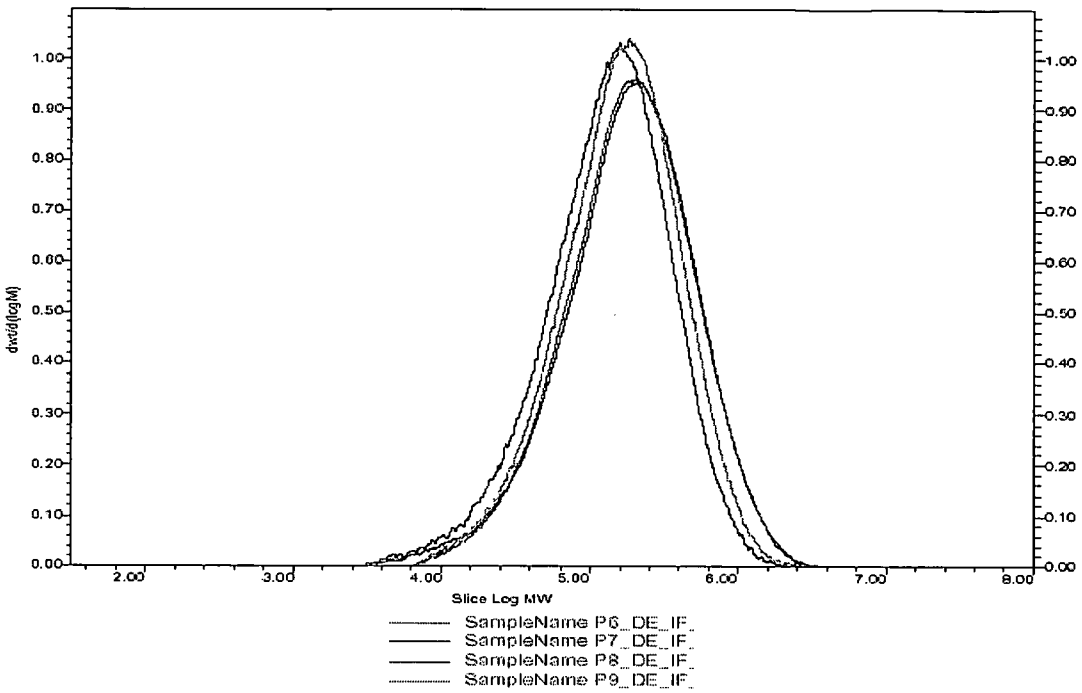

Figure 4.34 *GPC overlays of the homopolymer decalin insoluble fractions.*

The xylene insoluble fractions generally have broader molecular weight distribution (MWD) whilst the decalin insoluble fractions have narrower MWD. This is a result of the decrease in the Mw values for the decalin-extracted materials, while the $\overline{M_n}$ values remained constant. Polymer 6 shows significant differences between the MWD values of the xylene and decalin insoluble fractions. Polymer 7, with the highest xylene solubles percentage, shows the least variation in the MWD values of the xylene and decalin insoluble fractions. This could possibly mean that both solvents easily extracted the soluble materials present in Polymer 7.

Also, the decalin insoluble fractions of Polymer 7 are the only exception with higher MWD value than the corresponding xylene insoluble fractions. The fact that decalin insoluble fractions generally have narrower MWD may be an indication that decalin is extracting more homogenous fractions than the xylene.

4.8.2 Thermal properties of the homopolymer insoluble fractions.

Table 4.18 gives the DSC results of the xylene and decalin insoluble homopolymer fractions.

Table 4.18 *The thermal properties of xylene and decalin homopolymer insoluble fractions*

	Xylene insoluble fractions		Decalin insoluble fractions	
Polymer number	**Melting temperature (°C)**	**Crystallinity (%)**	**Melting temperature (°C)**	**Crystallinity (%)**
6	165	36	160	13
7	164	29	158	20
8	160	17	158	10
9	164	33	160	32

Polymer 6's xylene insoluble fraction, with a crystallinity value of 36%, has the highest peak melting temperature of 165 °C. However, the corresponding decalin insoluble fraction has a slightly lower peak melting temperature of 160 °C and is 13% crystalline. The main distinction between the two fractions lies in the significant differences in their respective crystallinity values. In general the xylene insoluble fractions have higher peak melting temperatures and percentage crystallinity. Figure 4.35 clearly illustrate the differences between the thermal properties of the xylene and decalin insoluble fractions. The xylene insoluble fractions have narrower melting curves whereas the decalin fractions melt over a wider temperature.

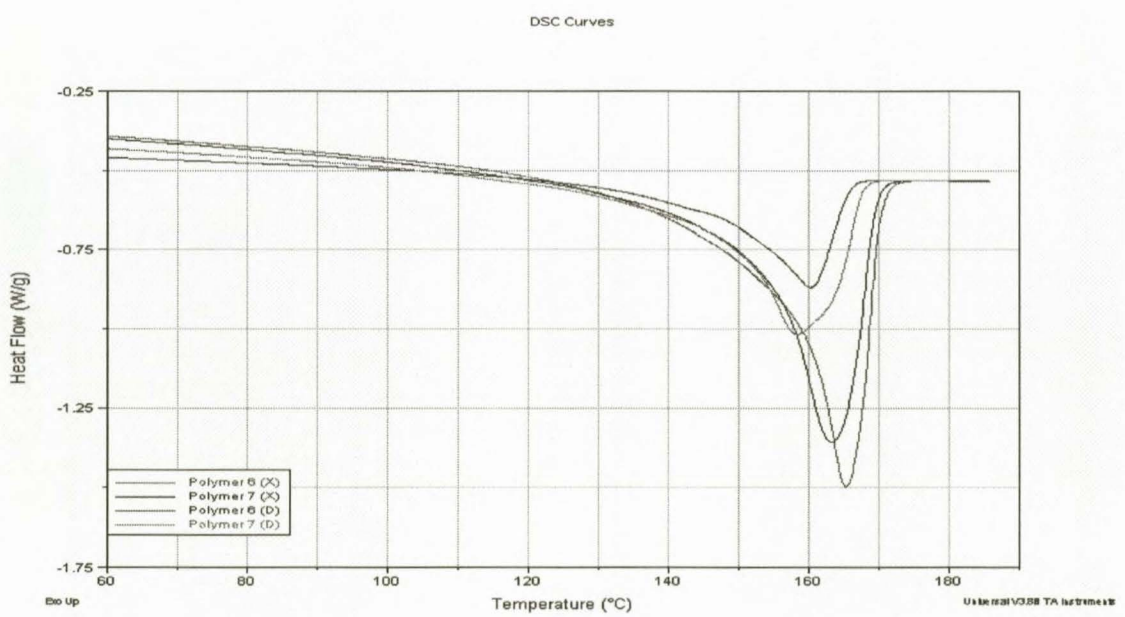

Figure 4.35 *The melting overlays of the homopolymer xylene and decalin insoluble fractions.*

The decalin homopolymer insoluble fractions show a reduced peak area when compared to the xylene insoluble fractions, indicative of a lower percentage crystallinity. It is possible that

some of the DSC's samples extracted by decalin (post-extraction) show broad peaks due to still being wet with decalin. The fact that the overall crystallinity of the material that had been extracted with decalin is lower than that of materials extracted with xylene also supports the premise that decalin extracts some crystalline material, that xylene does not. These crystalline materials might have not been detected by DSC in the soluble fractions probably due to insufficient crystalline units constituting the fractions as explained under Section 4.7.2.

4.8.3 The ^{13}C NMR analysis of the homopolymer insoluble fractions.

The insoluble homopolymer fractions were characterized using ^{13}C NMR spectrometry The Polymer 7 spectrum is shown in Figure 4.36 and represents the other homopolymer samples since their ^{13}C NMR spectra are similar.

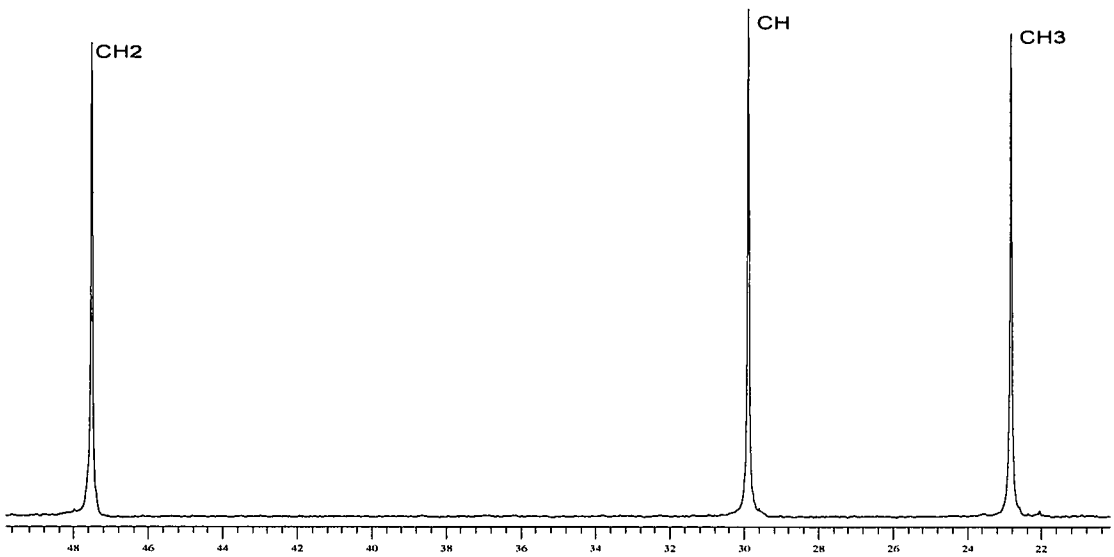

Figure 4.36 *The ^{13}C NMR spectrum of Polymer 7 xylene insoluble fraction.*

The spectrum shows that Polymer 7 xylene insoluble fractions are pure polypropylene with only the CH_3, CH_2 and CH peaks detectable. Peak integration was done on the methyl peak to determine the isotacticity and this was found to be approximately 94%. A similar exercise was performed on the corresponding decalin insoluble fraction shown in Figure 4.37 and the isotacticity in this case was measured to be 91%.

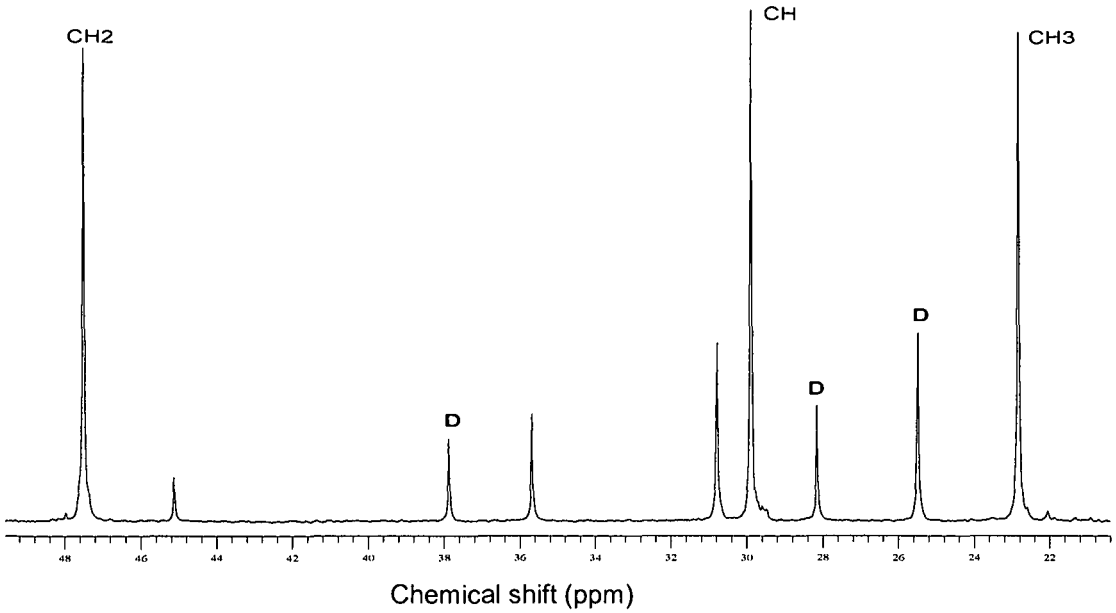

Figure 4.37 *The ^{13}C NMR spectrum of Polymer 7 decalin insoluble fraction.*

The xylene insoluble fractions have a slightly higher isotacticity than the corresponding decalin fraction. This is in line with the DSC results which showed the presence of more crystalline regions in the xylene insoluble fractions. The decalin insoluble fractions microstructure may be influenced by the presence of decalin (marked as D) in the fractions.

4.9 Characterisation of the xylene and decalin copolymer insoluble fractions.

4.9.1 GPC analysis of the propylene-ethylene random copolymer insoluble fractions.

The xylene and decalin insoluble fractions of the ethylene random copolymer samples were analyzed by GPC and the results are displayed in Table 4.19.

Table 4.19 *The GPC analysis of the random copolymer xylene and decalin insoluble fractions.*

	Xylene insoluble fractions			Decalin insoluble fractions		
Polymer number	$\overline{M}_w$	$\overline{M}_n$	MWD	$\overline{M}_w$	$\overline{M}_n$	MWD
1	290 000	89 000	3.3	210 000	100 000	2.1
2	300 000	88 000	3.4	195 000	80 000	2.5
3	670 000	155 000	4.3	280 000	115 000	2.5
4	290 000	87 000	2.3	195 000	80 000	2.4
5	410 000	130 000	3.1	240 000	120 000	2.0

The xylene and decalin insoluble fractions of the controlled rheology random copolymer samples labeled as Polymers 1, 2, 4 and 5 have lower molecular weight values than Polymer

3, which is a reactor grade. It is expected that the reactor grades should generally have higher Mw values than the controlled rheology grades.

From Table 4.19, the xylene insoluble fractions appear to have higher molecular weights than the decalin insoluble materials. Polymers 2 and 5, which are controlled rheology grades, show significant differences in the molecular weight of the corresponding xylene and decalin fractions. Also, the reactor grade labeled as Polymer 3 shows considerable differences in the molecular weight between its xylene and decalin insoluble fractions. Conversely, the MWD is generally higher for the xylene insoluble fractions than for the decalin insolubles.

In addition, the GPC results of the xylene and decalin soluble fractions were compared to the GPC results of the un-fractionated samples shown earlier in Table 4.6. In general, the xylene insoluble fractions have slightly higher molecular weights and molecular numbers than the un-fractionated materials. This result shows that the xylene has extracted most of the lower molecular weight portions as part of the soluble material portion. Conversely, all the decalin insoluble fractions have lower molecular weights than the un-fractionated samples, hence it is difficult to clearly define the type of fractions extracted by decalin.

4.9.2 Thermal properties of the propylene-ethylene random copolymer insoluble fractions.

The thermal properties of the xylene and decalin insoluble fractions are shown in Table 4.20.

Table 4.20 *The thermal properties of the xylene and decalin copolymer insoluble fractions.*

	Xylene insoluble fractions		Decalin insoluble fractions	
Polymer number	**Melting temperature (°C)**	**Crystallinity (%)**	**Melting temperature (°C)**	**Crystallinity (%)**
1	157	28	151	7
2	149	23	142	12
3	146	12	148	16
4	151	19	147	16
5	145	11	142	10

In general, xylene insoluble materials have a slightly higher peak melting temperature than decalin insoluble materials. Overall, teh decalin insoluble materials have a lower melting temperature and crystallinity than the xylene insoluble materials. Once again, this indicates that decalin extracts some crystalline material. While the insoluble fractions of Polymer 1 has the highest melting temperature of all the polymers, there seems to be no relationship between the melting temperature of the insoluble fractions of Polymers 2 to 5 and the ethylene content of these copolymers. Polymers 2 and 4 were originally nucleated, but

whether any nucleating agent was left after extraction is unknown. Be that as it may, differences in ethylene content is not reflected in the melting temperatures of the extracted material.

The DSC results of the xylene and decalin insoluble fractions of Polymers 1, 3 and 5 are shown in Figures 4.38 and 4.39, respectively, to illustrate the melting peak temperatures and the shape of the curve assumed by each fraction.

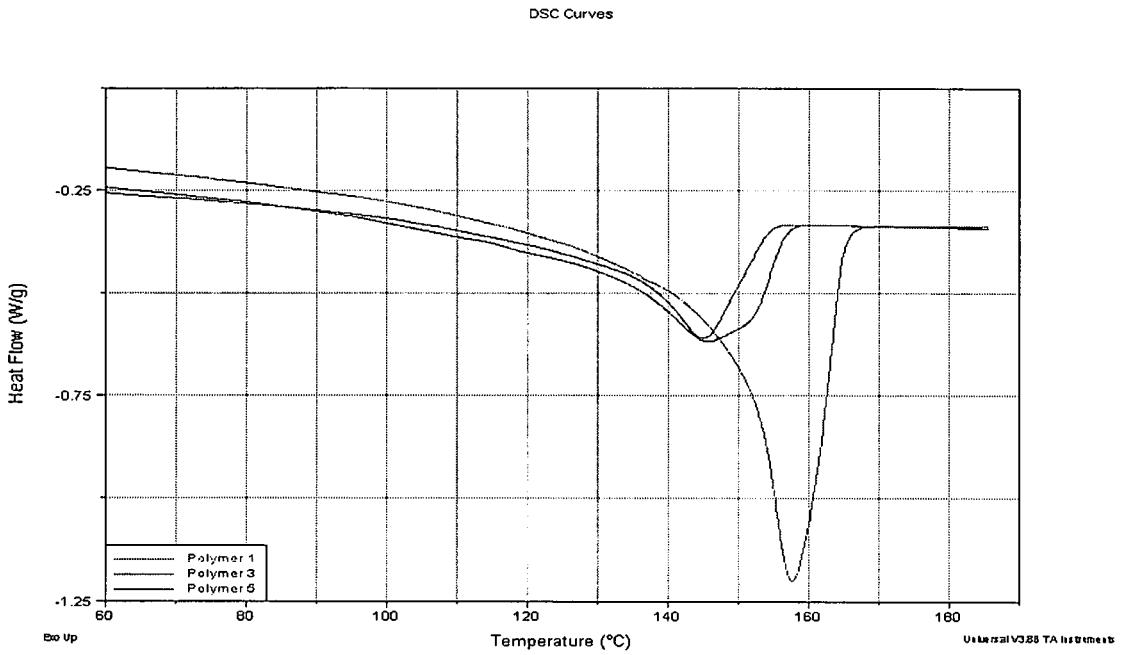

Figure 4.38 *The melting overlays of the ethylene random copolymer xylene insoluble fractions.*

A decrease in the percentage crystallinity of the xylene insoluble fractions is observed relative to the un-fractionated samples. Although this decrease is observed, the xylene fractions still have higher percentage crystallinity than the corresponding decalin insoluble fractions.

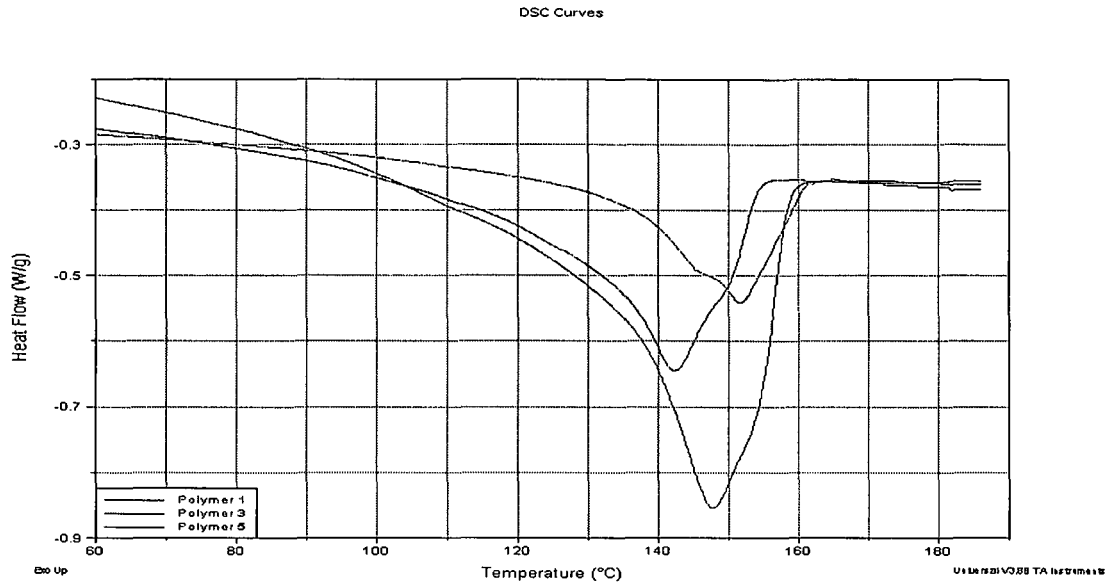

Figure 4.39 *The melting overlays of the ethylene random copolymer decalin insoluble fractions.*

A drop in the melting temperature is observed in the decalin insoluble fractions when compared to the un-fractionated samples. This can be attributed to the differences in the crystalline species and lamellar thickness between the un-fractionated samples and insoluble fractions. The Polymer 3 thermogram shows some broadening effect resulting from the possibility of the presence of more than one crystalline species in the polymer or it may still be wet with decalin.

4.9.3 Elucidation of the microstructural properties of the xylene and decalin insoluble fractions.

The solvent insoluble fractions were analyzed using ^{13}C NMR spectrometry. The ^{13}C NMR spectrum of the Polymer 1 xylene insoluble fraction is shown in Figure 4.40.

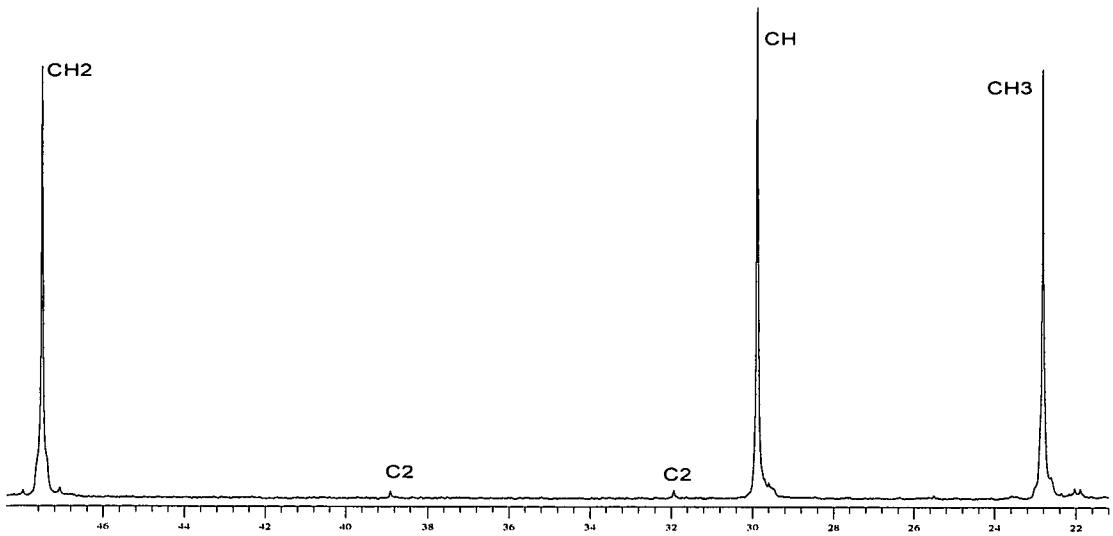

Figure 4.40 *The ^{13}C NMR spectrum of Polymer 1 xylene insoluble fraction.*

The ethylene peaks at approximately 32 ppm and 39 ppm are significantly reduced when compared to the un-fractionated sample (Figure 4.12). The extracted portion has significant amounts of ethylene rich material in it, this was expected. Polymer 1 xylene insoluble fraction spectrum shows that the material 85% isotactic.

The ^{13}C NMR spectrum of the decalin insoluble fraction of Polymer 1 showed that this fraction has a significant amount of residual decalin solvent in it and is thus not included in the report. Therefore, the spectrum of the decalin insoluble fraction of Polymer 2, shown in Figure 4.41, was used instead. It is representative of other ethylene random copolymer samples.

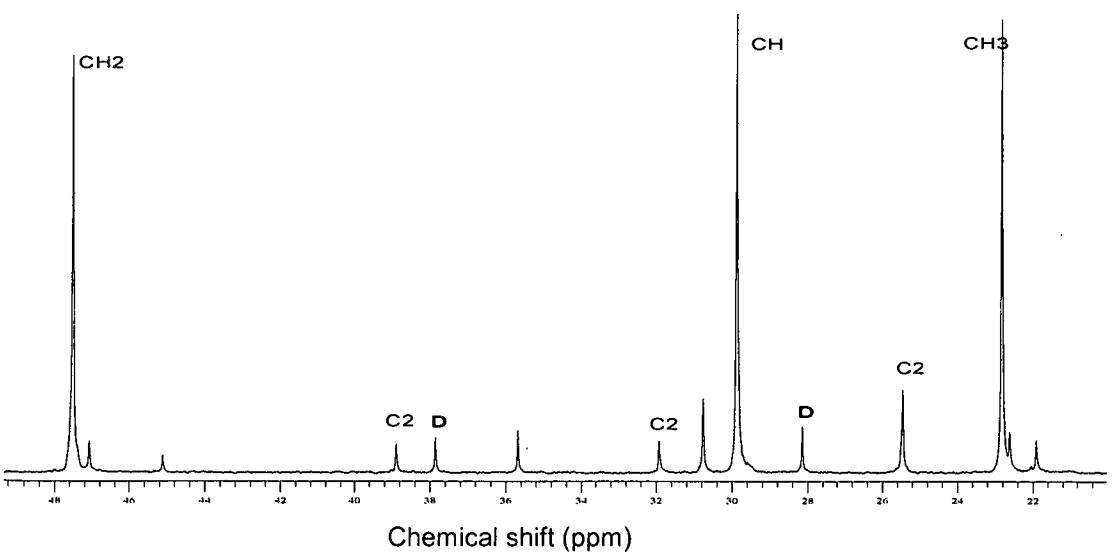

Figure 4.41 *The ^{13}C NMR spectrum of Polymer 2 decalin insoluble fractions.*

Figure 4.41 shows that Polymer 2 decalin insoluble fractions are 75% isotactic. Isolated ethylene insertions are clearly visible on the spectrum, particularly at 25 ppm, 32 ppm, 38 ppm and 47 ppm. The variation in ethylene content in Polymers 2 to 5 does not influence the microstructure of the decalin insoluble fractions to any noticeable degree. Figures 4.27 and 4.28 can be used as references for the location of the ethylene peaks along the spectrum. As noticed previously, decalin peaks are observed in the spectrum at about 28 ppm and also at 38 ppm (marked D in Figure 4.41). This emphasizes the difficulty in evaporating decalin solvent from the extracted fractions.

The ^{13}C NMR spectrum of the xylene insoluble fraction of Polymer 2 is illustrated in Figure 4.42 for comparison to the corresponding decalin fractions.

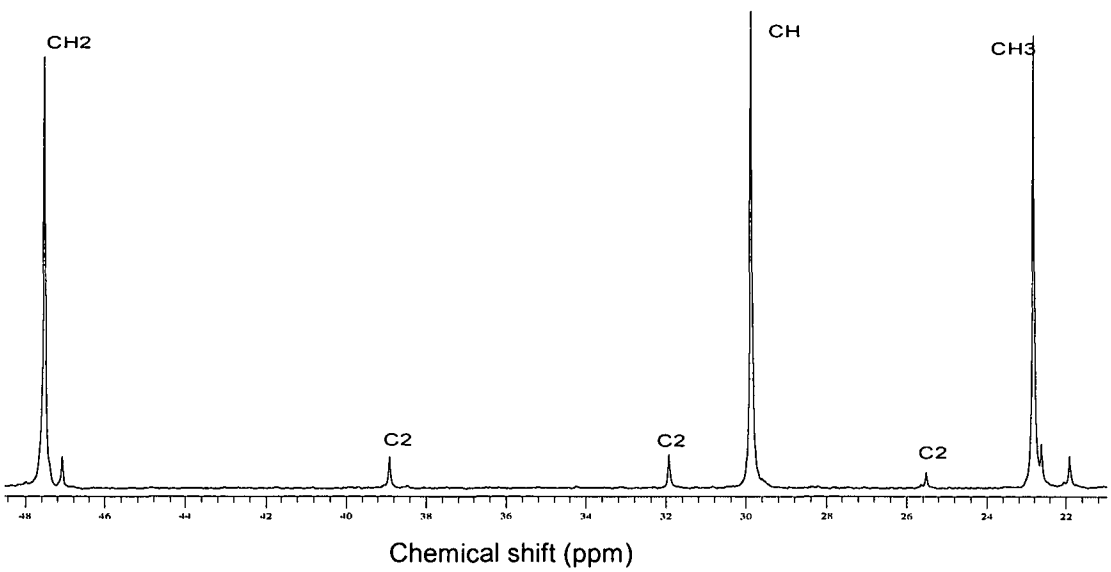

Figure 4.42 *The ^{13}C NMR spectrum of Polymer 2 xylene insoluble fractions.*

The spectrum shows that the xylene insoluble fraction of Polymer 2 is 80% isotactic, even though ethylene is present in the fraction. The ethylene peaks in the spectrum appears slightly reduced when compared to the decalin insoluble fraction. It was impossible, however, to quantify the exact ethylene content both for the xylene and decalin fractions. However, from Figures 4.41 and 4.42 it can be seen that the ethylene peak intensities are more pronounced in the decalin spectrum. This observation is in line with the ^{13}C NMR results of the soluble fractions which showed that the decalin soluble fractions were less ethylene rich.

4.10 Successive solvents extractions.

Material extracted by xylene were further successively extracted using hexane and heptane. This was performed in order to separate the fractions into more homogeneous fractions. The fractions thus generated are referred to as hexane and heptane soluble fractions. In all the

samples used in the successive extractions, none of them had the heptane insoluble fraction. The separated fractions were characterized by GPC, DSC and ^{13}C NMR spectrometry.

It is known that polymer separation is largely dependent on the polymer stereoregularity and to some extent the molecular weight also has an influence [9]. In the successive extractions, the principle employed in separating the polymer into various fractions was based on the increasing boiling points of hexane and heptane.

4.10.1 The GPC results of the successively extracted homopolymers.

Xylene soluble materials from homopolymer samples 6-9 were successively extracted utilizing hexane and heptane. The GPC results of the successive extractions are displayed in Table 4.21.

Table 4.21 *The GPC results of the successively extracted homopolymer samples.*

	Hexane soluble fractions (60 °C)			Heptane soluble fractions (90 °C)		
Polymer number	$\overline{Mw}$	$\overline{Mn}$	**MWD**	$\overline{Mw}$	$\overline{Mn}$	**MWD**
6	60 000	4 000	14.9	96 000	9 000	10.2
7	107 000	6 000	17.6	118 000	10 000	11.6
8	69 000	4 000	18.4	92 000	8 000	11.8
9	104 000	7 000	14.4	204 000	14 000	14.0

Table 4.21 shows that the successive extraction experiment resulted in a separation based alergely on molecular weight. Previously it was shown that the xylene soluble materials were essentially atactic [11].
This observation may be influenced by the extraction temperatures since polymers of higher molecular weight dissolve more easily at higher temperatures.

4.10.2 The ^{13}C NMR results of the successively extracted homopolymers.

Polymer 6 hexane and heptane soluble fractions were selected as typical samples. Figures 4.43 (a) and 4.43 (b) represent the ^{13}C NMR spectrum of the hexane soluble material extracted form the xylene soluble materials obtained from Polymer 6, and its methyl region, respectively.

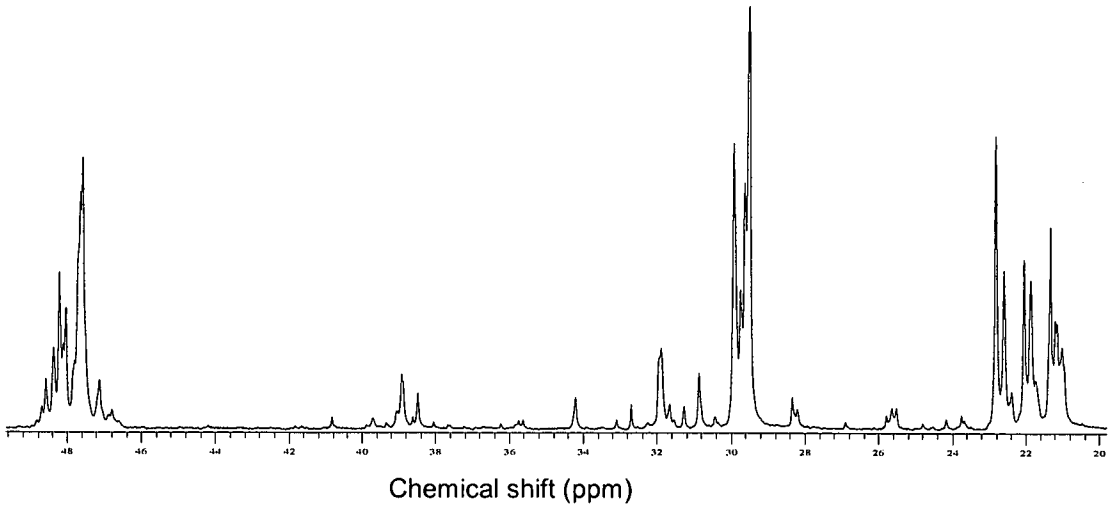

Figure 4.43 (a) *The ^{13}C NMR spectrum of Polymer 6 hexane extracted fraction.*

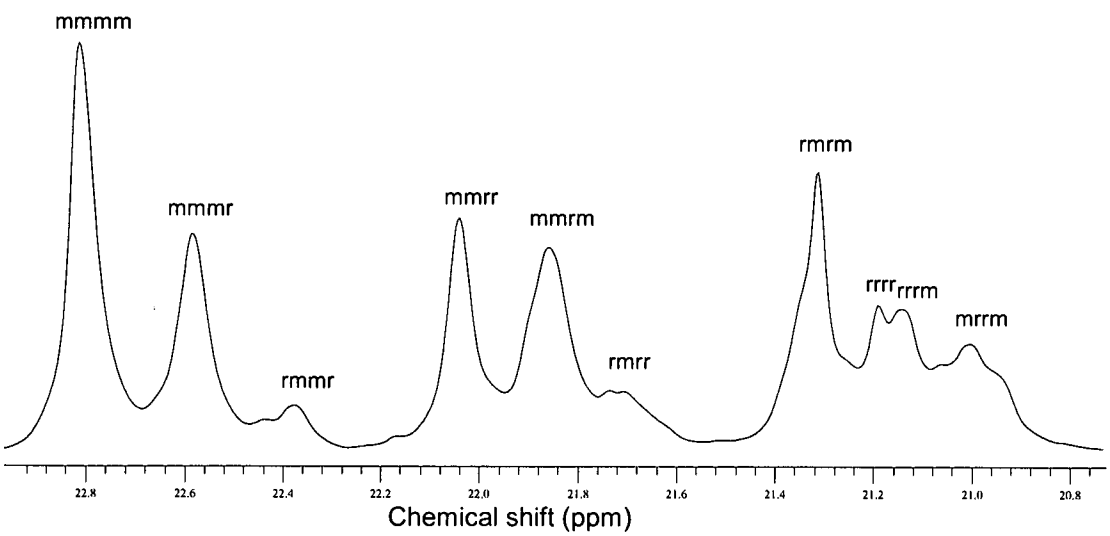

Figure 4.43 (b) *The methyl region of Polymer 6 hexane soluble fractions.*

Figures 4.43 (a) and 4.43 (b) confirm that the hexane soluble fractions are less stereoregular. GPC results showed that these fractions have lower $\overline{Mw}$ and a broad MWD. The integration of the methyl region confirms that these fractions are about 17% isotactic. The bulk of the material constituting the hexane soluble fractions is certainly atactic.

The ^{13}C NMR results of the heptane solubles are indicated in Figures 4.44 (a) and 4.44(b).

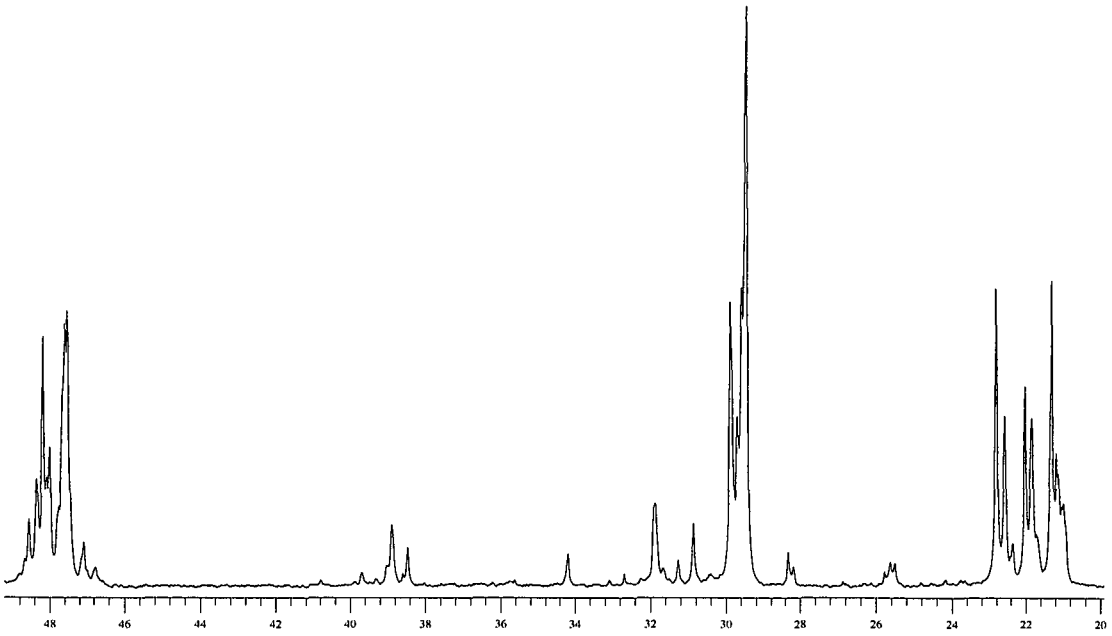

Figure 4.44 (a) *The ^{13}C NMR spectrum of Polymer 6 heptane extracted fraction.*

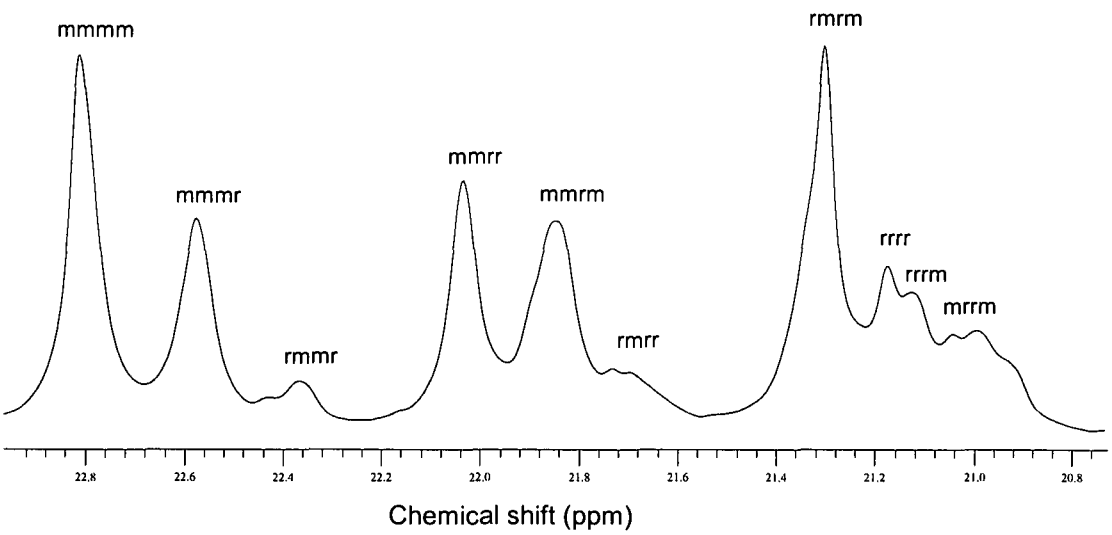

Figure 4.44 (b) *The methyl region of Polymer 6 heptane soluble fraction.*

The heptane soluble fraction was compared to the hexane soluble fraction and their microstructures were virtually identical. Isotacticity values are the same (17% and 16% for the hexane and heptane solubles, respectively). The peaks resonating between 20 ppm and 40 ppm result from the regioerrors caused by misinsertion of the propylene units into polymer backbone and the occurrence of chain termination. The distinction between the fractions is clearly only in the molecular weight and MWD. In this case, the heptane soluble fractions generally have higher molecular weight and a narrower MWD.

4.10.3 The GPC results of the successively extracted propylene-ethylene random copolymers.

The GPC results of the successively extracted ethylene random copolymer fractions are shown in Table 4.22.

Table 4.22 *The GPC results of the successively extracted propylene-ethylene random copolymer samples*

	Un-fractionated samples			Hexane soluble fractions (60 °C)			Heptane soluble fractions (90 °C)		
Polymer number	$\overline{Mw}$	$\overline{Mn}$	MWD	$\overline{Mw}$	$\overline{Mn}$	MWD	$\overline{Mw}$	$\overline{Mn}$	MWD
1	300 000	100 000	3.0	87 000	5 000	17.0	115 000	10 000	12.0
2	300 000	80 000	3.7	167 000	11 000	15.5	96 000	12 000	7.7
3	570 000	140 000	4.1	56 000	8 000	7.3	171 000	18 000	9.3
4	290 000	73 000	3.9	68 000	7 000	9.2	77 000	10 000	7.5
5	380 000	120 000	3.0	117 000	7 000	15.6	117 000	15 000	11.5

From Table 4.22 it is clear that the un-fractionated polymer material is separated into two distinct fractions characterised by the differences in molecular weight and MWD. In general, the hexane soluble fractions have the lower molecular weight and broader MWD than the heptane soluble fractions. The reason for these differences could be attributed to polymer solubility differences based on the solvent strength and extraction temperatures. During the process the material was not completely dissolved at both 60 °C and 90 °C. Polymer 5 has equal molecular weight for both the heptane and hexane soluble fractions and the distinction between the two fractions is in the MWD. In this case the heptane soluble fractions have a slightly narrower MWD.

4.10.4 The thermal properties of hexane and heptane extracted fractions.

The hexane and heptane soluble fractions were comprised of basically amorphous materials which did not yield any usable results from the DSC.

4.10.5 The ^{13}C NMR results of the successively extracted copolymer fractions.

The successively extracted fractions of the ethylene random copolymers were analysed on the NMR to distinguish between the microstructure of the hexane and heptane solubles.

Figures 4.45 (a) and 4.45 (b) gives the ^{13}C NMR spectrum and the methyl region of Polymer 1 (hexane soluble materials extracted from the xylene soluble material), respectively.

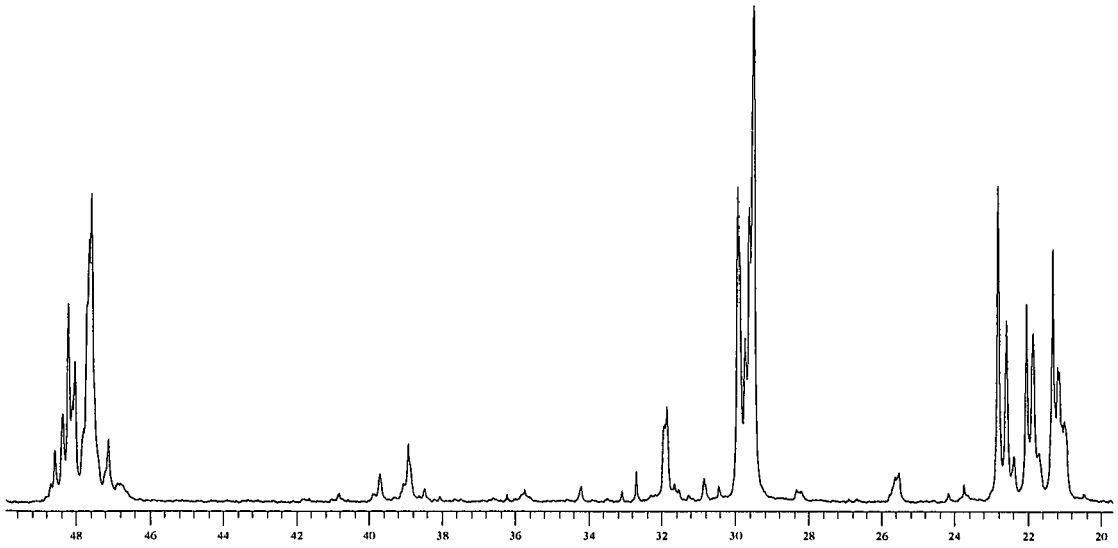

Figure 4.45 (a) *The ^{13}C NMR spectrum of Polymer 1 hexane extracted fractions.*

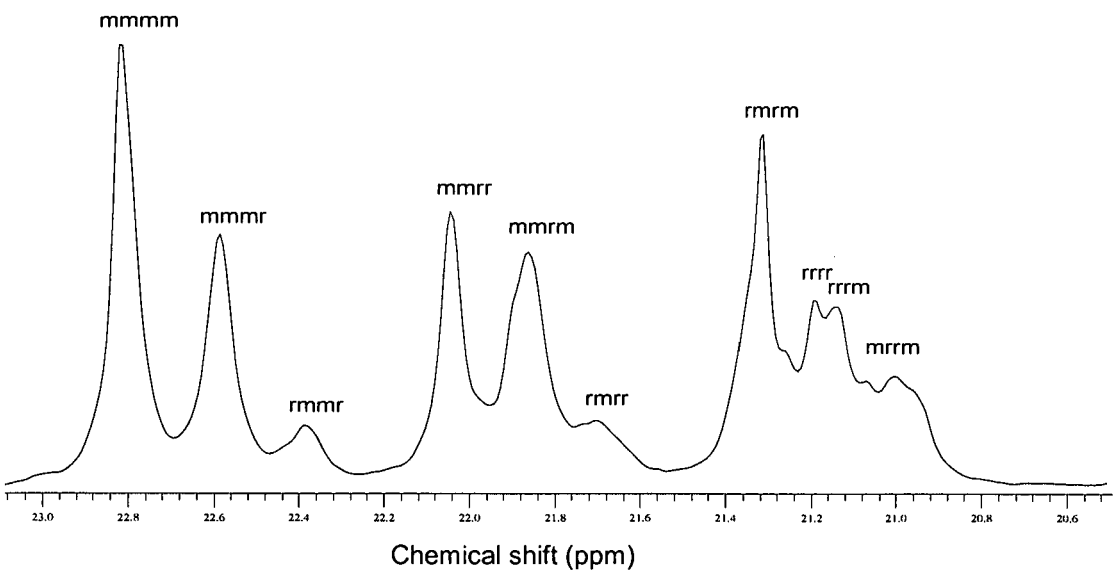

Figure 4.45 (b) *The methyl region of Polymer 1 hexane soluble fractions.*

The spectrum clearly shows that hexane extracted atactic material. Isotacticity is approximately 16.8%. The peaks resonating at about 26 ppm, 39 ppm, and 47 ppm confirm the presence of ethylene comonomer in the extracted materials.

The ^{13}C NMR spectrum of the heptane soluble material (extracted from the xylene soluble material) of Polymer 1 is shown in Figure 4.46 (a) and it almost resembles the hexane soluble fraction spectrum (Figure 4.45 (a)) entirely. An expanded version of the Polymer 1 heptane soluble fraction methyl region is shown in Figure 4.46 (b) to further elucidate the heptane fractions microstructure.

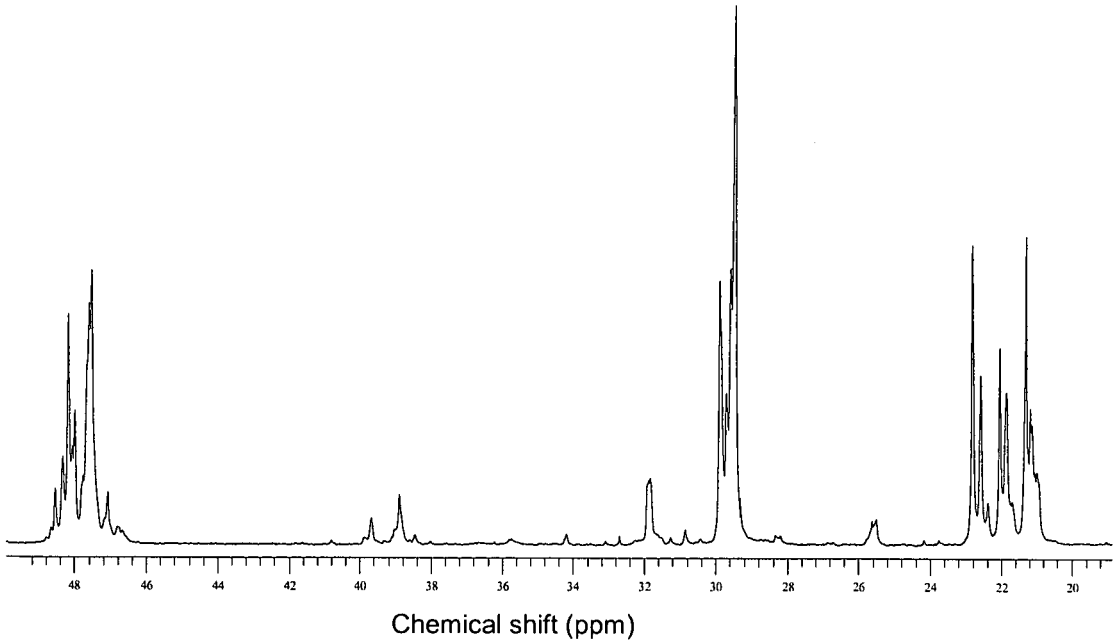

Figure 4.46 (a) *The ^{13}C NMR spectrum of Polymer 1 heptane extracted fraction.*

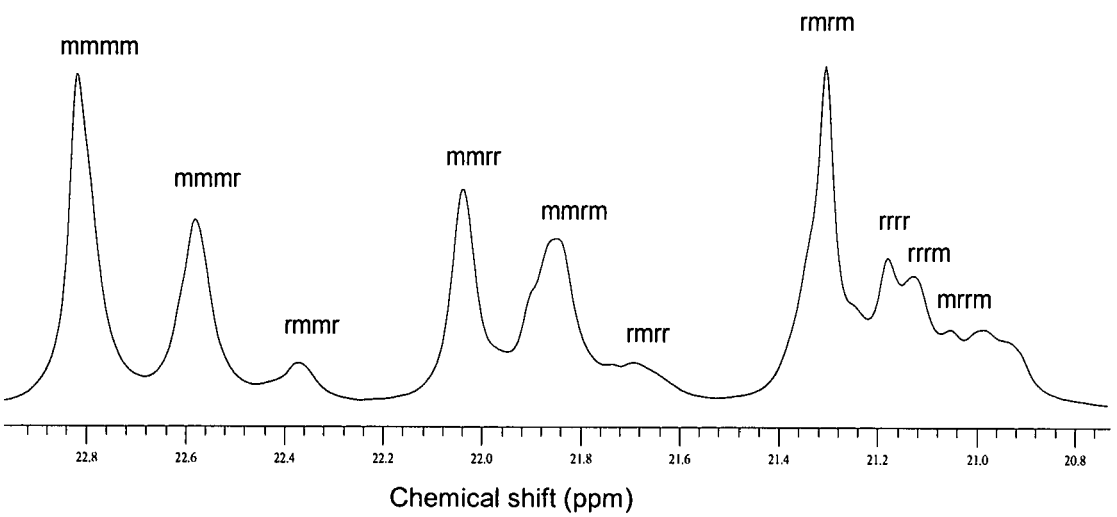

Figure 4.46 (b) *The methyl region of Polymer 1 heptane soluble fraction.*

Polymer 1's heptane soluble fraction has an isotacticity of 14.8% which is slightly lower than that of the corresponding hexane solubles, but this difference is of little significance.

The successively extracted fractions of Polymer 3 were also analyzed by ^{13}C NMR, in order to evaluate the microstructure. The evaluation of these fractions was performed with reference to Figure 4.27 and 4.28. The spectrum of the hexane soluble fraction is shown in Figure 4.47 (a) and its methyl region in Figure 4.47 (b). Noticeably, the ethylene peaks are strongly visible (at 26, 39 and 47 ppm) in the Polymer 3 spectrum. As Polymer 3 has a higher ethylene content than Polymer 1, this was expected.

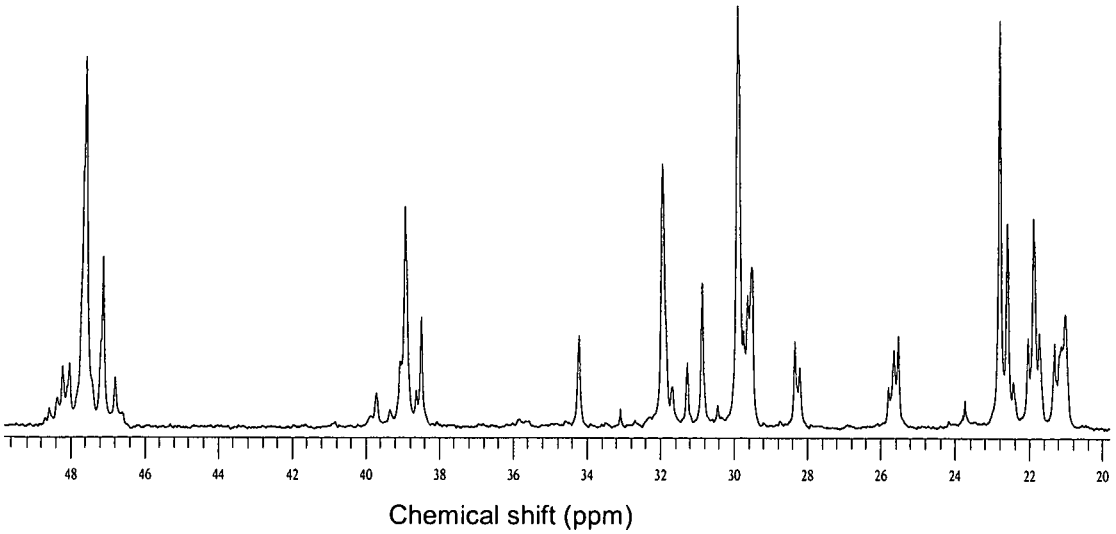

Figure 4.47 (a) *The ^{13}C NMR spectrum of the hexane soluble fraction of Polymer.*

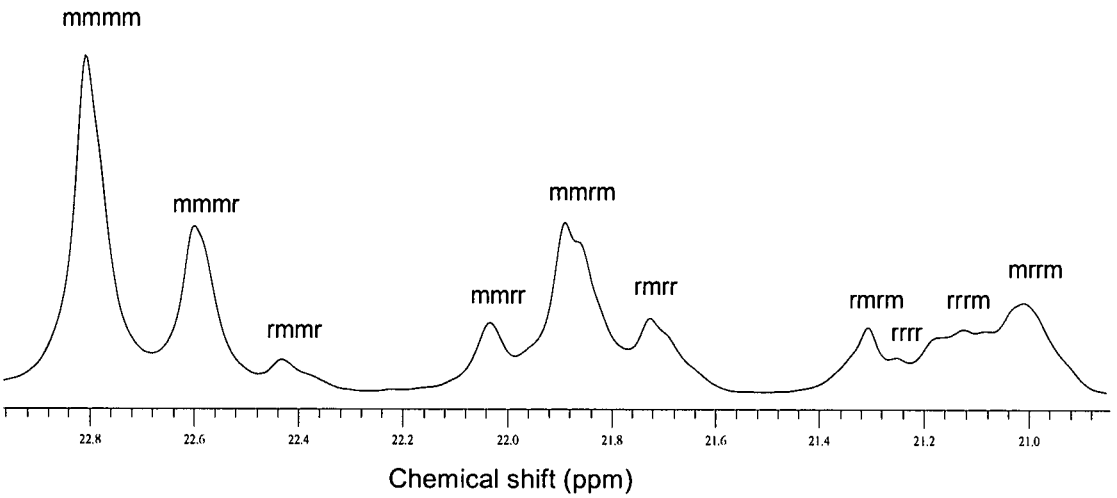

Figure 4.47 (b) *The ^{13}C NMR spectrum (methyl region) of the heptane soluble fraction of Polymer 3.*

Figures 4.47 (a) and 4.47 (b) were compared to the spectra of the heptane soluble fractions of Polymer 3, represented in Figures 4.48 (a) and 4.48 (b).

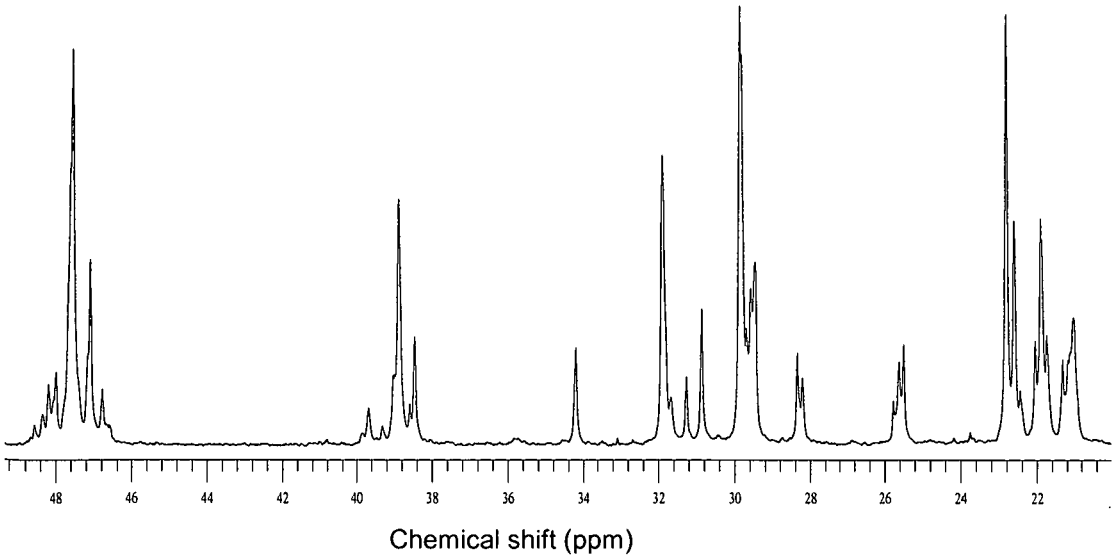

Figure 4.48 (a) *The ^{13}C NMR spectrum of the heptane soluble fraction of Polymer 3.*

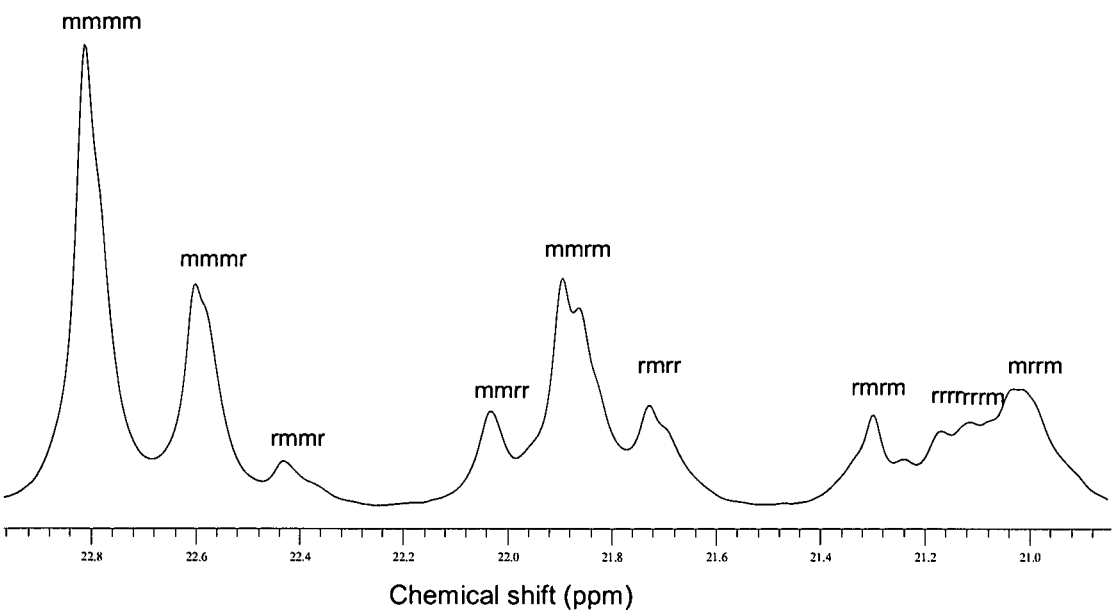

Figure 4.48 (b) *The ^{13}C NMR spectrum (methyl region) of the heptane soluble fraction of Polymer 3.*

The Polymer 3 hexane and heptane solubles spectra do not differ significantly. Their respective isotacticities are measured at approximately 23% for both fractions. The major difference between these two fractions is in the molecular weight. Both Polymer 3 hexane and heptane soluble fractions have higher isotacticity values than Polymer 1 fractions. From the spectra it appears as if the ethylene content of the hexane and heptane soluble materials of Polymer 3 is higher than that of Polymer 1.

The successive extraction results were compared to the xylene extractions. The comparative study made between the copolymer xylene, hexane and heptane fractions showed that there is no systematic relationship between the molecular weight and MWD of the respective

fractions. Heptane fractions generally showed higher molecular weight than the other fractions, whereas the hexane fractions had much broader MWD's.

4.11 References

1. Soares, J.B.P. and Hamielec, A.E. *Polymer*, Volume 37 No. 20 **(1996)**, pp. 4607 – 4614.
2. Ahn, T.O., Hong, S.C., Kim, J.H. and Lee, D. *Journal of Applied Polymer Science*, Volume 67 **(1998)**, pp. 2213 – 2222.
3. Resconi, L., Cavallo, L., Fait, A. and Piemontesi, F. *Chem. Rev.,* Volume 100 **(2000)**, pp. 1253 – 1345.
4. Busico, V. and Cipullo, R. *Progress in Polymer Science*, Volume 26 **(2001)**, pp. 443 – 533.
5. Xu, J., Yang, Y., Feng, L., Kong, X and Yang, S. *Journal of Applied Polymer Science,* Volume 62 **(1996)**, pp. 727 – 731.
6. Kioka, M., Makio,H., Mizuno, A. and Kashiwa, N. *Polymer*, Volume 35 Number 3 **(1994)**, pp. 580 – 583.
7. Moore, Jr, E.P. *Polypropylene Handbook*, **(1996)**, Hanser and Garner, New York.
8. Monrabal B. *Journal of Applied Polymer Science,* Volume 52 **(1994)** pp.491 – 499.
9. Lehtinen, A. and Paukkeri, R. *Macromolecules Chemistry Physics*, Volume 195 **(1994)**, pp. 1539 - 1556.
10. Harding, G.W. *Fractionation and characterisation of propylene copolymers.* MSc thesis, University of Stellenbosch, South Africa **(2005)**.
11. Kawamura, H., Hayashi, T., Inoue,Y. and Chujo, R. *Macromolecules*, Volume 22 **(1989)**, pp. 2181 – 2186.

Chapter 5. Conclusions and recommendations.

The R21 and wet xylene soluble results showed that these techniques are inappropriate for the determination of xylene solubles in copolymer materials. Moreover, the R21 technique is seen to be specific for a certain polymer (homopolymer vs. random) type, and is also significantly influenced by catalyst and donor differences.

Overall the relationships (or lack thereof) between "in-house" techniques and polymer properties are established. The fact that copolymers are complex structures are illustrated, and that the relationship between catalyst ratio and polymer properties is not only influenced by tacticity, but also by comonomer and comonomer distribution.

It is recommended that the calibration curve be established for the copolymer samples using decalin and xylene, respectively, to ensure accurate readings from the Mini Spec NMR. It is equally important to establish the Mini spec NMR calibration line for measuring homopolymer decalin solubles.

The effects of ethylene comonomer incorporation in polypropylene were thoroughly investigated. It was found that comonomer insertion causes melting peak temperature depression and lowered the overall crystallinity of copolymers relative to the homopolymers. It can also be concluded that ethylene content increases the amount of soluble fractions in the polymer.

Decalin seems to extract lower molecular weight material, as well as more isotactic material than xylene. This is consistent for both the homopolymers and copolymers.

Prep-TREF has separated the selected polymers according to crystallizability as expected. Although the trend of TREF, GPC and DSC results were as expected, they did not correlate well with the xylene, decalin and successive extractions results. Successive extractions indicate that extracting the xylene solubles with solvent like hexane and heptane separate the homopolymers into different molecular weights. In the case of the copolymers the successive extractions results seem inconclusive. It is recommended that optimisation work should be conducted to try and establish a correlation amongst these techniques.

Appendix

The ^{13}C NMR spectra

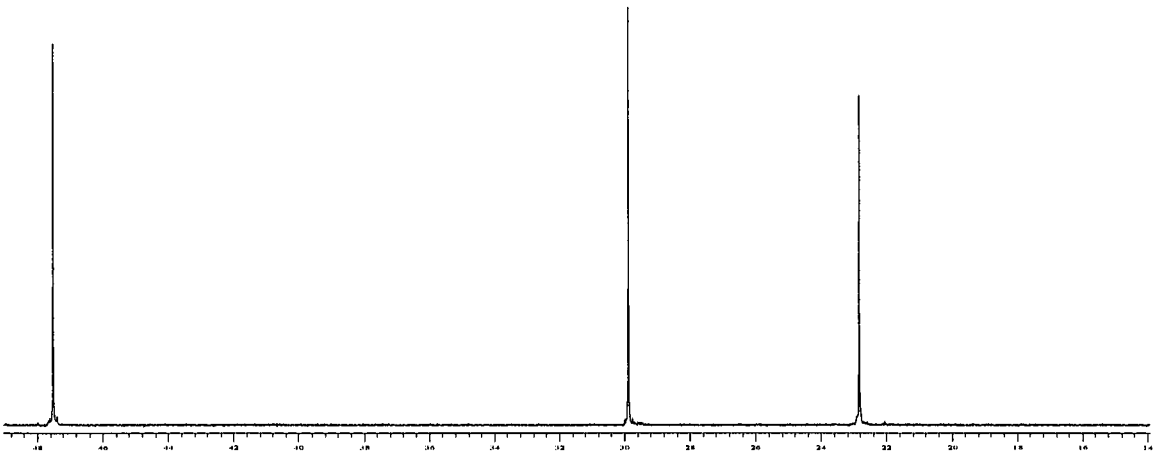

Appendix 1.1 (a): *^{13}C NMR of Polymer 6 un-fractionated sample.*

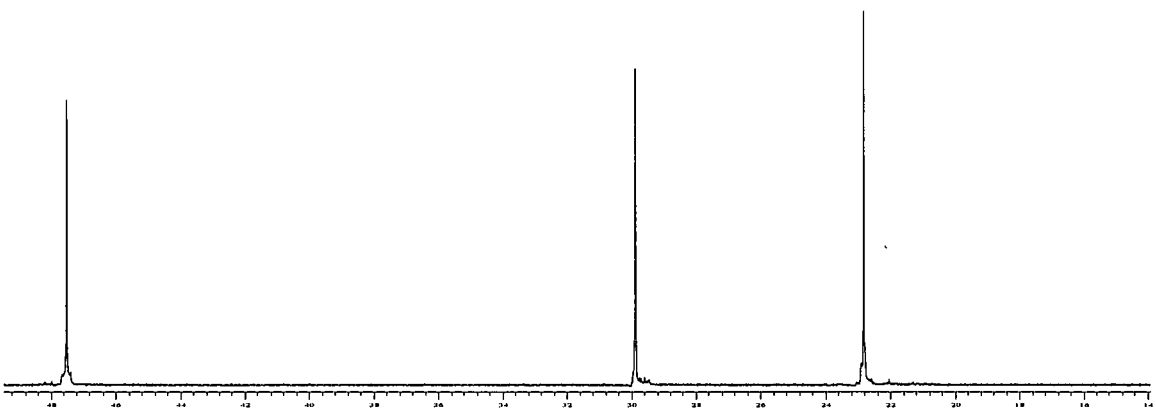

Appendix 1.1 (b): *^{13}C NMR of Polymer 8 un-fractionated sample.*

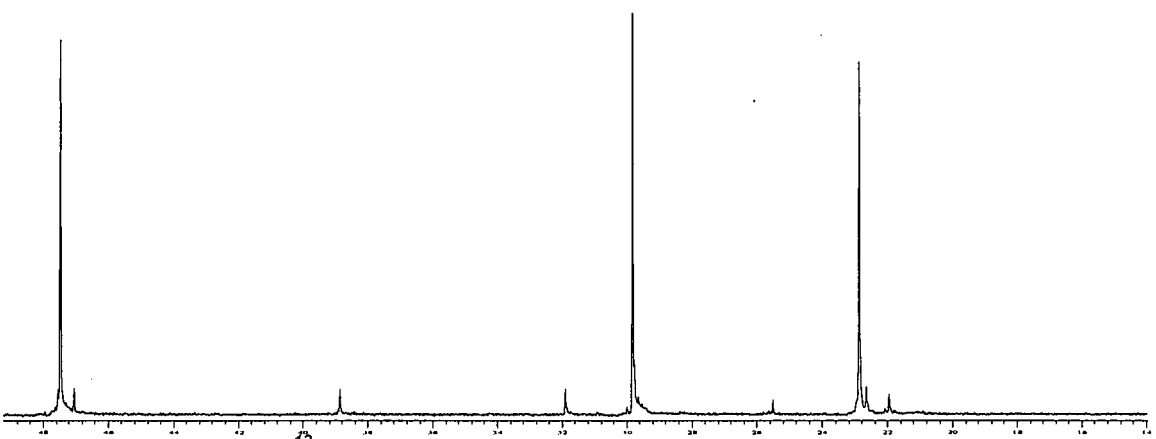

Appendix 1.2 (a): *^{13}C NMR of Polymer 3 un-fractionated sample.*

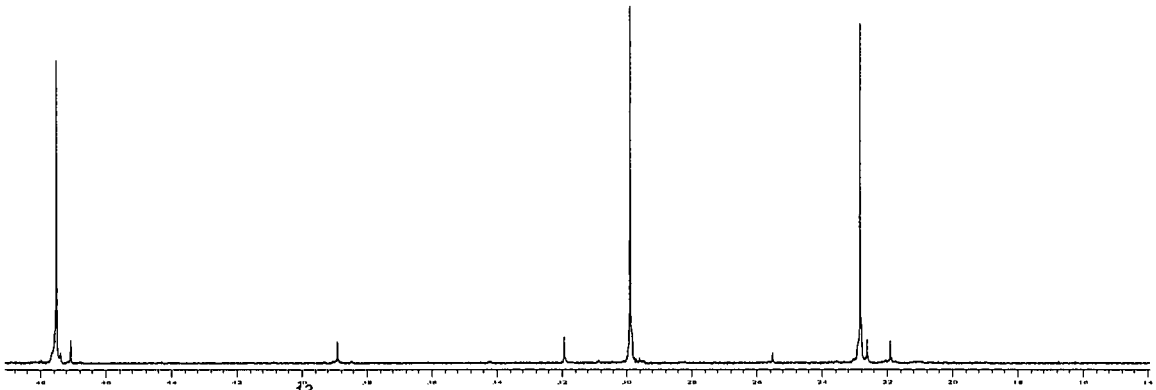

Appendix 1.2 (b): *^{13}C NMR of Polymer 4 un-fractionated sample.*

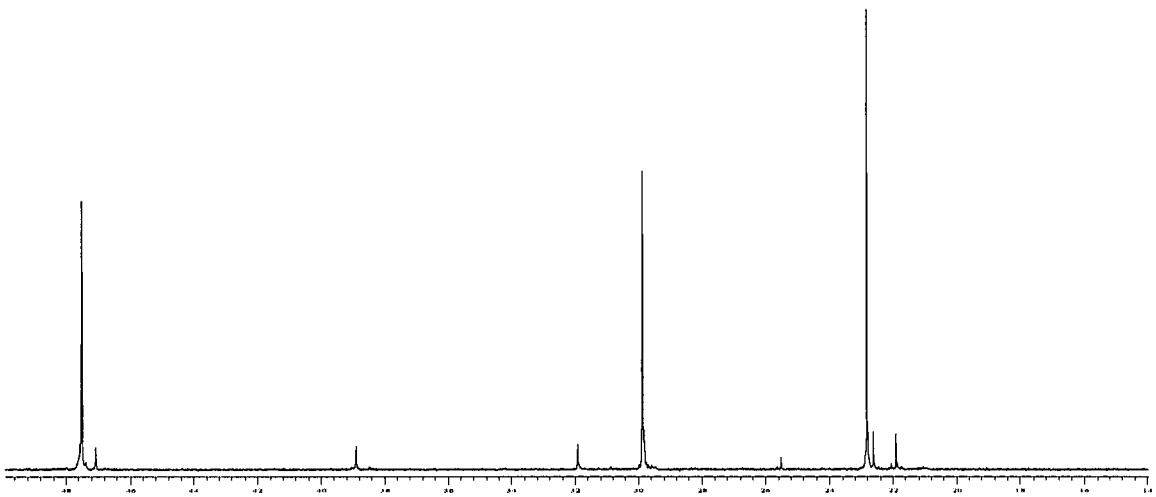

Appendix 1.2 (c): *^{13}C NMR of Polymer 5 un-fractionated sample.*